Since January 2020 Elsevier has created a COVID-19 resource centre with free information in English and Mandarin on the novel coronavirus COVID-19. The COVID-19 resource centre is hosted on Elsevier Connect, the company's public news and information website.

Elsevier hereby grants permission to make all its COVID-19-related research that is available on the COVID-19 resource centre - including this research content - immediately available in PubMed Central and other publicly funded repositories, such as the WHO COVID database with rights for unrestricted research re-use and analyses in any form or by any means with acknowledgement of the original source. These permissions are granted for free by Elsevier for as long as the COVID-19 resource centre remains active.

Coordination Chemistry Reviews 427 (2021) 213586

Contents lists available at ScienceDirect

Coordination Chemistry Reviews

journal homepage: www.elsevier.com/locate/ccr

Review

Zero-, one-, two- and three-dimensional supramolecular architectures sustained by Se···O chalcogen bonding: A crystallographic survey

Edward R.T. Tiekink [1]

Research Centre for Crystalline Materials, School of Science and Technology, 5 Jalan Universiti, Sunway University, Bandar Sunway, Selangor Darul Ehsan 47500, Malaysia

ARTICLE INFO

Article history:
Received 15 May 2020
Accepted 2 September 2020
Available online 17 October 2020

Keywords:
Supramolecular
Chalcogen bonding
Secondary bonding
Selenium
Oxygen

ABSTRACT

The Cambridge Structural Database was evaluated for crystals containing Se···O chalcogen bonding interactions. These secondary bonding interactions are found to operate independently of complementary intermolecular interactions in about 13% of the structures they can potentially form. This number rises significantly when more specific interactions are considered, e.g. Se···O(carbonyl) interactions occur in 50% of cases where they can potentially form. In about 55% of cases, the supramolecular assemblies sustained by Se···O(oxygen) interactions are one-dimensional architectures, with the next most prominent being zero-dimensional assemblies, at 30%.

© 2020 Elsevier B.V. All rights reserved.

Contents

[1] ORCID ID: 0000-0003-1401-1520.
E-mail address: edwardt@sunway.edu.my

https://doi.org/10.1016/j.ccr.2020.213586
0010-8545/© 2020 Elsevier B.V. All rights reserved.

1. Introduction

Being present in the three domains of life, i.e. Archaea, Bacteria and Eukarya, selenocysteine has long being recognised as the 21st proteinogenic amino acid [1–3]. Natural biological functions of selenocysteine relate to redox moderation and anti-oxidant effects such as in the mammalian oxidoreductase system, thioredoxin reductase (TrxR), where it is present in the active site [4]. In connection with thyroid disease, selenocysteine is also present in the active sites of deiodinase enzymes which can activate or inactivate thyroid hormones [5]. The crucial role of selenium in natural biological functions implies a selenium-deficient diet causes disease and requires intervention [6]. Complimenting dietary supplements, synthetic selenium compounds also play a role/have potential as therapeutics [7–10]. The most prominent selenium drug is Ebselen™, i.e. N-phenyl-1,2-benzisoselenazol-3(2H)-one, which is known to exhibit a variety of biological activities, partially owing to its ability to mimic the glutathione peroxidase enzyme, which regulates redox homeostasis and which protects cells from oxidative stress [7–10]. Other medicinal benefits of Ebselen™ include cytoprotective and neuroprotective properties, and potential therapeutic applications relate to anti-cancer, anti-bacterial and anti-inflammatory activities [7–10]. With this background, it is not surprising the biological mechanism(s) of Ebselen™ and related species have been investigated thoroughly [11,12]. These experimental and theoretical investigations often point to the importance of both inter- and intra-molecular Se···O interactions in crucial biological processes [11,12]. Stabilising Se···O interactions are now classified among chalcogen bonding interactions, a term possibly first employed in 1998 [15], whereby the Group XVI element functions as an electrophile [13,14]. It is stressed that the focus of the present review is upon the role of intermolecular Se···O contacts and upon the supramolecular aggregation patterns they sustain. In general terms, chalcogen interactions find very practical applications in a range of contexts beyond biology and medicine [16–18], such as in molecular/anion recognition [19–22], catalysts [23,24] and materials science [25,26]. With this level of activity, it is not surprising there are several authoritative reviews of chalcogen bonding [27–30], including reviews of different physiochemical procedures for their detection in phases other than in crystals [31–33], the primary importance of X-ray crystallographic investigations notwithstanding.

The most convenient method for identifying chalcogen bonding in the solid-state relies upon crystal structure analysis with the earliest investigations of chalcogen bonding depending on the evaluation of crystal structures for contacts occurring at separations intermediate between the respective sums of the covalent and van der Waals radii for the participating atoms. In these present times where all manner of intermolecular contacts/-supramolecular synthons are being "revealed", it might be tempting to suggest chalcogen bonding, and related tetrel and pnictogen interactions involving, respectively, Group XIV and XV elements acting as the electrophile, are a recent phenomenon. While obviously these interactions already exist in the crystals of the relevant compounds capable of forming such interactions and may not necessarily have been recognised or appreciated as being significant previously, it turns out the discussion of secondary bonding interactions actually goes back well over 50 years. Among the first bibliographic reviews of the topic are those by H.A. Bent [34], Noble Laureate O. Hassel [35] and N.W. Alcock [36], with these being followed up by a number of general overviews of the topic [37–40]. It is likely the first time the term secondary bonding was used in the context of these donor–acceptor interactions appeared in the title of a research paper was in a Conference Abstract published in 1975 [41] and then in a follow-up Journal article in 1977 [42]. The use of secondary bonding as a design element in crystal engineering endeavours was suggested as early as 1999 [43].

An initially disconcerting feature of many secondary bonding interactions, including halogen bonding [44], which also comes under the appellation secondary bonding [36], was that the interaction often occurred between two electron-rich species, i.e. a low oxidation state main group element, implying a lone-pair or even lone-pairs of electrons, and donors also having at least one lone-pair of electrons. Through the concept of a σ-hole, theory now aids the understanding of this apparent violation of basic electrostatic arguments. Conventionally the bonding in chalcogen bonds was described in terms of charge transfer from a lone-pair of electrons of the donor atom (D) to an anti-bonding orbital of the bond involving the chalcogen atom (A–X), i.e. $(D)n^2 \rightarrow \sigma^*(A–X)$, but the problem remains in that two electron-rich species are brought into close contact. The σ-hole concept, widely employed to explain the bonding in such circumstances [45,46], relates to the anisotropic distribution of charge about the bonded chalcogen atom. With reference to the bonding axis of a A–X bond, there is an equatorial band of electron density about the A atom, i.e. perpendicular to the A–X bond, and a significant electron-deficient region at the extension of the bonding axis, the σ-hole (or polar cap). It is the latter that can form stabilising interactions with nucleophilic species. The success and general applicability of this approach in rationalising the formation of chalcogen bonds as well as tetrel, pnictogen and halogen bonds [47] notwithstanding, recent studies point to the importance of orbital delocalisation as being relevant [48]. Having a model for bonding, the question then arises as to what are the energies of stabilisation are provided by chalcogen and related interactions. Naturally, the calculated energies will be highly dependent on the nature of the bonds about the interacting atoms, steric profiles of the interacting residues and whether a chalcogen or other intermolecular interaction is operating independently of supporting or competing intermolecular interactions not to mention the level of theory/basis sets employed in the performing of the calculations. Nevertheless, there appears a consensus from calculations [49–53] that the energies of stabilisation afforded by secondary bonding interactions are comparable and often exceed those provided by conventional hydrogen bonding interactions [54] and which, in turn, are comparable to the energies associated with other supramolecular synthons involving heavy elements such as π(chelate ring)···π(chelate) interactions [55].

It was in the context of a long-held interest in secondary bonding interactions and the supramolecular architectures they sustain [56–64] and in the aforementioned biological relevance of Se···O chalcogen bonding interactions that the present survey of Se···O interactions operating in crystals was undertaken. This review of the crystallographic literature serves to highlight the diverse nature of selenium atom environments, geometries, oxidation states and numbers and types of Se···O secondary bonding interactions formed by selenium and the wide variety of supramolecular architectures these chalcogen bonding interactions sustain.

2. Methodology

The Cambridge Structural Database (CSD; version 5.41) [65] was searched employing ConQuest (version 2.0.4) [66] for Se···O contacts present in crystals based on the distance criterion that the separation between the selenium and oxygen atoms had to be equal to or less than the sum of the van der Waals radii, i.e. assumed in the CSD as 3.42 Å [65]. Other general criteria were applied in order to keep the number of retrieved structures to a reasonable number and to ensure reliability in the data, namely structures with errors, were salts, polymeric and contained transition metal elements were omitted along with those with R > 0.075. In all 274 structures were retrieved. These were then evaluated manually to ensure that the Se···O interaction was operating in isolation of other obvious supramolecular synthons employing PLATON [67], Mercury [68] and DIAMOND [69].

Three classes of compounds were rejected from further analysis. Firstly, several structures that registered as a hit was in fact a false positive as the putative Se···O(hydroxyl) interaction was embedded within a hydroxyl-O–H···Se hydrogen bond. This is illustrated in Fig. 1a for (-)-t-butylphenylphosphinoselenoic acid [70], where hydroxyl-O–H···Se hydrogen bonding (Se···O = 3.30 Å) occurs between the two independent molecules comprising the asymmetric unit in the crystal. The second scenario leading to the omission of structures also involved hydrogen bonding. Thus, in bi-nuclear 2,2′-(diselane-1,2-diyl)bis(pyridin-3-ol) [71], two centrosymmetrically related molecules are connected into a dimeric aggregate via hydroxyl-O–H···N(pyridyl) hydrogen bonds as shown in Fig. 1b. Contributing to the stability of this aggregate are Se···O(hydroxyl) contacts (3.36 Å) which, obviously, are not operating independently and so examples such as this were omitted from the survey. The third class of omitted compounds featured complementary secondary bonding interactions. An example of this is shown in Fig. 1c where some of the supramolecular association operating in the 1:1 co-crystal formed between co-formers 2,2-dimethyl-N-(7-oxo-6,7-dihydro[1,2,5]selenadiazolo[3,4-d]pyrimidin-5-yl)propanamide and 2,2-dimethylpropanoic acid [72] are highlighted. While Se···O interactions (3.27 Å) are noted, these occur within a tetra-molecule assembly sustained by Se···N secondary bonding interactions (2.83 Å) and eight-membered {···HOCO···NCNH} synthons.

After manual screening, there remained 224 examples of supramolecular aggregation featuring Se···O secondary bonding interactions. All of these are illustrated in Appendix A along with detail of the full composition of the crystal, citation details, selected distances and angles, and comments on supramolecular aggregation along with image(s). The structures are generally arranged in terms of the supramolecular aggregation patterns sustained by the Se···O secondary bonding interactions operating in the crystals, i.e. zero-, one-, two- and three-dimensional. For completeness, Se···O interactions occurring in solvates and co-crystals are also included. Within each of these categories, discussion of selenium(II) atoms participating in Se···O interactions precedes those involving selenium(IV) centres and, when known, selenium

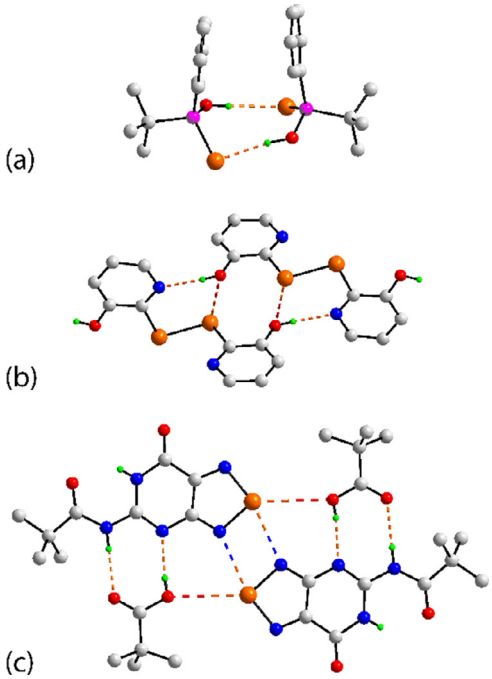

Fig. 1. Examples of excluded structures from the present survey owing to (a) the Se···O contact being embedded within a hydroxyl-O–H···Se hydrogen bond, (b) the Se···O contact occurring within an assembly also mediated by hydroxyl-O–H···N (pyridyl) hydrogen bonds and (c) the Se···O contacts occurring within a tetra-molecule aggregate already sustained by a combination of Se···N secondary bonding interactions and hydrogen bonding. Hydrogen bonds are shown as orange dashed lines, Se···O contacts as orange-red dashed lines and Se···N contacts as orange-blue dashed lines. In this and subsequent diagrams, only acidic-H atoms are shown. Colour code: selenium (orange), phosphorus (pink), oxygen (red), nitrogen (blue), carbon (grey) and hydrogen (green).

(VI) examples. Within in each oxidation state, mono-nuclear species are covered before bi-nuclear species, etc. and within each of these categories, aggregates sustained by one interaction are illustrated before those sustained by two interactions, etc. Generally, the examples are included in order of increasing Se···O distances. The exception to the last guideline occurs when there are significant numbers of closely related compounds. Comments on hydrogen bonding, when present in the crystal, are also included in Appendix A rather than in the main text unless pertinent to the discussion of the identified Se···O contacts. Finally, while the focus herein is upon intermolecular Se···O contacts, hypervalent intramolecular Se···O, and more rarely Se···F and Se···S contacts, are noted in a number of the structures included in this survey. In cases where these occur, details are also included in Appendix A.

3. Zero-dimensional assembles mediated by Se···O chalcogen bonding

In 55 structures zero-dimensional assemblies are formed mediated by Se···O chalcogen bonding interactions. These can be connected by one Se···O contact, usually two Se···O contacts but aggregates sustained by up to 10 Se···O contacts are known. Selenium(II), (IV) and (VI) species are all shown to form zero-dimensional aggregates.

3.1. Selenium(II) species

There are a total of 32 selenium(II) species, **1**–**32** [11,73–96,98–101], forming Se···O contacts leading to zero-dimensional aggregates. The chemical diagrams for the interacting species in these structures are shown in Fig. 2.

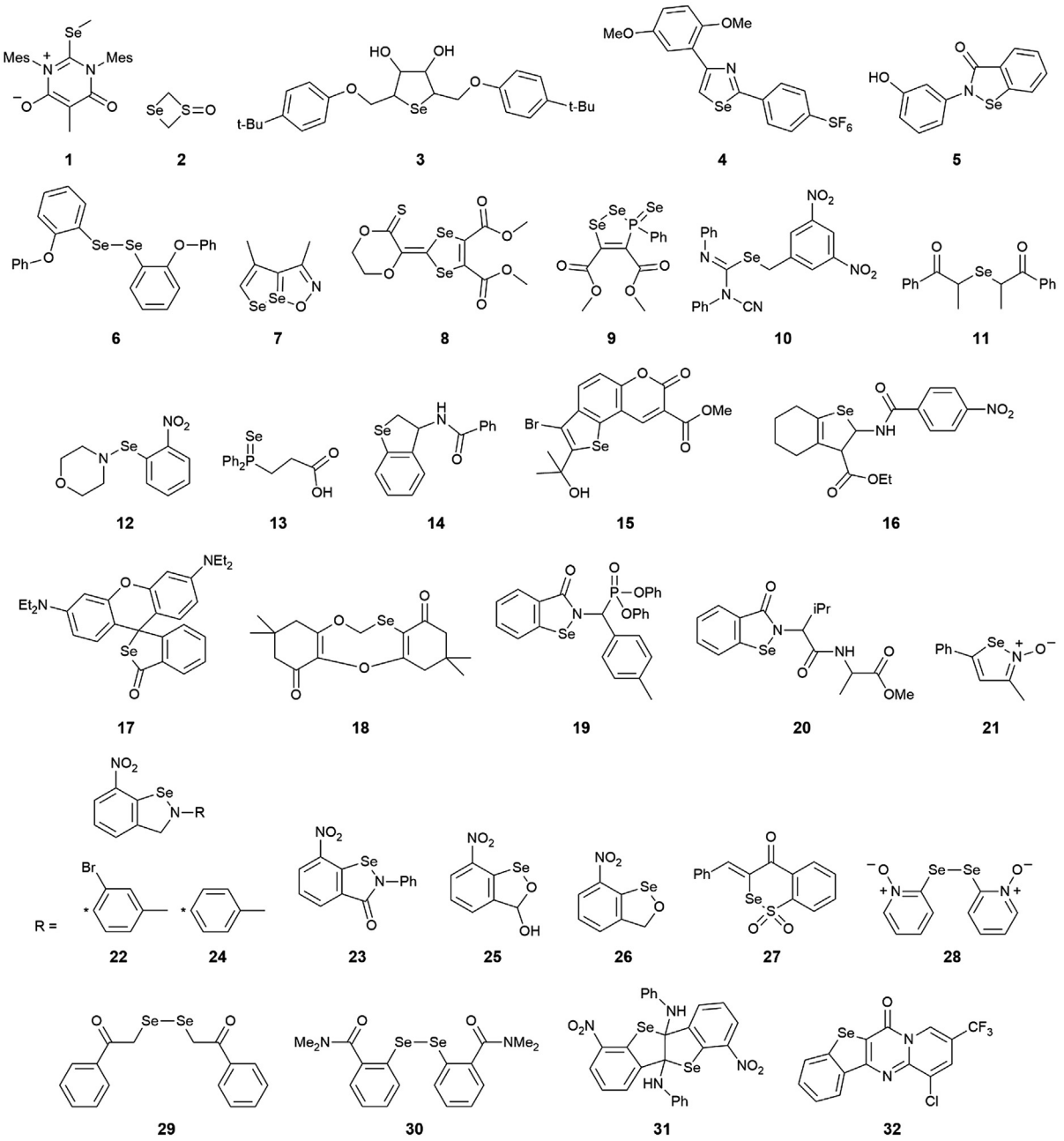

Fig. 2. Chemical diagrams for the interacting species, **1**–**32**, in selenium(II) crystals featuring Se···O contacts leading to zero-dimensional aggregates. The point of attachment at the nitrogen atoms in **22** and **24** are indicated by an asterisk.

3.1.1. Aggregates sustained by a single Se···O contact

The common feature of mono-selenium(II) molecules **1**–**5** [11,73–76] is that dimeric aggregates are sustained by a single Se···O chalcogen bonding interaction; in each of **2**–**5**, the selenium atom is incorporated within a ring. For **2** [74], **4** [76] and **5** [11], Fig. 3a, the contact forms between the two independent molecules comprising the crystallographic asymmetric unit. In **1** [73], there are four independent molecules and two pairs are connected by a single Se···O(carbonyl) interaction. In **3** [75], there are eight independent selenium(II)-containing molecules and four DMSO molecules in the asymmetric unit. In this instance, only one pair of selenium(II)-containing molecules is connected by a single Se···O (hydroxyl) contact. This is a relatively rare case as, usually, in cases where multiple molecules comprise the crystallographic asymmetric unit, all participate in the formation of Se···O contacts (vide infra). In diselenide **6** [77], a Se···O(ether) interaction is featured between the two independent molecules of the asymmetric unit, Fig. 3b. Compound **7** [78] features both selenium(II) and selenium(IV) centres connected within a ring with the selenium(II) atom of one of these connecting to an oxygen atom of the second independent molecule via a Se···O(N-oxo) contact as shown in Fig. 3c. In **8** [79], with four independent molecules in the asymmetric unit, two pairs of molecules are connected by a single Se···O (methoxy) contact. A similar situation pertains in tri-nuclear **9** [80], where a single Se···O(methoxy) contact links the two independent molecules, Fig. 3d. The molecule of **9** is notable in that in addition to two ring selenium atoms, a phosphorus-bound selenide selenium(II) atom is present but, it is one of the ring selenium

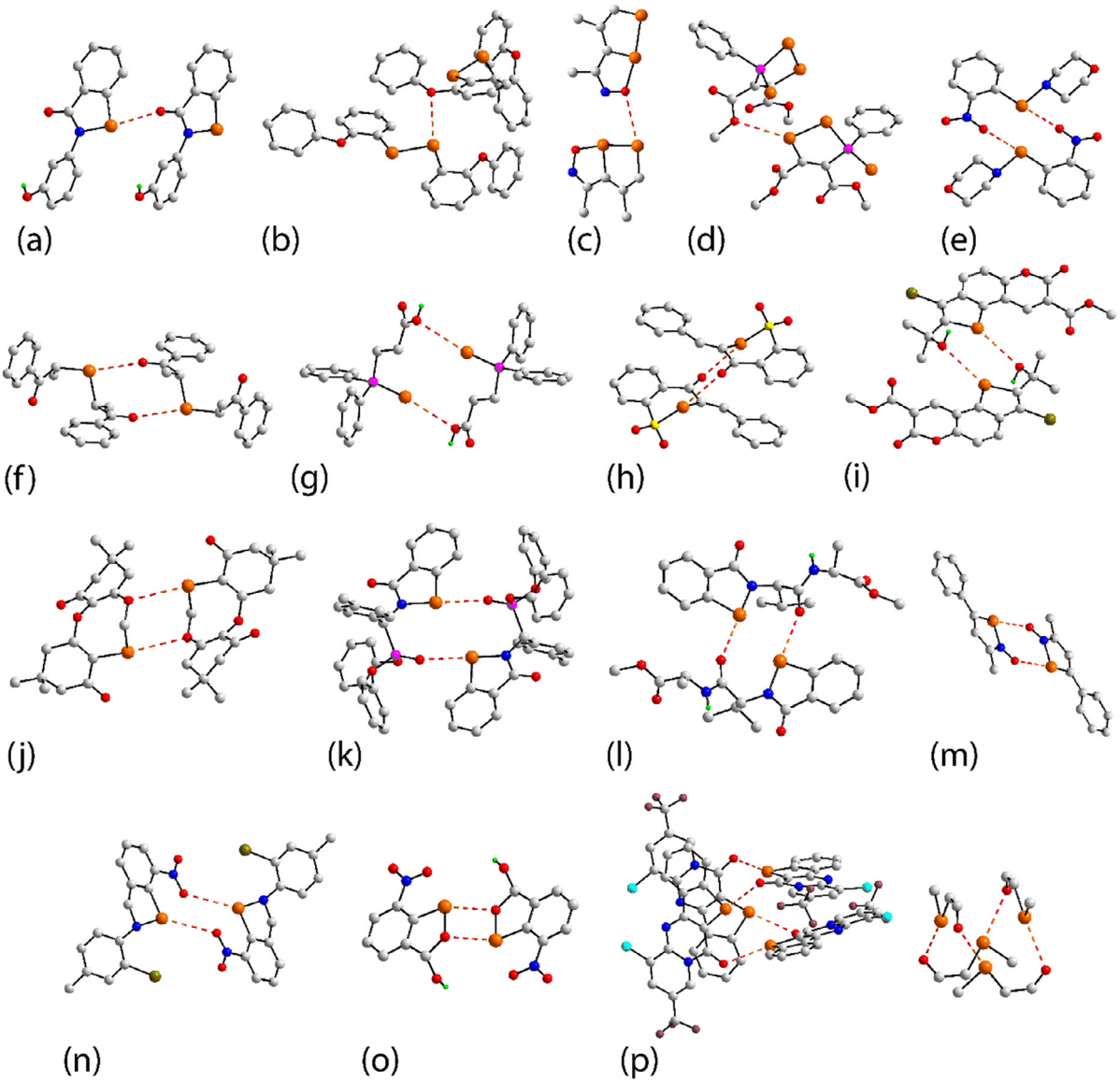

Fig. 3. Representative examples of supramolecular association in selenium(II) crystals leading to zero-dimensional aggregation patterns based on Se···O chalcogen bonding interactions: (a) **5** [11; Se···O = 2.96 Å], (b) **6** [77; 3.25 Å], (c) **7** [78; 3.41 Å], (d) **9** [80; 3.31 Å], (e) **12** [83; 3.34 Å], (f) **11** [82; 3.27 Å], (g) **13** [84; 3.36 Å], (h) **27** [96; 3.14 Å], (i) **15** [86; 3.27 Å], (j) **18** [89; 3.37 Å], (k) **19** [90; 2.80 Å], (l) **20** [91; 2.85 Å], (m) **21** [92; 2.93 Å], (n) **22** [93; 3.24 Å], (o) **25** [95; 2.91 Å] and (p) **32** [101; 2.98 Å] (including simplified view). Additional colour codes: bromide (olive-green), chloride (cyan), yellow (sulphur), fluoride (plum).

atoms that engages in the Se···O(methoxy) interaction. Despite the presence of multiple selenium atoms in **6**–**9**, only one of the possible selenium atoms in each is engaged in a Se···O contact.

3.1.2. Aggregates sustained by two Se···O contacts

The overwhelming majority of mono-nuclear selenium(II) molecules in this category adopt a two-molecule motif sustained by two Se···O contacts. This motif is found in the crystals of **10**–**27** [81–96]. Molecules **10**–**12** feature acyclic, two-coordinated selenium, **13** is a selenide and those of **14**–**27** are also two-coordinated but with the selenium atom incorporated within a ring. In **10** [81] and **20** [91] the Se···O interactions occur between the two independent molecules comprising the asymmetric unit whereas in the remaining examples, they occur between centrosymmetrically related molecules. The selenium atoms in **10** [81] and **12** [83], Fig. 3e, associate with nitro-oxygen atoms, in **11** [82] with carbonyl-oxygen, Fig. 3f, and in **13** [84], Fig. 3g, with hydroxyl-oxygen, the selenium donor being a phosphorous-bound selenide atom. While attention is directed towards intermolecular Se···O interactions in the present survey, it is worth highlighting here that several of these species discussed herein also feature close intramolecular Se···O contacts. This feature first occurs in this survey in **12** where, owing to the close proximity of a pendant nitro substituent, an intramolecular Se···O(nitro) contact of 2.58 Å occurs which is significantly shorter than the intermolecular Se···O(nitro) separation of 3.34 Å. While details of these intramolecular Se···O contacts, and rare examples of intramolecular Se···F and Se···O contacts, are not discussed herein, comments on these are included in Appendix A.

The ring-selenium atoms are generally incorporated within five-membered rings but form part of a six membered ring in **27** [96] and part of an eight-membered ring in **18** [89]. The molecules in **14** [85], **16** [87] and **27** [96], the latter having potential sulphoxide-oxygen atoms capable of forming Se···O contacts, Fig. 3h, associate via Se···O(carbonyl) contacts. In the crystals of **15** [86], Se···O(hydroxyl) contacts are formed despite the presence

of bromide atoms, Fig. 3i, and in each of **17** [88] and **18** [89], Fig. 3j, Se···O(ether) contacts are formed despite the presence of potential carbonyl-oxygen donors. Phosphorus-bound oxide atoms provide the oxygen atoms to form the dimeric aggregate in **19** [90], Fig. 3k, amide-O in **20** [91], Fig. 3l, and N-oxide in **21** [92], Fig. 3m. The dimeric aggregates formed in **22** [93], Fig. 3n, **23** [94] and **24** [93] are sustained by Se···O(nitro) interactions despite the presence of potential competitive interactions with bromide (**22**) and carbonyl-O (**23**). The two remaining molecules in this section feature adjacent selenium and oxygen atoms in the five-membered ring and each of these, i.e. **25** [95] and **26** [95], assemble about a centre of inversion to form a supramolecular four-membered $\{\cdots Se–O\}_2$ synthon. In **25**, Fig. 3o, there are nitro- and hydroxyl-oxygen atoms also capable of forming Se···O interactions but, do not. A related $\{\cdots Se–N\}_2$ synthon was observed in Fig. 1c and has been discussed in terms of being a reliable synthon in the supramolecular chemistry of selenium-nitrogen materials [97]. The foregoing highlights the fact that a myriad of oxygen atoms can participate in Se···O interactions and no definitive preference for one type oxygen atom over another is obvious.

There are four examples of bi-nuclear selenium(II) species forming centrosymmetric aggregates. In diselenide **28** [98], Se···O (N-oxide) interactions sustain the dimer while Se···O(carbonyl) contacts are found in each of **29** [99] and **30** [100]. In **31** [93], one of the ring-selenium atoms of the bi-nuclear molecule associates with a nitro-oxygen atom, similar to that seen in Fig. 3n. An extraordinary mode of association via Se···O(carbonyl) contacts is found in **32** [101]. Here, a four-molecule aggregate is formed about a four-fold rotatory inversion axis ($\bar{4}$) as shown in the images of Fig. 3p.

3.2. Selenium(IV) and selenium(VI) species

Less common but, nevertheless well represented in this survey are selenium(IV) compounds, which differ by having a single lone-pair of electrons as opposed to two for selenium(II) species. Even less frequently observed herein are selenium(VI) species, devoid of stereochemically-active lone-pairs on the selenium centre. The interactions selenium(VI) species form with oxygen reflect more conventional Lewis acid-Lewis base interactions. There are 18 selenium(IV) species, **33**–**50** [100,102–115], and five selenium(VI) species, **51**–**55** [116–119], forming Se···O contacts leading to zero-dimensional aggregates, with the chemical diagrams for the interacting species in these shown in Fig. 4.

3.2.1. Aggregates of selenium(IV) species sustained by two Se···O contacts

The majority of the selenium(IV) compounds form centrosymmetric dimers, indeed 14 of the 18 crystals feature this motif, and each of these is constructed about a four-membered $\{\cdots Se–O\}_2$ synthon. Compounds **33** [102], **34** [103], **35**–**37** [104] conform to the general formula R(R′)Se=O. The dimeric aggregate for **34**, being representative for this series, is shown in Fig. 5a, and is sustained by Se···O(oxide) interactions and is notable for the presence of potentially competitive but, non-interacting sulphur, fluoride and bromide donors. Two structures conform to the formula R(R′O)Se=O. In **38** [100], with R′ = H, the interaction sustaining the dimer is Se···O(carbonyl), Fig. 5b, while the Se···O(oxide) interactions persist in **39** [105], R′ = Me. Similar Se···O(oxide) interactions sustain dimers in instances when the selenium is incorporated in a five-membered ring as in the crystals of **40** [106] and **41** [107]. The first non-selenium oxide molecule is this section is **42** [108], Fig. 5c, where the selenium atom is C,O-chelated by two distinct ligands leading to four- and five-membered rings; the dimer is stabilised by Se···O (alkoxide) contacts. A similar contact occurs in the triorganoselenium species **43** [109], Fig. 5d, where the selenium atom is incorporated within a six-membered ring. The molecules in **44** [110], Fig. 5e, are connected by Se···O(N-oxo) interactions and those in **45** [111], Fig. 5f, and bi-nuclear **46** [112], Fig. 5g, by Se···O(alkoxide) and Se···O(oxide) interactions, respectively. The structure of **44** is the earliest reported crystal structure included in the present survey,

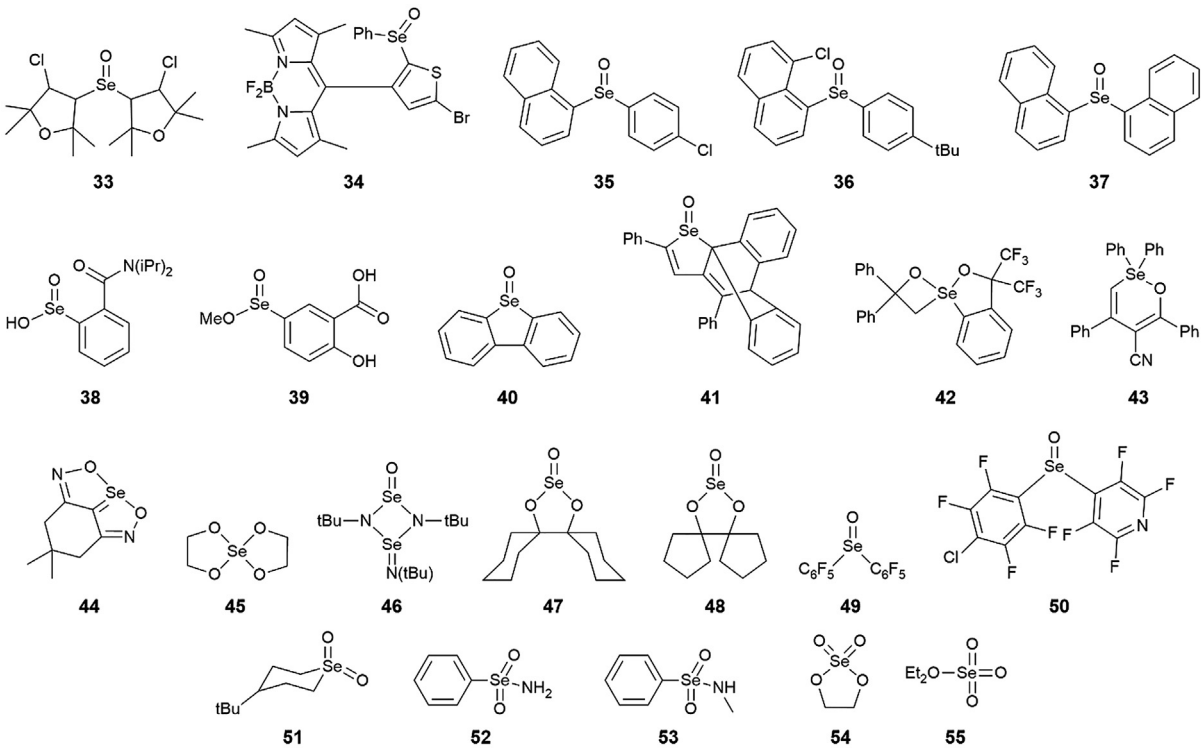

Fig. 4. Chemical diagrams for the interacting species, **33**–**55**, in selenium(IV) and selenium(VI) crystals featuring Se···O contacts leading to zero-dimensional aggregates.

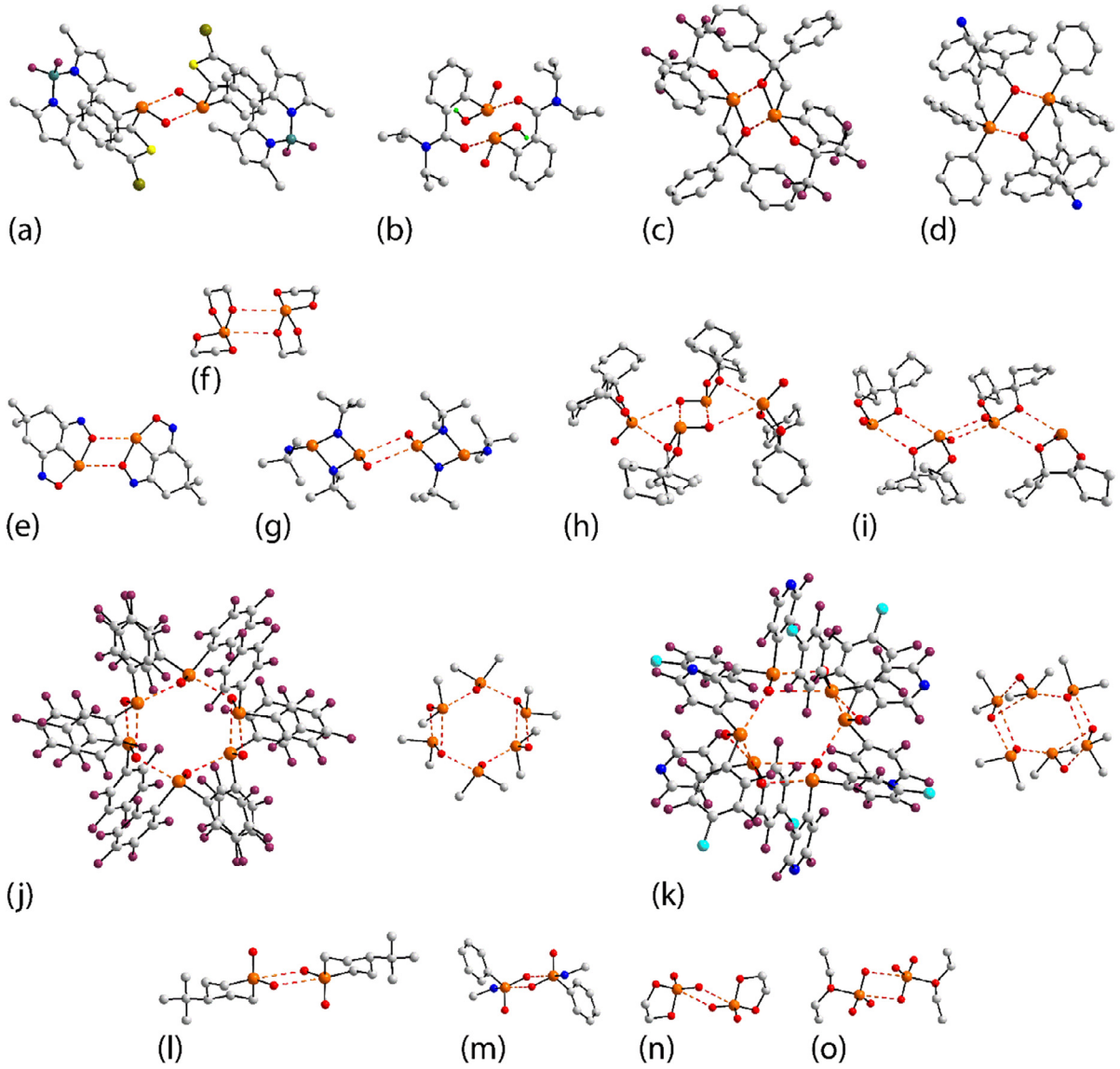

Fig. 5. Representative examples of supramolecular association in selenium(IV) and selenium(VI) crystals leading to zero-dimensional aggregation patterns based on Se···O chalcogen bonding interactions: (a) **34** [103; Se···O = 2.92 Å], (b) **38** [100; 2.85 Å], (c) **42** [108; 3.22 Å], (d) **43** [109; 3.00 Å], (e) **44** [110; 3.20 Å], (f) **45** [111; 3.29 Å], (g) **46** [112; 3.19 Å], (h) **47** [113; 2.81–3.24 Å], (i) **48** [113; 2.96–3.20 Å], (j) **49** [114; 2.60–3.20 Å], (k) **50** [115; 2.66–3.33 Å], (l) **51** [116; 3.35 Å], (m) **53** [117; 3.23 Å], (n) **54** [118; 3.17 Å] and (o) **55** [119; 3.11 Å]; the cores in hexameric **49** and **50** are also included.

being described in 1972. It is also noted here that the authors of this paper discussed the supramolecular association mediated by Se···O secondary bonding in their description of the molecular packing in this crystal. Higher nuclearity aggregates are noted in the remaining selenium(IV) structures to be described in this section.

3.2.2. Aggregates of selenium(IV) species sustained by more than two Se···O contacts

Each of **47** and **48** [113] assemble into tetrameric aggregates in the solid-state. In the crystal of **47**, there are two independent molecules in the asymmetric unit. One of these assembles about a centre of inversion by the familiar four-membered {···Se–O}$_2$ synthon. Attached to either side of this aggregate are two of the second independent molecules whereby each selenium of each of the terminal molecules effectively bridges the oxo atom, already engaged in a Se···O contact implying this atom is bifurcated, and an alkoxide-oxygen atom of the O,O-chelating ligand, Fig. 5h. The tetrameric aggregate in **48**, Fig. 5i, has the same centrosymmetric {Se···O}$_2$ core but, the terminal connections are also of the type {Se···O}$_2$, also formed by the second independent molecules. This compound is of particular interest as the asymmetric unit comprises four independent molecules. Two engage as shown in Fig. 5i, while the other two engage to form a supramolecular chain as discussed below, see **175** [113]. The last two selenium(IV) aggregates to be described are hexameric.

In the crystal of **49** [114], three independent molecules comprise the asymmetric unit. A hexagon of selenium atoms, with a pronounced chair conformation, is formed about a centre of inversion, with the connections between them being of the type Se···O (oxide), Fig. 5j. In this scheme, two of the independent molecules associate via the four-membered {···Se–O}$_2$ synthon with two of these bridged by two of the third independent molecules. Thus, two of the selenium atom forms two Se···O(oxide) contacts and four make a single Se···O(oxide) contact. In terms of the oxide donors, two form two Se···O(oxide) contacts and the remaining four oxide-oxygen atoms participate in a single contact, indicating the hexamer is sustained by eight Se···O(oxide) interactions in all. A related situation pertains for the hexamer formed in the crystal

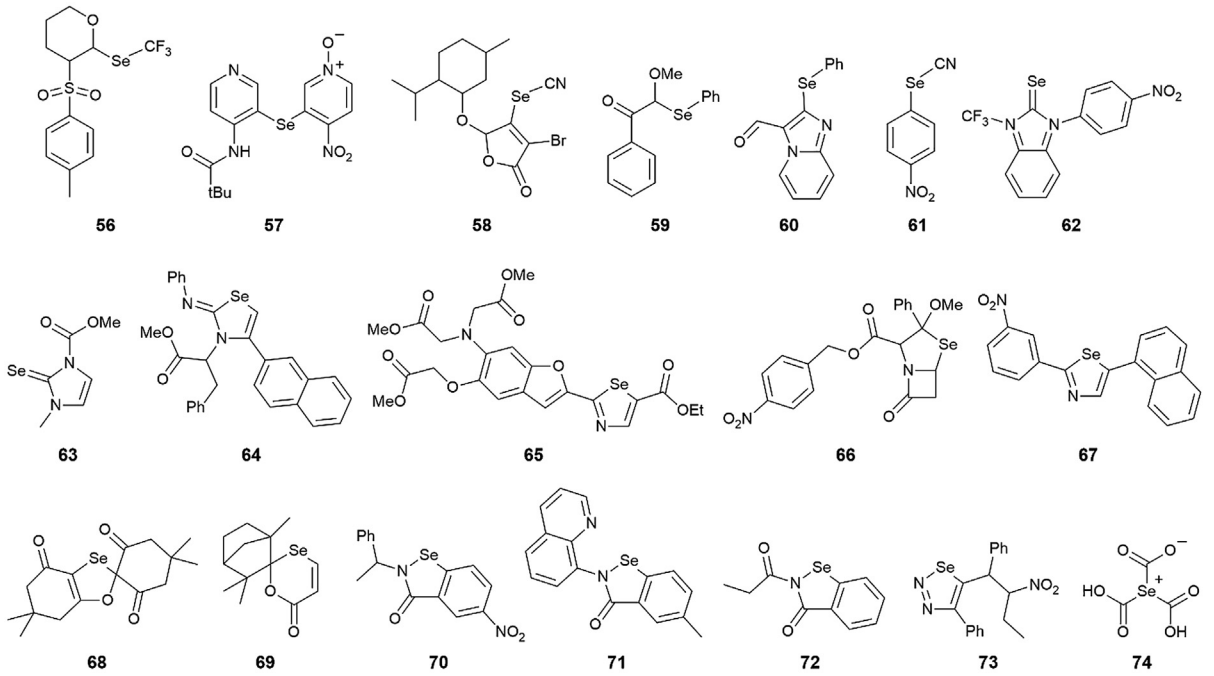

Fig. 6. Chemical diagrams for the interacting species, **56**–**74**, in selenium(II) crystals featuring Se···O contacts leading to linear one-dimensional aggregates.

of **50** [115], Fig. 5k. The core and asymmetry in the hexamer comprising **50** is as descried for **49**. However, in the case of **50**, there are two independent and linked {···Se–O}$_2$ synthons which are bridged over the centre of inversion via a pair of Se···O(oxide) interactions. So, four of the selenium atoms form two Se···O(oxide) contacts and two make a single Se···O(oxide) contact, leading to a total of 10 Se···O(oxide) contacts sustaining the hexamer.

3.2.3. Aggregates of selenium(VI) species sustained by Se···O contacts

There are five selenium(VI) species featuring Se…O interactions, each leading to a centrosymmetric, dimeric aggregate. Compounds **51** [116], **52** [117], **53** [117] and **54** [118] feature Se(=O)$_2$ entities, while that of **55** [119] is an adduct of Se(=O)$_3$. A {···Se–O}$_2$ core is found in each of the five dimers. In diorgano **51**, the selenium atom is incorporated within a six-membered ring, Fig. 5l. Two species feature CNO_2 coordination geometries, i.e. **52** and **53**, Fig. 5m. An O,O-chelating ligand, leading to a five-membered ring, is seen in **54**, Fig. 5n. In the only example of a molecule based on Se(=O)$_3$ core is the ether adduct, **55**, Fig. 5o.

4. One-dimensional assembles mediated by Se···O chalcogen bonding

The most numerous among the supramolecular aggregation patterns described herein are one-dimensional chains. In all, 125 structures fall in this category, being over half of all examples included in this survey. The following description is based on the oxidation state of the selenium atom forming the Se···O chalcogen bonding contact, the nuclearity of the molecule and the topology of the resultant chain, i.e. linear, zig-zag, helical and twisted.

4.1. Mono-nuclear selenium(II) species forming linear supramolecular chains

The chemical diagrams of the 19 mono-nuclear selenium(II) molecules aggregating to form linear supramolecular chains in their crystals based on Se···O chalcogen bonding contacts, i.e. **56**–**74** [12,120–137], are shown in Fig. 6.

A variety of selenium(II) and oxygen atom environments participate in Se···O contacts leading to linear, one-dimensional chains. The first six molecules have the common feature that they are diorganoselenium(II) species with the selenium atom not enclosed within a ring. Fig. 7a shows the formation of Se···O(ether) contacts giving rise to the chain in the crystal of **56** [120]. Molecules **57** [121], **58** [122], **59** [123] and **60** [124] employ carbonyl-oxygen atoms in the chalcogen bonding interaction. As seen in Fig. 7b for **57**, Se···O(carbonyl) interactions form in preference to putative Se···O(N-oxo, nitro) contacts. A similar situation pertains in **58** where bromide, cyano-nitrogen and two kinds of ether-oxygen atoms are available for secondary bonding interactions. The presence of Se···O(nitro) interactions are responsible for chain formation in the crystal of **61** [11], Fig. 7c. In **62** [125], Fig. 7d, Se···O (nitro) interactions are also formed. The interacting selenium atom in **62** is a rare example of a selenide forming Se···O interactions, as is the case for **63** [126], which forms Se···O(methoxy) contacts.

The selenium atom is incorporated within a five-membered ring and is flanked by two carbon atoms in five molecules: **64** [127], **65** [128], **66** [129], **67** [130] and **68** [131]. The Se···O(carbonyl) contacts in the chain formed by **64** are highlighted in Fig. 7e. The structure of **64** is notable as two independent molecules comprise the asymmetric unit and each self-assembles into a linear supramolecular chain. A similar mode association is found in the crystal of **68**, where each of the two independent molecules self-associate into a linear chain. By contrast, in **65**–**67** the Se···O association involves ether-, methoxy- and nitro-oxygen atoms. In **69** [132], the selenium atom is incorporated within a six-membered ring and molecules assemble via Se···O(carbonyl) contacts, Fig. 7f. In each of the four remaining five-membered ring-containing molecules, the selenium atom is flanked by carbon and nitrogen atoms. In **70** [133], **71** [134] and **72** [135], Fig. 7g, the molecules are linked by Se···O(carbonyl) interactions whereas in **73** [136], Fig. 7h, Se···O(nitro) contacts are evident. The last structure is this category to be described is that of **74** [137] where the selenium atom formally carries a positive charge and one of three carboxylic acid substituents is deprotonated. As seen from Fig. 7i, the linear chain is sustained by Se···O(carbonyl)

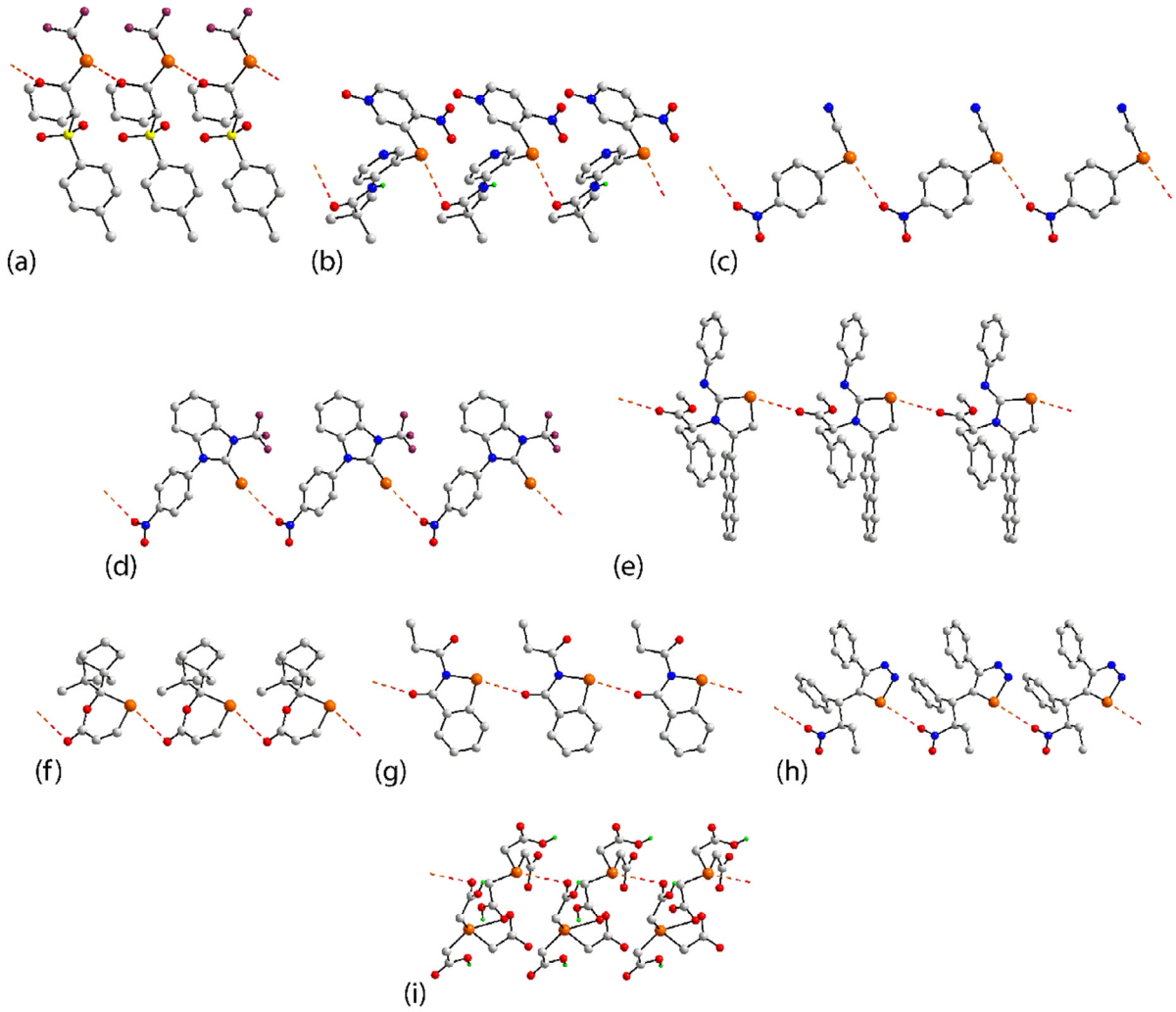

Fig. 7. Representative examples of supramolecular association in selenium(II) crystals leading to linear, one-dimensional chains based on Se···O chalcogen bonding interactions: (a) **56** [120; Se···O = 3.08 Å], (b) **57** [121; 3.12 Å], (c) **61** [11; 3.29 Å], (d) **62** [125; 3.29 Å], (e) **64** [128; 3.09 Å], (f) **69** [132; 3.39 Å], (g) **72** [135; 3.19 Å], (h) **73** [136; 3.19 Å] and (i) **74** [137; 3.21 Å].

interactions; the carboxylate residue is engaged in charge-assisted hydrogen bonding, precluding it from participating in Se···O contacts.

4.2. Mono-nuclear selenium(II) species forming zig-zag supramolecular chains

The chemical diagrams of the 32 mono-nuclear selenium(II) molecules, i.e. **75**–**106** [11, 74,101,133, 138–162], forming zig-zag supramolecular chains in their crystals based on Se···O chalcogen bonding contacts are shown in Fig. 8. With two exceptions, as detailed below, the zig-zag chains are propagated by crystallographic glide symmetry.

Seven compounds have the selenium atom not constrained within a ring while the remaining 25 feature cyclised selenium, usually within a five-membered ring. A representative example of a zig-zag chain is shown in Fig. 9a, for **75** [138]. Here, Se···O(carbonyl) interactions are in play, as in crystals of **76** [139] and **77** [140]. In **78** [141], Fig. 7b, an example rich in heteroatoms, Se···O(-sulphoxide) interactions are evident, as they are in **79** [142], Fig. 9c, with a rare C,S-donor set for selenium. The structures of **80** [143] and **81** [144] are examples of selenides are engaged in Se···O interactions. In **80**, there are two independent molecules in the asymmetric unit and each of these self-associates into a supramolecular chain via C═Se···O(nitro) interactions, one of these is shown in Fig. 9d. In **81**, where the selenide is phosphorus-bound, the zig-zag chain, Fig. 9e, arises as a result of P═S···O(ether) contacts. The remaining molecules to be covered have the selenium atom incorporated with a ring.

In the next six molecules, each selenium(II) atom has a C,C-donor set. The selenium atom in **82** [74] forms part of a four-membered ring and the molecules assemble into a zig-zag chain via Se···O(sulphoxide) contacts, Fig. 9f. The chains in **83** [145] are sustained by Se···O(methoxy) interactions, and in **84** [146], **85** [101], **86** [147] and **87** [148] by Se···O(carbonyl) interactions. Compound **85**, Fig. 9g, is one of two molecules in this section assembling into a zig-zag chain not propagated by glide symmetry. In this case, there are two independent molecules which associate to form the supramolecular chain.

Next, is a series of molecules constructed about a 5-selanylidene-1H-pyrrol-2-one core, i.e. **88**–**99** [11,149–157], featuring a variety of substituents, R, at the nitrogen atom: R = CH_2Ph (**88**) [149], Ph, polymorphs **89** [11] and **90** [150], Ph-C(=O)OH-4 (**91**) [151], Ph-Br-4 (**92**) [152], Me (**93**) [153], H, acid **94** [152], Ph-Br-2 (**95**) [154], Ph-Me-3 (**96**) [155], Ph-Me-2 (**97**) [156], Ph-OH-3 (**98**) [11] and, lastly, R = a fused 1-ethylpiperidine-2,6-dione/naphthalene derivative (**99**) [157]. The common mode of the supramolecular association is the formation of Se···O(carbonyl)

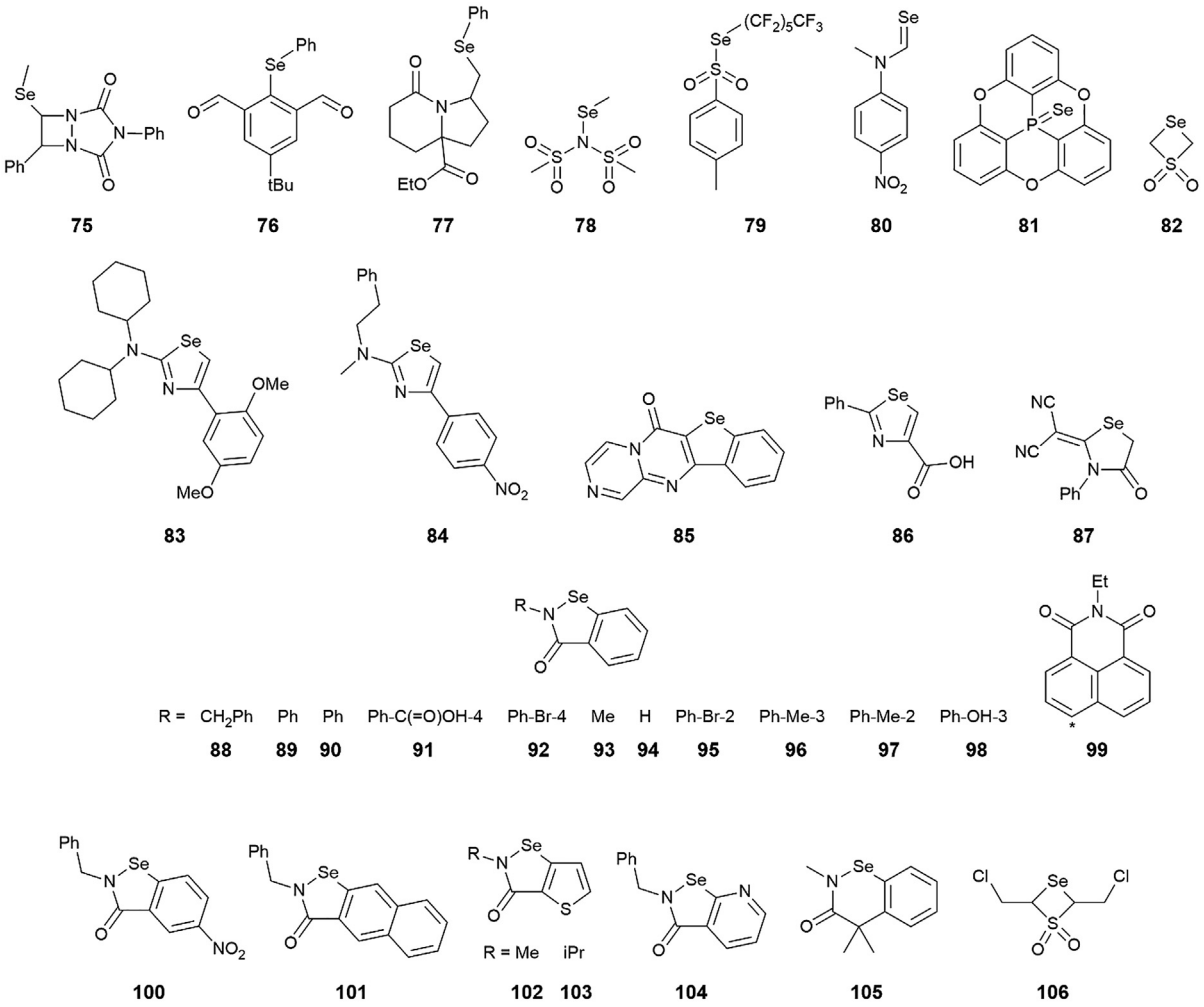

Fig. 8. Chemical diagrams for the interacting species, **75**–**106**, in selenium(II) crystals featuring Se···O contacts leading to zig-zag one-dimensional chains. The point of attachment at the nitrogen atom in **99** is indicated by an asterisk.

interactions, as illustrated for **95** [154] in Fig. 9h. Generally, these contacts are short, ranging from 2.53 Å in **88** [149] to 2.86 Å for **99** [157], suggesting considerable covalent character in these secondary bonding interactions. As indicated above, **89** and **90** are polymorphs. These exhibit the same supramolecular aggregation via Se···O(carbonyl) interactions with very similar Se···O separations of 2.53 and 2.57 Å, respectively. Of interest is the R = H derivative, **94**, i.e. the acid form, where three independent molecules comprise the asymmetric unit. One molecule self-assembles into a zig-zag chain (glide symmetry). The two other molecules associate via a Se···O(carbonyl) interaction and the resultant dimeric aggregates assemble into a zig-zag chain, again propagated by glide symmetry. Variations of the above are seen in **100** [133], where the fused C_6 ring carries a nitro substituent, and **101** [158], where the fused C_6 ring is fused to a second C_6 ring, and in **102** and **103** [159], where the fused C_6 ring is substituted by a thienyl ring; each of the resultant zig-zag chains are sustained by Se···O(carbonyl) interactions. The Se···O(carbonyl) interactions persist in **104** [160], where the fused C_6 ring of the above examples is now a pyridyl ring and **105** [161], where the selenium atom is incorporated into a six-membered ring. The final molecule in this section, **106** [162], Fig. 9i, is notable in that the selenium atom, embedded within a four-membered ring, forms two Se···O(sulphoxide) interactions to sustain the zig-zag chain.

4.3. Mono-nuclear selenium(II) species forming helical and twisted supramolecular chains

The chemical diagrams of the mono-nuclear selenium(II) molecules, i.e. **107**–**123** [152,163–177] and **124**–**126** [159,178,179], forming, respectively, helical and twisted supramolecular chains in their crystals based on Se···O chalcogen bonding contacts are shown in Fig. 10.

The supramolecular chains with helical symmetry are typically propagated by crystallographic 2_1 screw symmetry, with two exceptions only, and, while less numerous than zig-zag supramolecular chains sustained by Se···O interactions, comprise 17 examples. Six of the molecules do not have selenium incorporated within a ring, and four of these have selenium within a C_2-donor set: **107** [163], **108** [164], **109** [165], Fig. 10a, and **110** [166], and two of the examples are selenides **111** [167] and **112** [168], Fig. 11b. Highlighting the diversity of oxygen-donors in these chains, in **107** and **109** they feature Se···O(carbonyl) contacts, **108** Se···(methoxy), **110** Se···O(sulphoxide), **111** Se···O(hydroxyl) and the chains in **112** are sustained by Se···O(ether) interactions. The remaining helical structures feature cyclised selenium atoms. The five-membered rings in **113** [169], **114** [170] and **115** [171] also feature C_2 donor sets as does the selenium atom in **116** [172], Fig. 11c, which is now incorporated within a six-membered ring. The donor atoms forming the Se···O interactions

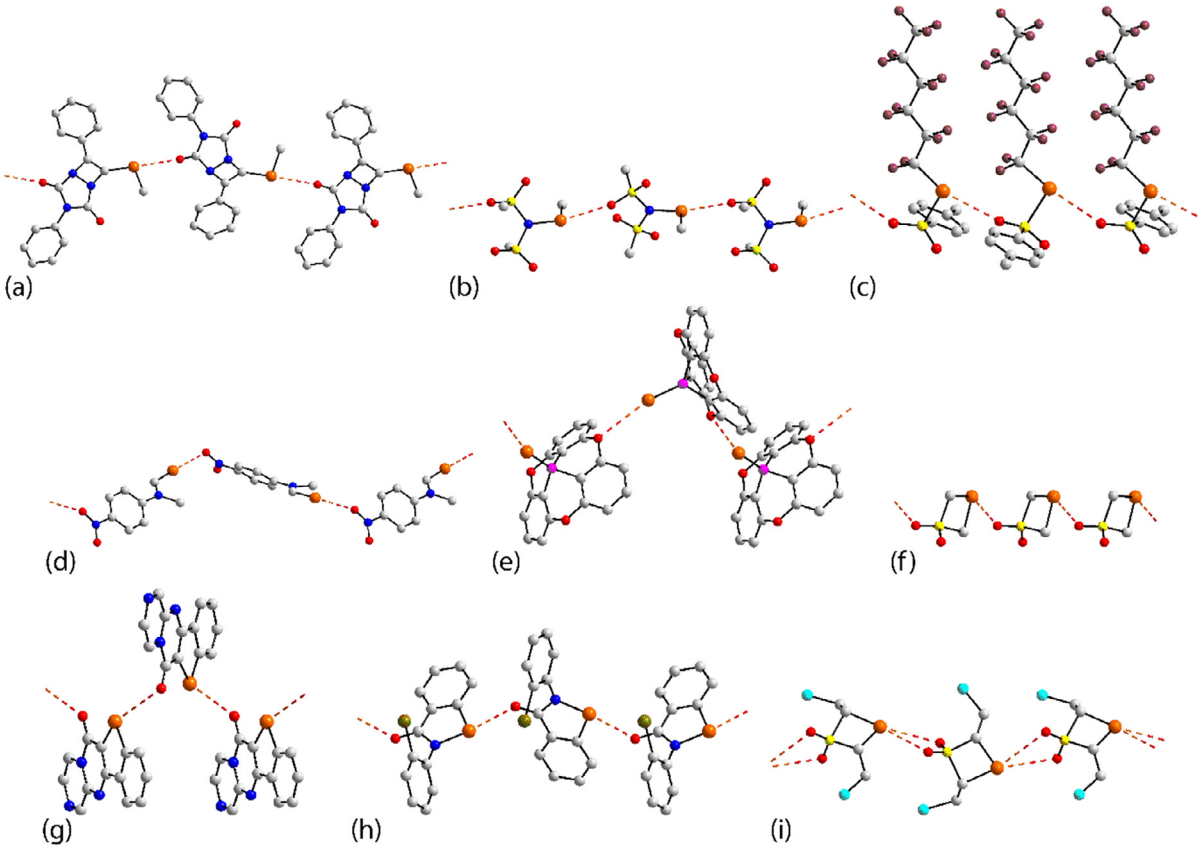

Fig. 9. Representative examples of supramolecular association in selenium(II) crystals leading to linear, one-dimensional chains based on Se···O chalcogen bonding interactions: (a) **75** [138; Se···O = 3.05 Å], (b) **77** [140; 3.06 Å], (c) **78** [141; 3.16 Å], (d) **80** [143; 3.12 Å], (e) **81** [144; 3.41 Å], (f) **82** [74; 3.05 Å], (g) **85** [101; 3.36 Å], (h) **95** [154; 2.67 Å] and (i) **106** [162; 3.29 & 3.35 Å].

are hydroxyl in **113** but, carbonyl in **114**–**116**; in **114**, both ether and hydroxyl donors are available but not employed in Se···O contacts. The remaining ring structures contain hetero-atoms, all having at least one nitrogen atom, with two exceptions. In **117** [173], the helical chain is sustained by a charge-assisted Se···O(N-oxo) interaction with the separation being a short 2.41 Å. Molecules **118** [152], **119** [174], **120** [152] and **121** [175] all feature the 5-selanylidene-1H-pyrrol-2-one core, as seen above in the sequence of molecules **88**–**99**. The chains in **118** and **120** are sustained by Se···O(hydroxyl) interaction despite having potential carbonyl donors, whereas the chains in **119** and **121** feature Se···O(carbonyl) interactions. It is noted that **118** has two polymorphs: in **5**, Fig. 3a, the two independent molecules of the asymmetric unit assemble by a single Se···O(carbonyl) interaction and in second polymorph, **98**, molecules assemble into a zig-zag chain, but via Se···O(hydroxyl) interactions as in **118**. The helical chain formed in **119** is especially noteworthy in that rather than the usually observed 2_1 symmetry, the chain is propagated by crystallographic 6_1 screw symmetry, Fig. 11d. In **122** [176], where there are two nitrogen atoms in the ring, flanking the selenium atom, the helical chain is sustained by Se···O(carbonyl) interactions, Fig. 11e. The supramolecular aggregation in **123** [177] is quite unusual, featuring three distinct Se···O contacts for the selenium atoms derived from the two independent molecules comprising the asymmetric unit. As viewed from Fig. 11f, one selenium atom forms a single contact with a nitro-oxygen atom while the other selenium atom spans the two oxygen atoms of a symmetry related five-membered ring. The shortest Se···O contact of 2.90 Å in the chain is associated with the Se···O(carbonyl) interaction. The other unusual feature of the resulting supramolecular chain is that it is propagated by crystallographic 4_1 screw symmetry.

There are three molecules, **124** [159], **125** [178] and **126** [179], assembling in their crystals to form twisted chains. In **124**, Fig. 10g, and **125**, two independent molecules comprise the asymmetric unit with the twisted arrangement arising due to the relative orientations of the independent molecules in the chains propagated by translational symmetry; chains are sustained by Se···O(carbonyl) contacts. The molecule in **126**, Fig. 10h, has crystallographic two-fold symmetry with the selenium atom lying on the axis. Each selenium atom forms two Se···O(nitro) contacts with centrosymmetrically related molecules.

4.4. Multi-nuclear selenium(II) species forming supramolecular chains

Most of the molecules in this category are bi-nuclear but, there are several examples of tri- and tetra-nuclear selenium(II) compounds. The chemical structures for the molecules forming the supramolecular chains, i.e. **127**–**159** [80,92,95,104,180–205], are shown in Fig. 12.

4.4.1. Bi-nuclear selenium(II) species forming linear chains

A linear chain is observed in crystals of **127** [180], Fig. 13a, an example whereby the selenium atom is not embedded within a ring and where only one of the selenium atoms is engaged in a Se···O contact; in this case the donor is a carbonyl-oxygen atom. When embedded within a five-membered ring, the selenium atoms can be next to each other as in **128** [181] and **129** [182], Fig. 13b, or in a six-membered ring, i.e. **130** [183]. Again, only

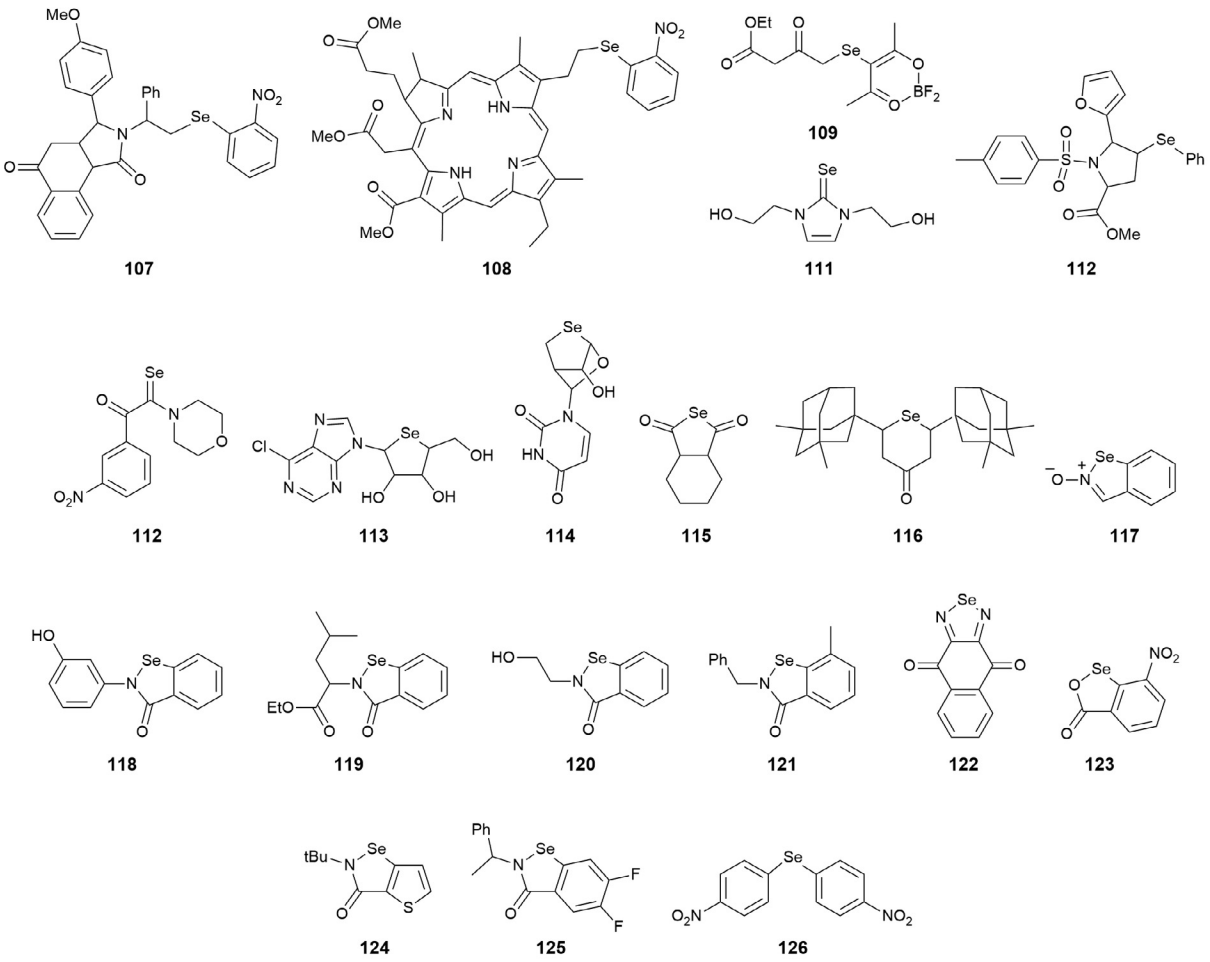

Fig. 10. Chemical diagrams for the interacting species, **107**–**123**, in selenium(II) crystals featuring Se···O contacts leading to helical one-dimensional chains, and **124**–**126**, leading to twisted chains.

one of the selenium atoms in **128**–**130** forms a Se···O contact, with the donors being ether-, sulphoxide- and carbonyl-oxygen, respectively. The structure of **129** is especially noteworthy in that two molecules comprise the asymmetric unit, and these possess amide donors capable of forming hydrogen bonding interactions. One of the independent molecules forms a supramolecular chain, as just mentioned, and these are connected into a double-chain by conventional amide-N–H···O(sulphoxide) hydrogen bonds involving the same sulphoxide-oxygen atom forming the Se···O contacts. The second independent molecule also forms a supramolecular chain but, mediated solely by amide-N–H···O(sulphoxide) hydrogen bonds, there being no Se···O interactions of note. The adoption of Se···O and/or amide-N–H···O(sulphoxide) hydrogen bonds suggests, at least to a first approximation, some equivalence in the energies of stabilisation afforded by these modes of association. In **131** [184], the association leading to a linear chain involves both selenium atoms connecting to the carbonyl-oxygen atom of a translationally related molecule, Fig. 13c. A double-chain is noted for **132** [185], Fig. 13d. Here, two selenium atoms occur diagonally opposite positions in a centrosymmetric C_2Se_2 square, and each forms a Se···O(carbonyl) interaction to form a linear chain. Two independent molecules also comprise the asymmetric unit of **133** [186]. One of these self-associates into a linear chain via Se···O(sulphoxide) contacts whereby one selenium atom forms two contacts with translationally related molecules leading to seven-membered {···Se···OSSeSeSO} synthons. Centrosymmetrically related chains assemble into a double-chain, also via Se···O(sulphoxide) contacts, but involving the second selenium atom (forming the shortest Se···O contact) and six-membered $\{\cdots OSSe\}_2$ synthons, as shown in the views of Fig. 13e.

4.4.2. Bi-nuclear selenium(II) species forming zig-zag chains

Four molecules of the general formula RSeSeR form supramolecular zig-zag chains in their crystals; these along with the other chains described in this section are propagated by glide symmetry. These are sustained by an average of one Se···O(sulphoxide) contact per molecule in **134** [186], Fig. 13f, Se···O(nitro) in **135** [187] and Se···O(carbonyl) in each of **136** [188] and **137** [189]. A variation is noted for **138** [95], Fig. 13g, where the selenium atoms are connected by an oxo-bridge and one of these forms Se···O(nitro) contacts. The selenium atoms are adjacent to each other in the five-membered ring of **139** [190] and one of these participates in Se···O(sulphoxide) interactions to form the zig-zag chain. In the five-membered rings of each of **140** [191] and **141** [192], Fig. 13h, the selenium atoms are separated by a carbon atom, and the chain is mediated by Se···O(carbonyl) interactions. In **142** [80], Se···O(hydroxyl) interactions involving the ring-bound selenium atom mediate the formation of the zig-zag chain rather than putative interactions involving the phosphorus-bound selenide atom. A variation in the general theme of one Se···O link per molecule to sustain the zig-zag chain is noted for **143** and **144** [190], Fig. 13i, where each selenium atom, occupying adjacent positions in a five-membered ring, participates in Se···O(sulphoxide) interactions with the same sulphoxide-oxygen atom.

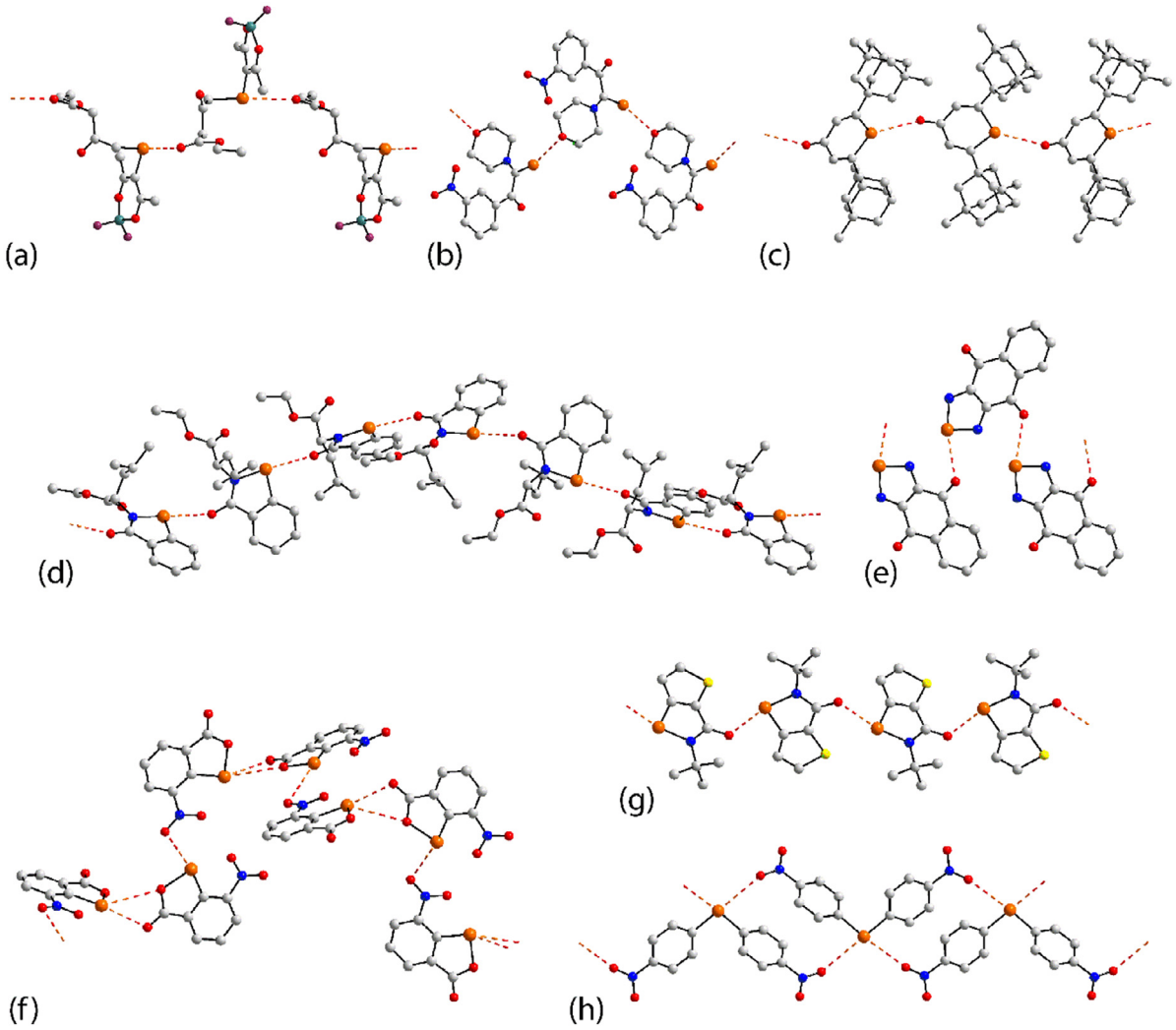

Fig. 11. Representative examples of supramolecular association in selenium(II) crystals leading to helical, one-dimensional chains based on Se···O chalcogen bonding interactions: (a) **109** [165; Se···O = 3.04 Å], (b) **112** [168; 3.39 Å], (c) **116** [172; 3.18 Å], (d) **119** [174; 2.83 Å], (e) **122** [176; 2.95 Å], (f) **123** [177; 2.90, 3.30 & 3.38 Å], (g) **124** [159; 2.55 Å] and (h) **126** [179; 3.26 Å]. Additional colour code: teal, boron.

4.4.3. Bi-nuclear selenium(II) species forming helical chains

The common feature of the seven helical chains formed by bi-nuclear selenium(II) molecules is that each is propagated by 2_1 screw symmetry. The first six molecules employ a single selenium atom in forming the Se···O chalcogen bond: **145**, **146** [193], Fig. 14a, **147** [194], **148** [195], **149** [196] and **150** [197]. The oxygen donors span a range of types, i.e. sulphoxide (**145** and **146**), ether (**147**) and carbonyl (**148** and **150**) and phenoxide (**149**). In **151** [198], Fig. 14b, the adjacent selenium atoms are embedded within a five-membered ring and form contacts to the same carbonyl-oxygen atom to form the helical chain, i.e. bearing a close resemblance to the aggregation pattern seen in **143** and **144**, Fig. 13i. The bi-nuclear molecule in **152** [199], has two-fold symmetry with the axis bisecting the Se–Se bond, and each selenium atom forms a Se···O(nitro) contact to a centrosymmetrically related molecule with the result a twisted chain ensues, Fig. 14c.

4.4.4. Multi-nuclear selenium(II) species forming chains of various topologies

There are two tri-nuclear selenium(II) species forming supramolecular chains in their crystals. As a result of Se···O(carbonyl) interactions whereby two of the three selenium atoms, each within a five-membered ring, form a contact to the same carbonyl-oxygen atom, a linear chain is formed in the crystal of **153** [152], Fig. 14d. In **154** [200], where there is an "open" selenium atom and two selenium atoms within five-membered rings, it is the former that forms a Se···O(ether) contact to generate a zig-zag chain via glide symmetry, Fig. 14e.

The remaining five selenium(II)-containing species in this section are tetra-nuclear. In **155** [201], two five-membered rings, each with a 1,3-disposition of selenium atoms, are connected to form the tetra-nuclear molecule. In the crystal, only one of the selenium atoms forms a Se···O(carbonyl) interaction with translationally related molecules so that a linear chain is formed, Fig. 14f. The macrocyclic compound, **156** [202], employs two of its selenium atoms to sustain a linear assembly via Se···(methoxy) interactions and eight-membered $\{\cdots SeC_2O\}_2$ synthons, Fig. 14g. The molecule **157** [203] is clearly related to **155** but, in this case, this assembles into a zig-zag chain (glide symmetry), Fig. 14h. The remaining molecules, **158** [204], and **159** [205], assemble into helical chains, for **158**, Fig. 14i, propagated by 2_1 screw symmetry. An interesting variation is noted for **159** in that the four selenium atoms line up in a chain within an eight-membered ring; two independent molecules comprise the asymmetric unit. The independent molecules assemble via a Se···O(carbonyl) contact and the resultant dimeric aggregate then assembles, via additional Se···O(carbonyl) contacts,

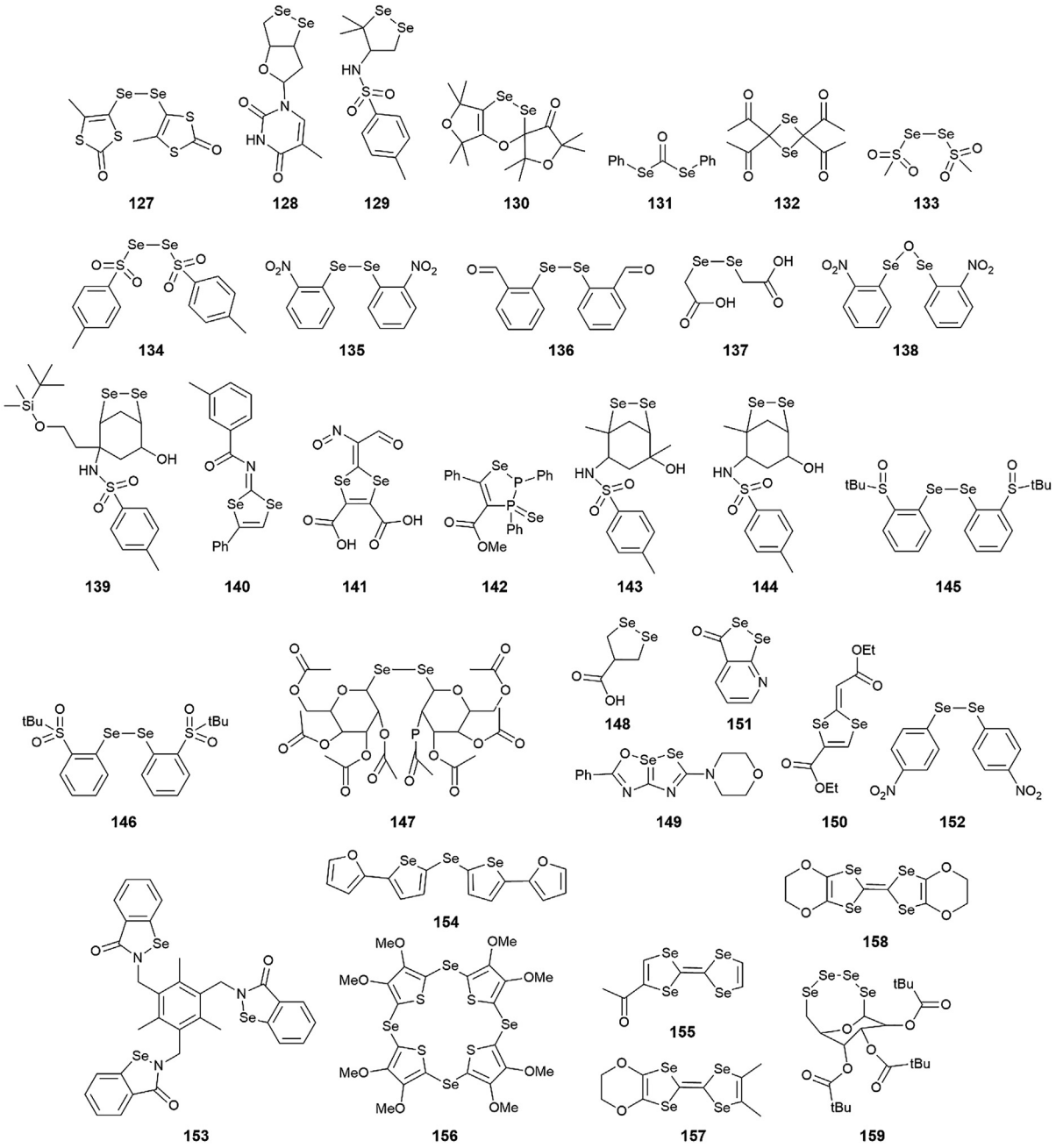

Fig. 12. Chemical diagrams for the interacting species, **127**–**159** [80,95,152,159,180–205], in multi-nuclear selenium(II) crystals featuring Se···O contacts leading to supramolecular one-dimensional chains.

into a supramolecular helical chain propagated by 3_1 screw symmetry, Fig. 14j.

4.5. Multi-nuclear selenium(IV) species forming supramolecular chains

While far less represented than their selenium(II) counterparts, there are 21 examples of selenium(IV) compounds, usually selenoxide derivatives, self-associating in their crystals to form one-dimensional chains via Se···O chalcogen bonding. The chemical diagrams for these species, i.e. **160**–**180** [93,104,105,113,188,206–217], are shown in Fig. 15.

The three selenoxides, **160** [104], **161** [104] and **162** [206], Fig. 16a, feature C_2O-donor sets and associate in their crystals to form linear, supramolecular chains via Se···O(nitro) interactions in **160**, and Se···O(methoxy) interactions in **161** and **162**. Double-chains are often observed in the crystals of the selenium(IV) compounds in this category owing to the formation of multiple Se···O interactions. This is exemplified by **163** [207], Fig. 16b. Here, centrosymmetrically related molecules are connected by a pair of Se···O(oxide) interactions, leading to a $\{\cdots Se–O\}_2$ core, and the resultant dimeric aggregates assemble into a linear, double-chain so each selenium atom forms two Se···O contacts. Similar patterns are noted in **164** [208], Fig. 16c, and **165** [209] but, with the bridges leading to the chains being interactions of the type Se···O(nitro); in **164**, the Se···O(carbonyl) separations are shorter than the Se···O(nitro) contacts whereas the opposite trend pertains in **165**, underscoring the difficulty of correlating distances associated with weak interactions as discussed in section 8. In **166** [210], Fig. 16d, with a chelating O,O-ligand leading to a five-membered ring, the double-chain arises as the successive, centrosymmetri-

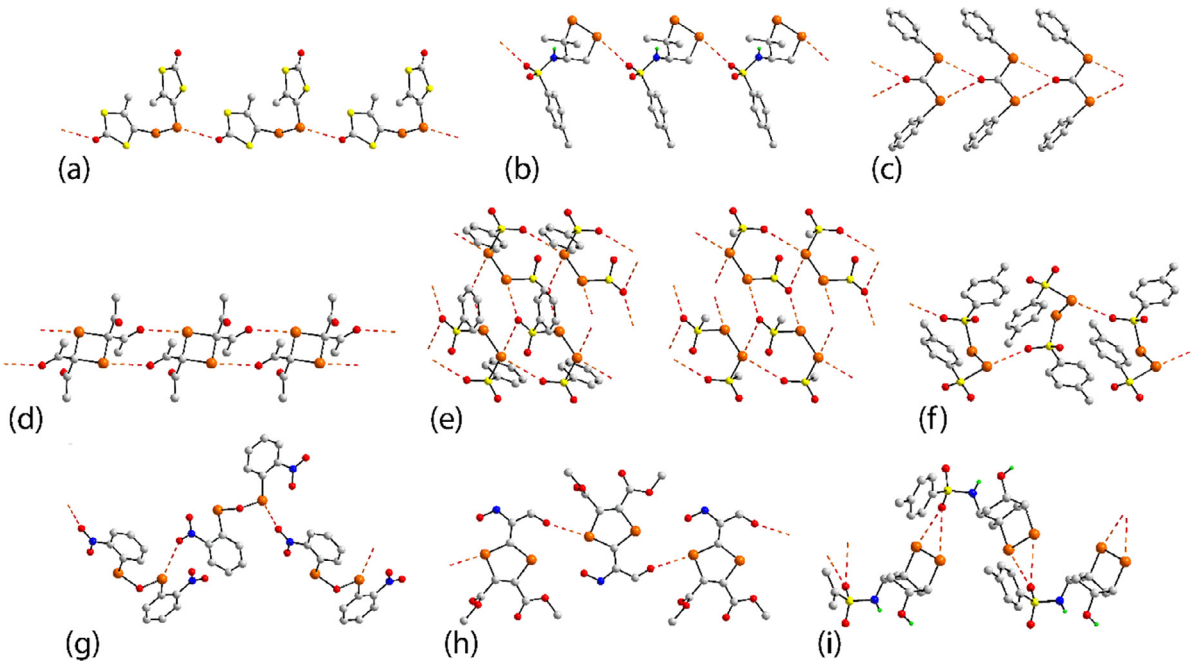

Fig. 13. Representative examples of supramolecular association in selenium(II) crystals leading to one-dimensional chains of varying topology on Se···O chalcogen bonding interactions: (a) **127** [180; Se···O = 3.29 Å], (b) **129** [182; 3.22 Å], (c) **131** [184; 3.35 Å], (d) **132** [185; 3.04 Å], (e) **133** and view with only *ipso*-carbon atoms [186; 3.09, 3.37 & 3.35 Å], (f) **134** [186; 3.03 Å], (g) **138** [95; 3.25 Å], (h) **141** [192; 3.05 Å] and (i) **144** [190; 3.18 & 3.36 Å].

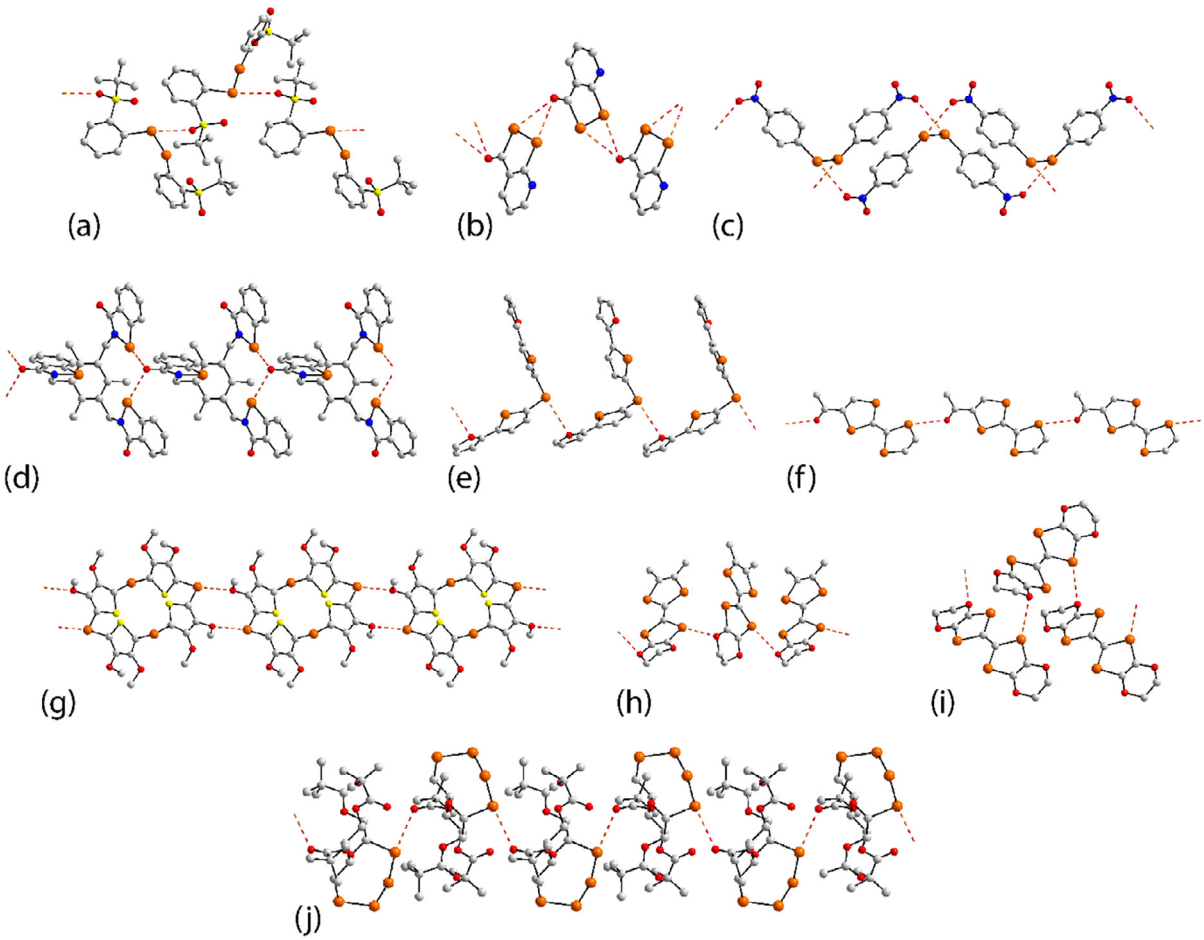

Fig. 14. Representative examples of supramolecular association in multi-nuclear selenium(II) crystals leading to one-dimensional chains of varying topology based on Se···O chalcogen bonding interactions: (a) **146** [193; Se···O = 3.19 Å], (b) **151** [198; 3.24 & 3.24 Å], (c) **152** [199; 3.22 Å], (d) **153** [152; 2.99 & 3.12 Å], (e) **154** [200; 3.34 Å], (f) **155** [201; 3.22 Å], (g) **156** [202; 3.03 Å], (h) **157** [203; 3.13 Å], (i) **158** [204; 3.35 Å] and (j) **159** [205; 3.16 & 3.17 Å].

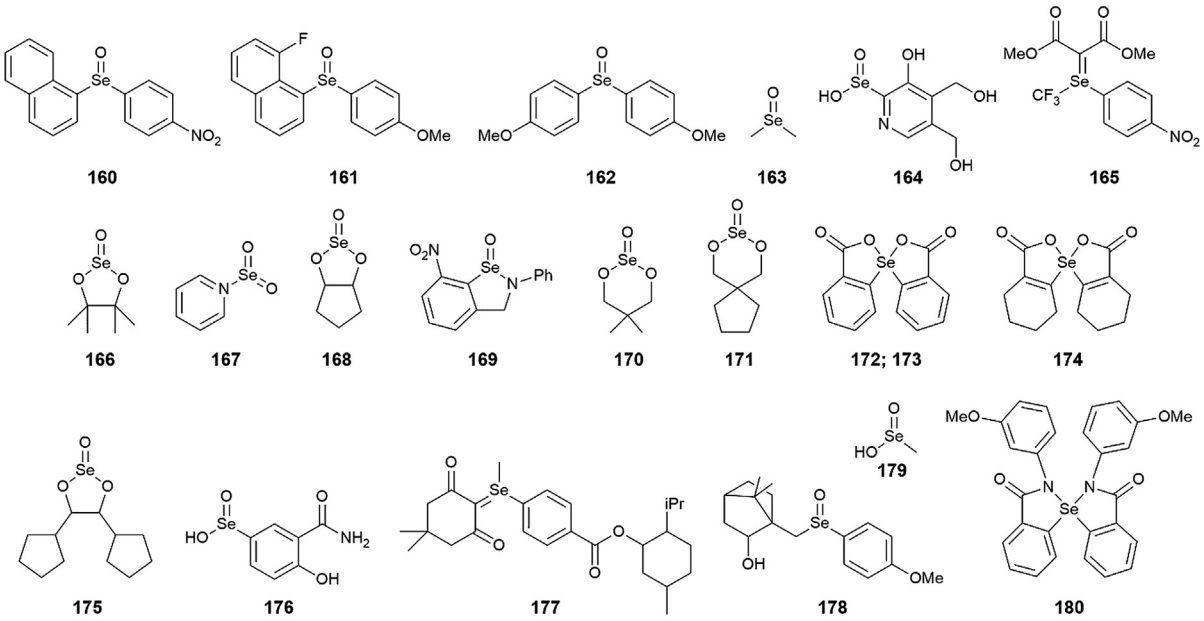

Fig. 15. Chemical diagrams for the interacting species, **160**–**180**, in selenium(IV) crystals featuring Se···O contacts leading to supramolecular one-dimensional chains.

cally related aggregates are connected by Se···O(alkoxide) interactions. In the dioxide species, **167** [211], Fig. 16e, the centrosymmetric aggregates are connected to translationally related dimers via a pair of Se···O(oxide) contacts so each selenium atom participates in three Se···O interactions. A more complicated mode of association between molecules occurs in **168** [113], Fig. 16f, for which two independent molecules comprise the asymmetric unit. One of the independent molecules assembles to form a dimer and translationally related dimers are bridged by a pair of the second independent molecule. There are six independent Se···O contacts involving oxide- (4) and alkoxide-oxygen (2) donors, and each selenium atom participates in three Se···O interactions.

Molecules **169** [93], **170** [113], Fig. 16g, and **171** [113], each with C_2O donor sets, assemble into zig-zag chains mediated by a

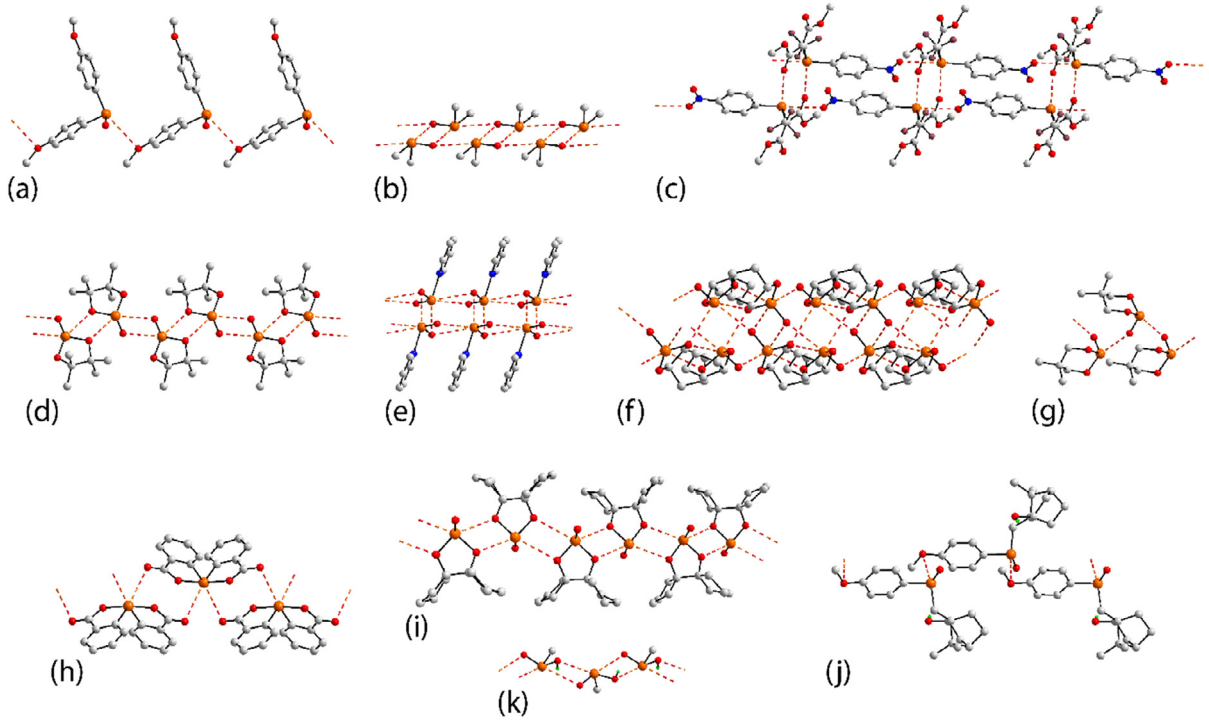

Fig. 16. Representative examples of supramolecular association in multi-nuclear selenium(II) crystals leading to one-dimensional chains of varying topology based on Se···O chalcogen bonding interactions: (a) **162** [206; Se···O = 3.37 Å], (b) **163** [207; 3.24 & 3.32 Å], (c) **165** [209; 3.14 & 3.22 Å], (d) **166** [210; 2.89 & 2.93 Å], (e) **167** [211; 3.00, 3.26 & 3.29 Å], (f) **168** [113; 2.69–3.20 Å], (g) **170** [113; 2.78 Å], (h) **173** [212; 3.22 Å], (i) **175** [113; 2.84–3.21 Å], (j) **178** [215; 3.40 Å] and (k) **179** [216; 3.16 & 3.31 Å].

single Se···O(oxide) contact in each case. In **171**, two independent molecules comprise the asymmetric unit and these are connected by a single Se···O(oxide) interaction and these dimers then assemble into a zig-zag chain via additional Se···O(oxide) interactions. Compounds **172** [188] and **173** [212], in which the selenium centres are O,O-chelated by two chelating ligands, are polymorphic. In **172**, a single Se···O(carbonyl) interaction, on average, sustains a zig-zag assembly (glide symmetry). By contrast, in **173**, Fig. 16h, the selenium atom lies on a two-fold axis of symmetry and there are, on average two Se···O(carbonyl) interactions per molecule with the Se···O(carbonyl) distance of 3.22 Å being longer than 3.02 Å observed in **172**, as would be expected. The molecule in **174** [213], also has the selenium atom lying on a two-fold axis of symmetry and a similar mode of association as for **173** is noted in its crystal. The supramolecular association **175** [113] is of particular interest. Here, there are four independent molecules in the asymmetric unit and each participates in Se···O contacts. Two of the independent molecules assemble into a tetrameric aggregate via Se···O(oxide) and Se···O(alkoxide) interactions as shown for aggregate **48** [113] in Fig. 5h. In the second assembly found in the crystal of **175**, involving the two remaining independent molecules, only Se···O(alkoxide) interactions are formed leading to a zig-zag chain with each selenium atom forming two Se···O interactions, Fig. 16i.

Helical chains (2_1 screw symmetry) are found in crystals of **176** [105], **177** [214] and **178** [215], Fig. 16j, sustained by either Se···O(carbonyl), **176** and **177**, or Se···O(methoxy), **178**, interactions. A helical chain, also with 2_1 screw symmetry, occurs in the crystal of **179** [216], Fig. 16k, as the selenium atom accepts bond Se···O(oxide) and Se···O(hydroxyl) interactions, rather than the single Se···O interactions of the previous three examples. Finally, in **180** [217] two independent molecules comprise the asymmetric unit and each selenium atom participates in two Se···O(carbonyl) interactions with the chain, propagated by translational symmetry, having a twisted topology owing to the relative orientation of the independent molecules comprising the repeat unit.

5. Two-dimensional assemblies mediated by Se···O chalcogen bonding

When Se···O chalcogen bonding extends in two dimensions, supramolecular layers are formed: this has been noted in a total of 20 crystals, with 12 selenium(II) and eight selenium(IV) examples. The chemical diagrams for **181**–**200** [95,113,133,186,218–231] are shown in Fig. 17.

5.1. Two-dimensional assemblies formed by selenium(II) compounds

Several different motifs are noted in the two-dimensional arrays formed by the compounds in this section. In the crystal of mono-nuclear **181** [218], Fig. 18a, molecules assemble about a centre of inversion, being connected by Se···O(nitro) interactions and eight-membered $\{\cdots Se\cdots ONO\}_2$ synthons. The connections extend laterally as each selenium forms two contacts as does each nitro group, via both oxygen atoms, with the resultant layer being corrugated. The selenium atom also forms two contacts in **182** [219] but, with the same, bifurcated carbonyl-oxygen atom to sustain a flat, hexagonal-like grid, Fig. 18b. In the following structures, disparate Se···O interactions sustain the resulting two-dimensional array. In **183** [220], the selenium atom forms two interactions with carbonyl- and hydroxyl-oxygen atoms, derived from symmetry related molecules, which are linked by a hydroxyl-O–H···O(carbonyl) hydrogen bond. In **184** [133], the connections are of the type Se···O(carbonyl) and Se···O(nitro), and analogous contacts are formed in **185** [221], Fig. 18c. The layers in each of **183**–**185** have a jagged topology. There are two bi-nuclear selenium(II) compounds adopting two-dimensional aggregation patterns. In the first of these, **186** [222], each selenium atom forms a contact to a carbonyl-oxygen atom of two different molecules, Fig. 18d, leading to a flat, hexagonal pattern akin to that for **182**, Fig. 18b. In a variation, in **187** [223], each selenium atom again forms a single contact but, two different carbonyl-oxygen atoms, Fig. 18e, leading to a corrugated topology. A polymorph of **187** exists, i.e. **132**, which

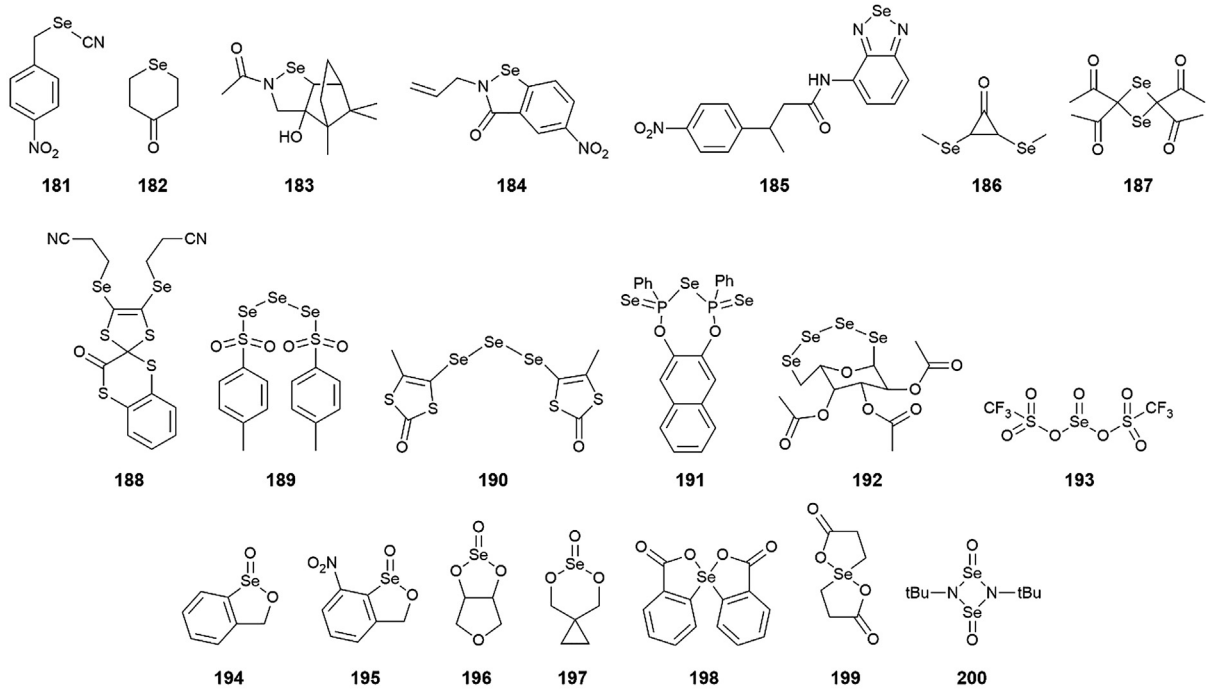

Fig. 17. Chemical diagrams for the interacting species, **181**–**200**, in selenium(II) and selenium(IV) crystals featuring Se···O contacts leading to supramolecular, two-dimensional arrays.

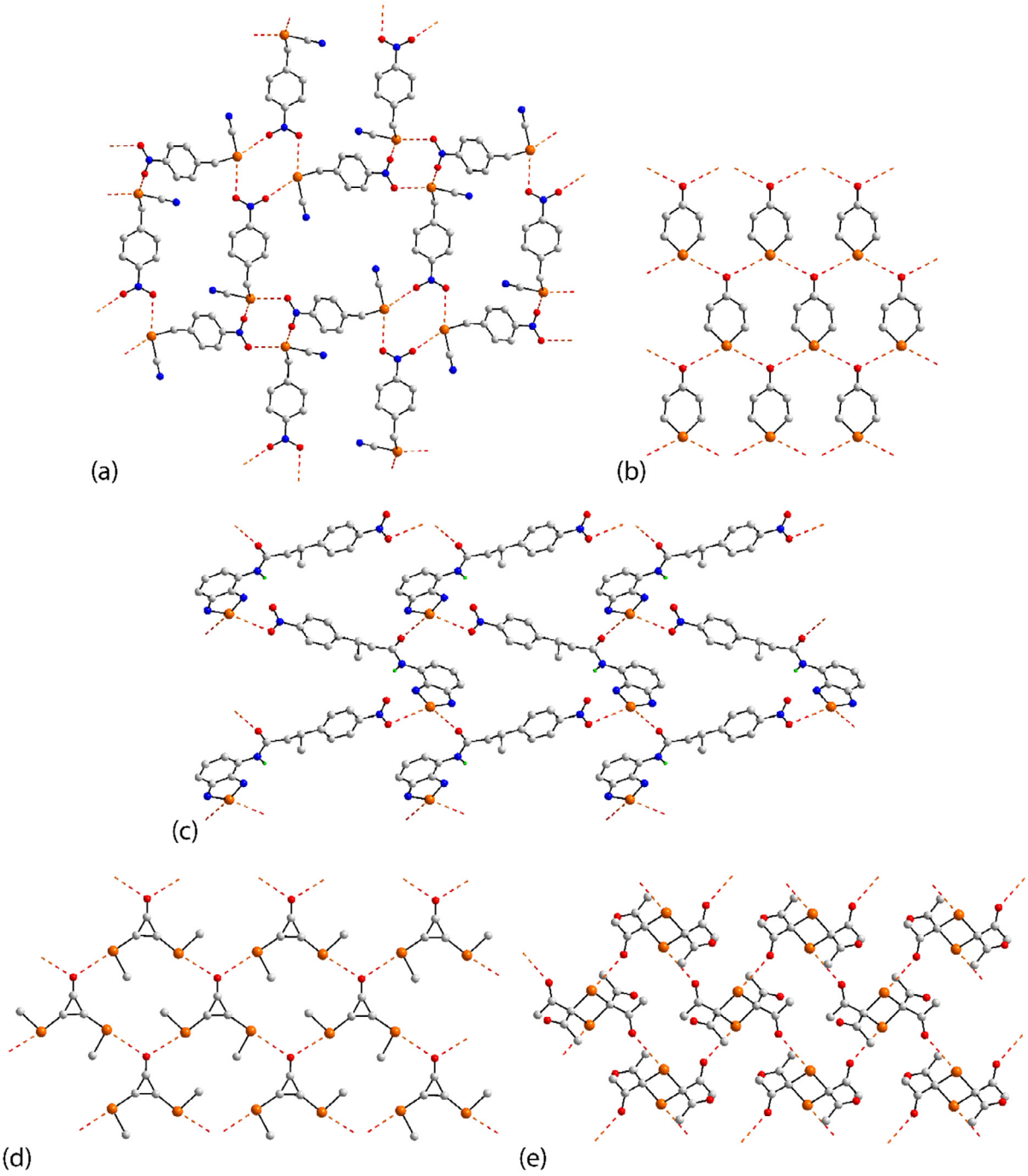

Fig. 18. Examples of supramolecular association in mono- and bi-nuclear selenium(II) crystals leading to two-dimensional arrays based on Se···O chalcogen bonding interactions: (a) **181** [218; Se···O = 3.01 & 3.17 Å], (b) **182** [219; 3.25 Å], (c) **185** [221; 3.06 & 3.16 Å], (d) **186** [222; 3.06 & 3.18 Å] and (e) **187** [223; 3.14 Å].

adopts a linear, one-dimensional chain in its crystal, Fig. 13d, forming the same number of Se···O(carbonyl) interactions. The difference in aggregation patterns arise as in **132**, centrosymmetric, eight-membered $\{\cdots SeC_2O\}_2$ synthons are formed whereas in **187**, the molecules assemble through more open, 16-membered $\{\cdots SeC_2O\}_4$ synthons, Fig. 18e.

Somewhat squarer arrangements are seen in the crystals of bi-nuclear **188** [224], Fig. 19a, where each molecule participates in four Se···O(carbonyl) interactions, with one of the selenium atoms forming two interactions and one of the carbonyl-oxygen atoms forming two interactions; the layer is corrugated. An even more square appearance is seen for **189** [186], Fig. 19b, where the central atom of the tri-nuclear molecule participates in two Se···O(sulphoxide) interactions with two different molecules while at the same time donating two sulphoxide-oxygen atoms to another two symmetry related molecules; the resultant layer is flat. In tri-nuclear **190** [225], which has two-fold symmetry with the central selenium atom lying on the axis, it is the external selenium atoms of the Se_3 chain that each form a single Se···O(carbonyl) interaction and each of the carbonyl-oxygen atoms also participates in a Se···O contact, Fig. 19c, leading to a corrugated layer. In tri-nuclear **191** [226], which has mirror symmetry with the central selenium lying on the plane, the selenide atoms lie to the periphery of the Se═P–Se–P═Se hetero-chain. In this instance,

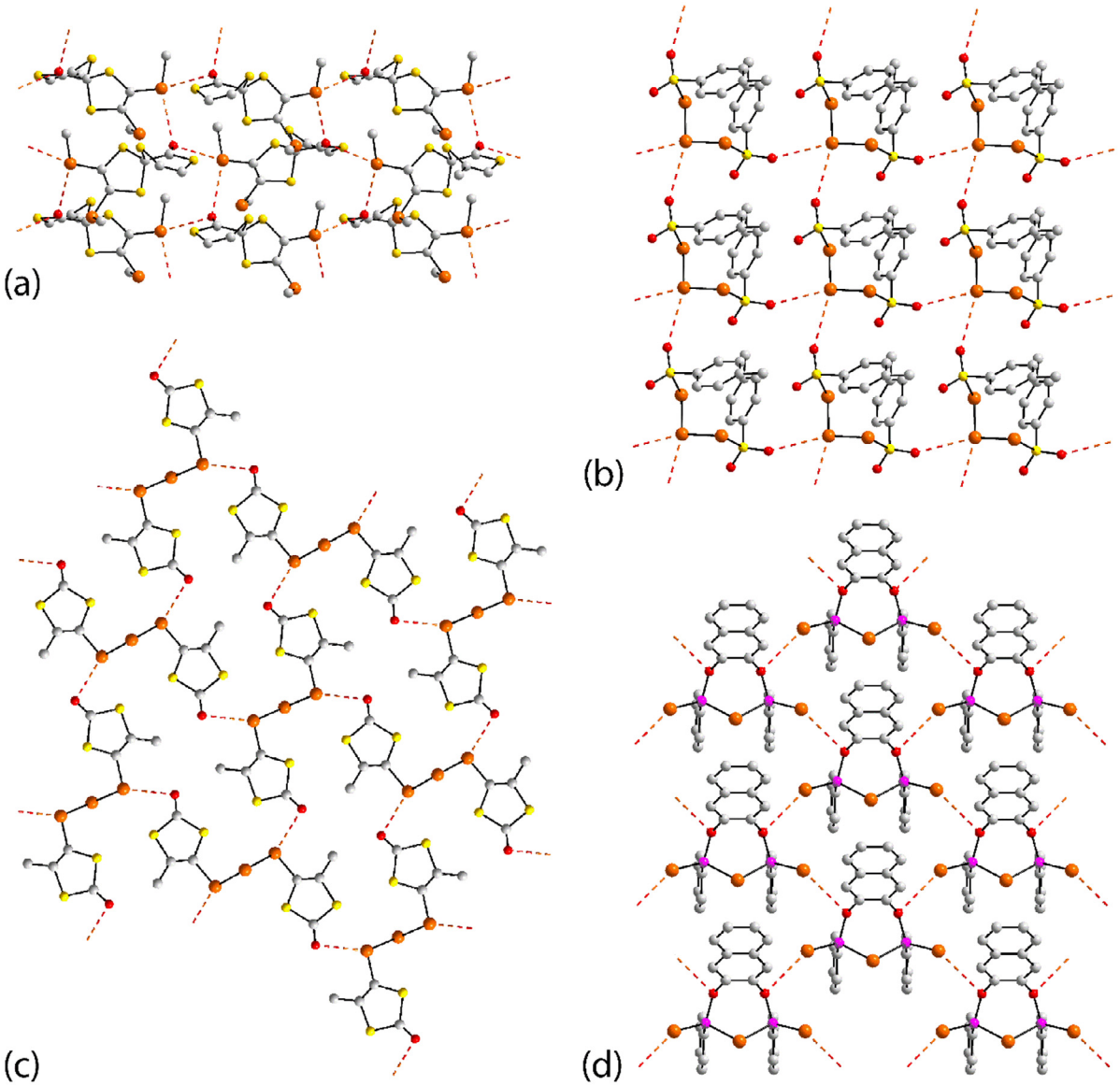

Fig. 19. Examples of supramolecular association in selenium(II) crystals leading to two-dimensional arrays based on Se···O chalcogen bonding interactions: (a) **188** [224; Se···O = 3.29 & 3.41 Å], (b) **189** [186; 3.22 Å], (c) **190** [225; 3.17 Å] and (d) **191** [226; 3.33 Å].

the selenide atoms form Se···O(phenoxide) contacts that generate a grid with a flat topology, Fig. 19d.

The final selenium(II) compound adopting a two-dimensional array in its crystal is also the only example of a tetra-nuclear compound in this category, **192** [205]. Here, the four selenium atoms are in a Se_4 chain and, as seen from Fig. 20, it is the 1,3-selenium atoms forming the Se···O(carbonyl) interactions with two different carbonyl-atoms that are responsible for the formation of the layer, which has a distinctive saw-tooth topology.

5.2. Two-dimensional assemblies formed by selenium(IV) compounds

A smaller number of selenium(IV) compounds assemble into two-dimensional arrays. The structure of **193** [227] is the only example in this series where the selenium atom is not incorporated within a ring. This open arrangement coupled with the selenium atom is within an O_3-donor set enables the formation of three interactions with each of the coordinated triflate anions, two of which are Se–O covalent bonds; each of the non-coordinating oxygen atoms participates in a Se···O(sulphonate) interaction, as seen from the detail of the selenium-atom environment of Fig. 21a. The packing comprises inter-digitated rows of molecules connected by the aforementioned Se···O(sulphonate) interactions to form a flat layer. In **194** [228], molecules are connected into centrosymmetric dimers via Se···O(alkoxide) interactions and these in turn are connected into a grid by Se···O(oxide) interactions which form the shorter of the separations, Fig. 21b. Disparate Se···O interactions are evident in **195** [95] and **196** [113]. In the former, approximately orthogonal chains sustained by Se···O(nitro) and Se···O(oxide) interactions assemble molecules into a two-dimensional array, Fig. 21c. In **196**, Se···O(alkoxide) and Se···O(oxide) interactions cooperate in a similar fashion. The resultant layer in each of **195** and **196** is jagged.

The selenium atom in **197** [113] is incorporated within a six-membered ring and forms a total of three Se···O interactions in the crystal, Fig. 22a. Centrosymmetrically related molecules are connected by via Se···O(alkoxide) interactions, forming the shorter distances, and these are connected into a flat, two-dimensional

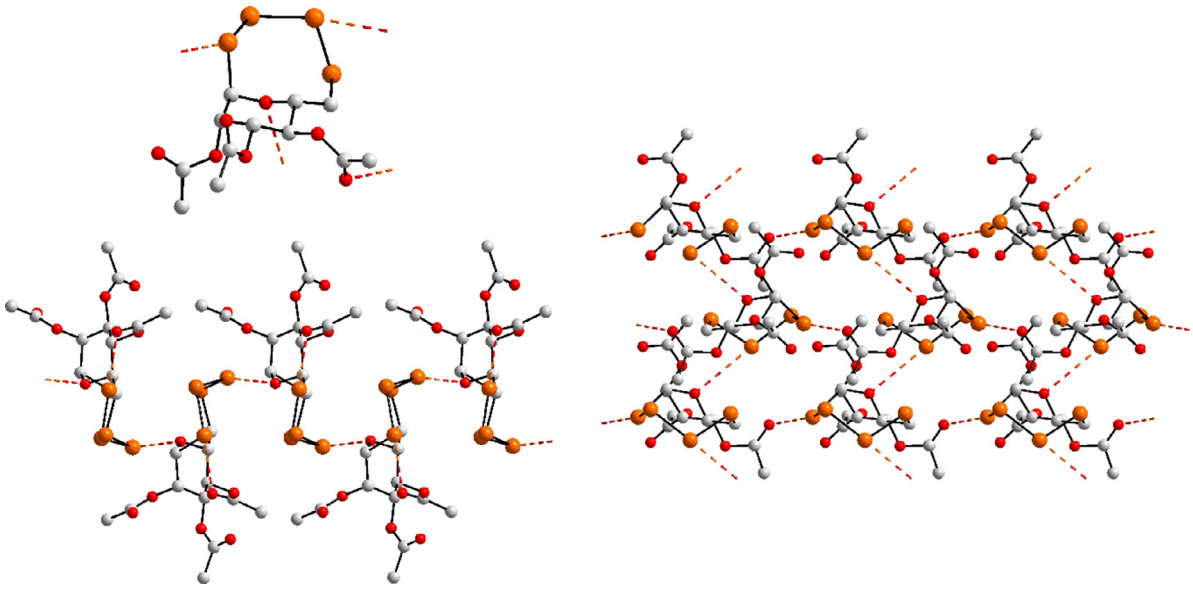

Fig. 20. Supramolecular association in **192** [205; Se···O = 3.34 & 3.42 Å], leading to two-dimensional arrays based on Se···O chalcogen bonding: detail of the Se···O(carbonyl) interactions as well as a side-on and plan view of the layer.

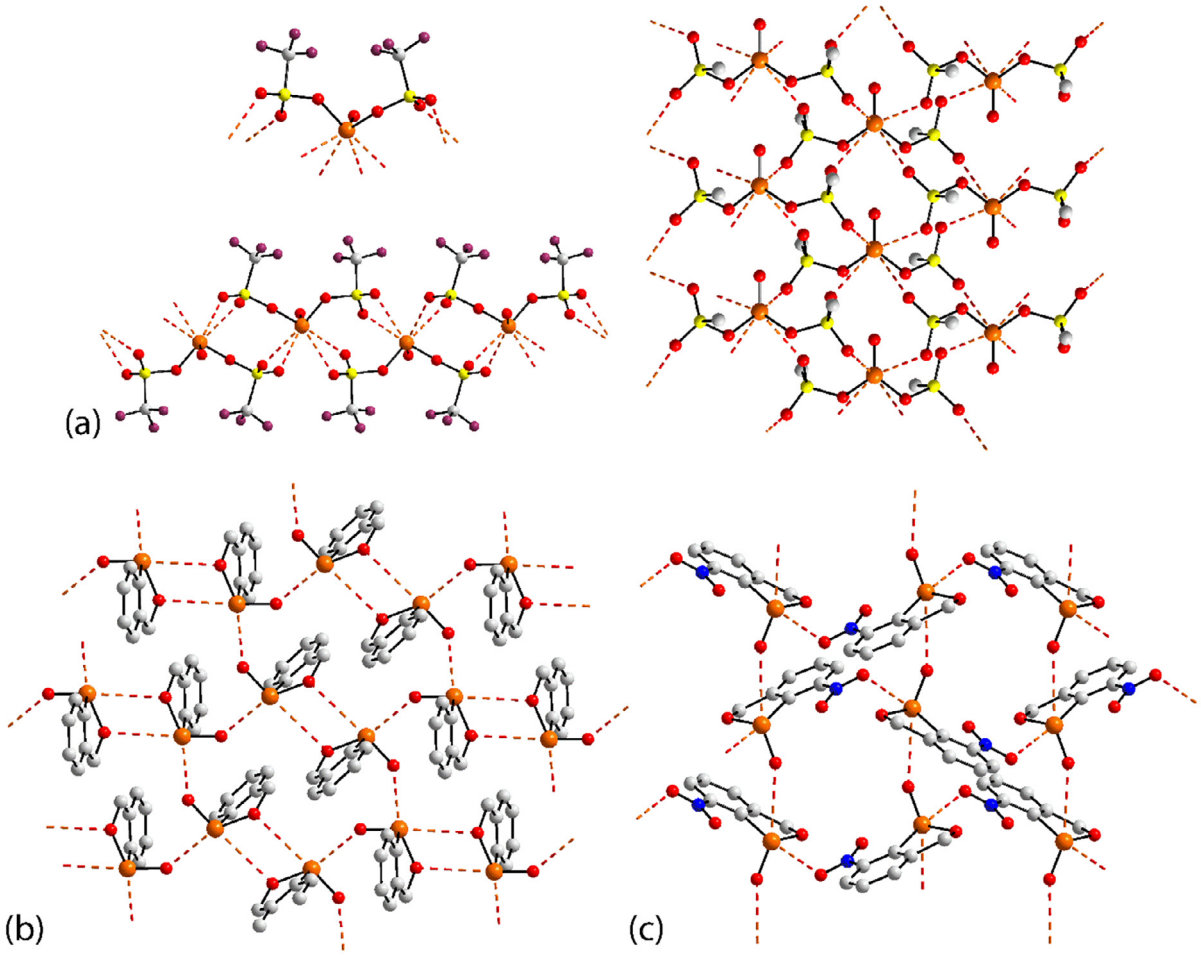

Fig. 21. Examples of supramolecular association in selenium(IV) crystals leading to two-dimensional arrays based on Se···O chalcogen bonding interactions: (a) **193** [227; Se···O = 2.76, 2.91, 3.14 & 3.14 Å] showing detail of the Se···O(sulphoxide) interactions as well as a side-on and plan view (fluoride atoms omitted) of the layer, (b) **194** [228; 2.76 & 3.29 Å] and (c) **195** [95; 3.13 & 3.26 Å].

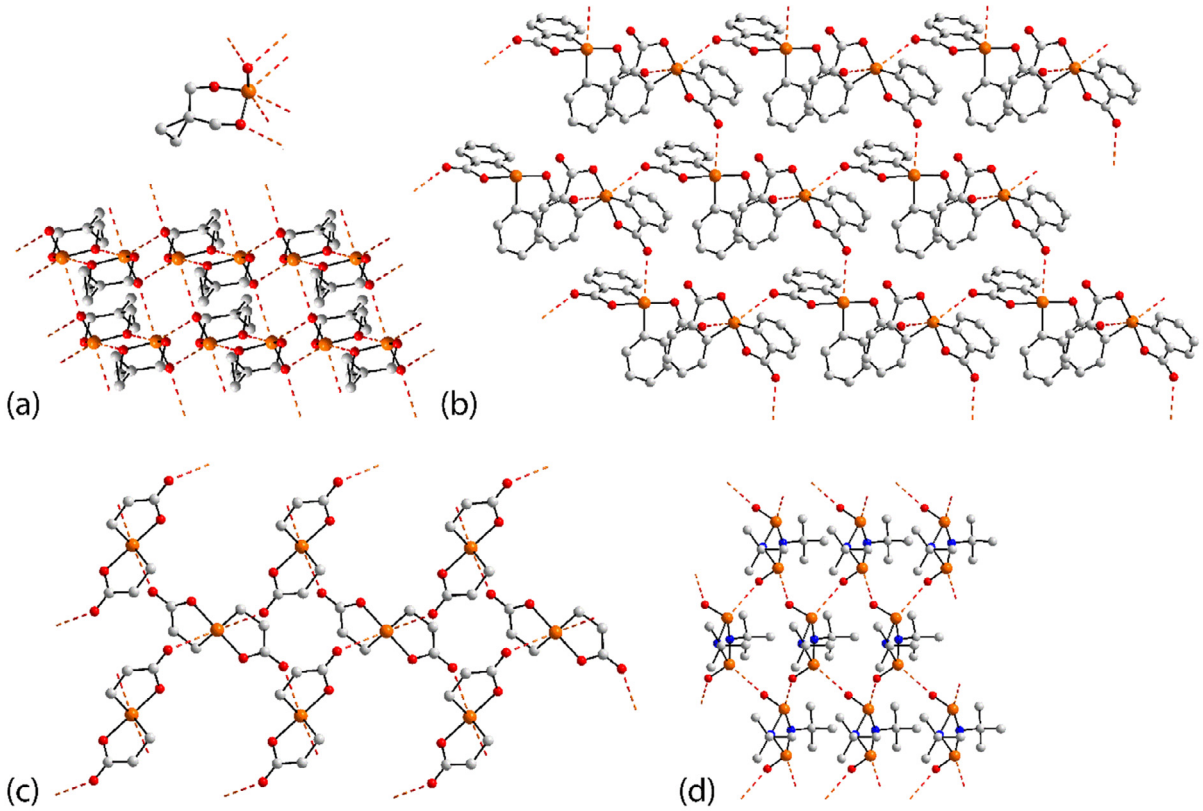

Fig. 22. Examples of supramolecular association in selenium(IV) crystals leading to two-dimensional arrays based on Se···O chalcogen bonding interactions: (a) **197** [113; Se···O = 2.82, 3.13 & 3.18 Å] showing detail of the Se···O interactions as well as a plan view of the layer, (b) **198** [229; 2.96, 2.97 & 3.16 Å], (c) **199** [230; 3.09 Å] and (d) **200** [231; 3.06 Å].

array by Se···O(oxide) interactions. Two independent molecules comprise the asymmetric unit of **198** [229] and these are connected by Se···O(carbonyl) interactions to form the array shown in Fig. 22b; the topology of the layer is flat. The selenium atom in the first independent molecule forms two Se···O contacts and the carbonyl-O atom one, with the second independent molecule follows the opposite trend. This flexibility in association via Se···O contacts is reflected in the following observation. Compound **198** is of particular interest as three polymorphs have been reported. Earlier in this survey, aggregation patterns were reported for the first two of these, i.e. **172** and **173**, Fig. 16h, each of which adopts a zig-zag chain in their crystal sustained, on average, by one and two Se···O(carbonyl) interactions, respectively. The selenium atom in **199** [230] is bis-chelated by C,O-donors and lies on a two-fold axis of symmetry. The selenium atom forms two Se···O(contacts) to form a flat, two-dimensional array, Fig. 22c. The only bi-nuclear compound in this section is found in **200** [231] where diagonally opposite selenium atoms are incorporated within a four-membered ring; the molecule has mirror symmetry with the nitrogen atoms of N_2Se_2 core lying on the plane. Each of the selenium and carbonyl-oxygen atoms forms a single Se···O(carbonyl) contact extending laterally to form a corrugated layer, Fig. 22d.

6. Three-dimensional assemblies mediated by Se···O chalcogen bonding

There are only three examples of selenium compounds comprising one chemical entity in the crystal assembling into a three-dimensional architecture based on Se···O chalcogen bonding. The chemical structures for these oxide-rich molecules, i.e. **201**–**203** [118,232], are shown in Fig. 23.

Only one selenium(II) molecule assembles to form a three-dimensional architecture in its crystal, namely **201** [232]. The bi-nuclear molecule has mirror symmetry containing both selenium atoms and relating the two cyclobutadiene residues. Here, each selenium atom forms four Se···O(carbonyl) interactions and each of the carbonyl-oxygen atoms forms two interactions to selenium as highlighted in Fig. 24a. The resulting architecture resembles a skewed honeycomb array. The two remaining molecules feature selenium(VI) centres, i.e. tri-nuclear **202** [118] and tetra-nuclear **203** [118]. In the former, which lacks symmetry, only the oxide-oxygen atoms participate in Se···O interactions with each forming a single contact and each selenium atom forming two Se···O(oxide) contacts, Fig. 24b. Layers with a zig-zag topology are discernible in the packing, Fig. 24b, being connected by three distinct Se···O(oxide) contacts. The molecule in **204** is disposed about a four-fold centre of inversion ($\bar{4}$) with each $Se(=O)_2$ unit involved in two donor and two acceptor Se···O(oxide) contacts, Fig. 24c. The resulting architecture comprises tetra-nuclear molecules assembled into columns, with a square appearance, connected orthogonally by the

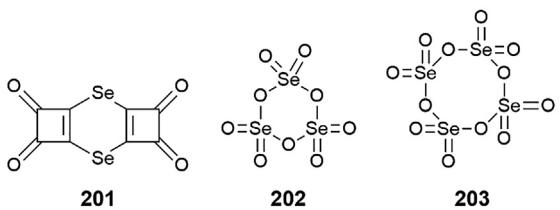

Fig. 23. Chemical diagrams for the interacting species, **201**–**203**, in selenium(II) and selenium(VI) crystals featuring Se···O contacts leading to supramolecular, three-dimensional arrays.

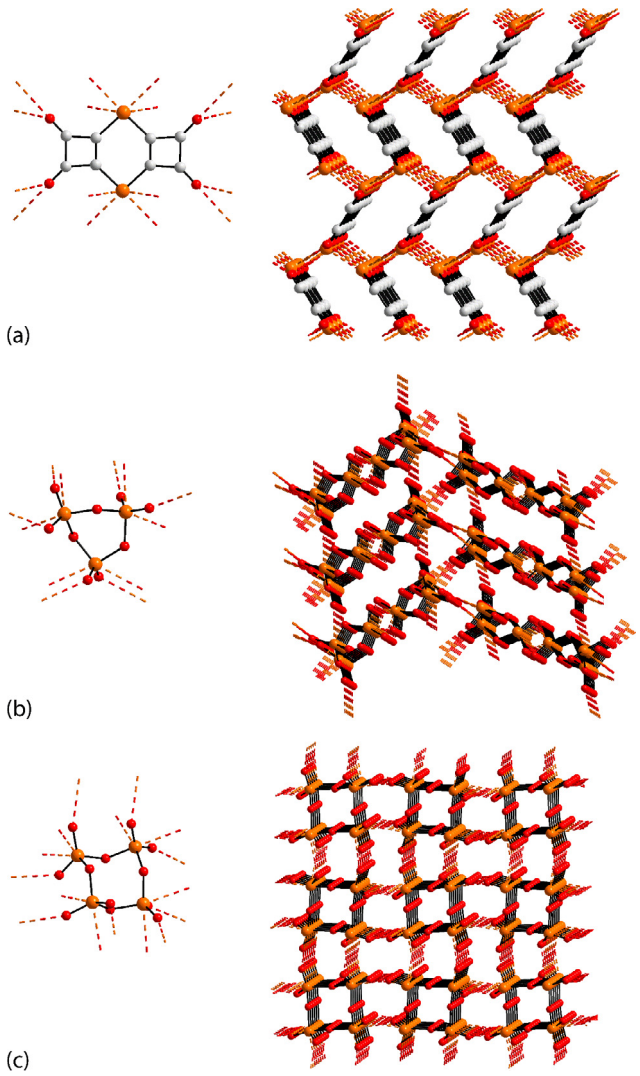

Fig. 24. Supramolecular association in selenium(II) and selenium(VI) crystals leading to three-dimensional arrays based on Se···O chalcogen bonding interactions showing detail of the Se···O interactions as well as a perspective of the three-dimensional assembly: (a) **201** [232; Se···O = 3.19 & 3.39 Å], (b) **202** [118; 3.03–3.33 Å] and (c) **203** [118; 3.13 & 3.15 Å].

Se···O(oxide) contacts which define columns with a rectangular appearance, Fig. 24c.

7. Supramolecular assemblies of multi-component species mediated by Se···O chalcogen bonding

For completeness, in this section Se···O chalcogen bonding interactions in multi-component crystals are surveyed. Firstly, solvates are described followed by co-crystals. The chemical structures of the 20 compounds covered in this section, **204**–**224** [118,233–245] are shown in Fig. 25.

7.1. Supramolecular assemblies in solvates of selenium compounds

Each of the mono-, bi- and tri-nuclear selenium(II) compounds, i.e. **204** [233], **205** [234] and **206** [235], illustrated in Fig. 26a-c, respectively, feature a single Se···O contact between the molecule and solvent, i.e. dimethylformamide in **204** and **206**, and methanol in **205**. In tetra-nuclear **207** [235], which is disposed about a centre of inversion, there are two co-crystallised dimethylformamide molecules and the oxygen atom from each of these symmetrically spans two selenium atoms to form a three-molecule aggregate shown in Fig. 26d.

A one-dimensional chain with a zig-zag topology (glide symmetry) is formed in the crystal of **208** [236] whereby the dimethylsulphoxide-oxygen atom symmetrically bridges two selenium atoms to form the arrangement shown in Fig. 26e.

The focus now turns towards selenium(IV) species. A three-molecule aggregate is formed in **209** [237] where the dioxane molecule, situated about a centre of inversion, bridges two molecules as shown in Fig. 26f. A hydrated, linear supramolecular chain is formed in the crystal of **210** [238]. The water molecule is connected to the selenium atom, being separated by 2.92 Å, and the resultant two molecule aggregates assemble into a chain via Se···O(hydroxyl) chalcogen bonds (3.03 Å) as shown in Fig. 26g.

In the mono-selenium(IV) compound **211** [239], linear chains are sustained by Se···O(oxide) contacts and these are connected into a three-dimensional array by links provided by bridging dioxane molecules, Fig. 27a. Thus, each selenium forms three Se···O interaction with the shorter of the separations involving Se···O (ether) contacts.

There are two mixed selenium(IV)/(VI) compounds in this category, i.e. **212** [118] and **213** [118], and a pivotal role for the co-crystallised dioxane molecules is evident in each. The tetra-nuclear molecule in **212** is disposed about a centre of inversion. There are two molecules of solvent for each tetra-nuclear molecule and it is the selenium(IV) centres that associate with two symmetry dioxane molecules to form a two-dimensional grid, Fig. 27b. In the second mixed valence compound, **213** [118], two tri-nuclear molecules and four dioxane molecules comprise the asymmetric unit. As shown in the left-hand image of Fig. 27c, molecules are assembled into a two-dimensional array with an undulating topology via Se···O(ether) interactions as each dioxane molecule is bridging and each selenium(IV) centre forms two contacts of this type. The links between layers to form a three-dimensional architecture are of the type Se···O(oxide), where the oxide-donors are bound to the selenium(VI) centres. The Se···O(oxide) interactions form separations systematically longer than the Se···O(ether) contacts, Fig. 27c.

A three-dimensional architecture is also found in the crystals of the selenium(VI) compound, **214** [118], a 1:1 dioxane solvate, with the bi-nuclear molecule bisected by two-fold axis of symmetry and with the dioxane molecule disposed about a centre of inversion. As seen in Fig. 27d, molecules are assembled into rows via Se···O(oxide) interactions and rows are connected by Se···O(ether) interactions derived from the bridging dioxane molecules. A systematic trend is noted in Se···O distances as for **213** in that the separations involving the Se···O(ether) contacts are shorter than the Se···O(oxide) contacts.

7.2. Supramolecular assemblies in selenium(II) co-crystals

In this final section, a number of selenium(II) and selenium(IV) aggregates are described, with all but one example being zero-dimensional in consideration of Se···O interactions alone. The selenium(II) atom in mono-nuclear **215** [240] forms four Se···O(ether) contacts to sustain a two-molecule aggregate, Fig. 28a. The asymmetric unit of **216** [241] comprises two selenium(II) molecules and the organic co-former, i.e. is a 2:1 co-crystal, one of the selenium(II) molecules makes a single Se···O(hydroxyl) interaction to form the two-molecule aggregate shown in Fig. 28b. In the 1:2 co-crystal **217** [242], each of the selenium atoms in the bi-nuclear molecule forms a Se···O(carbonyl) interaction to form a three-molecule aggregate, Fig. 28c. Another bi-nuclear molecule where the selenium atoms are connected to each other within a five-membered ring, **218** [243], forms a 2:1 co-crystal with a

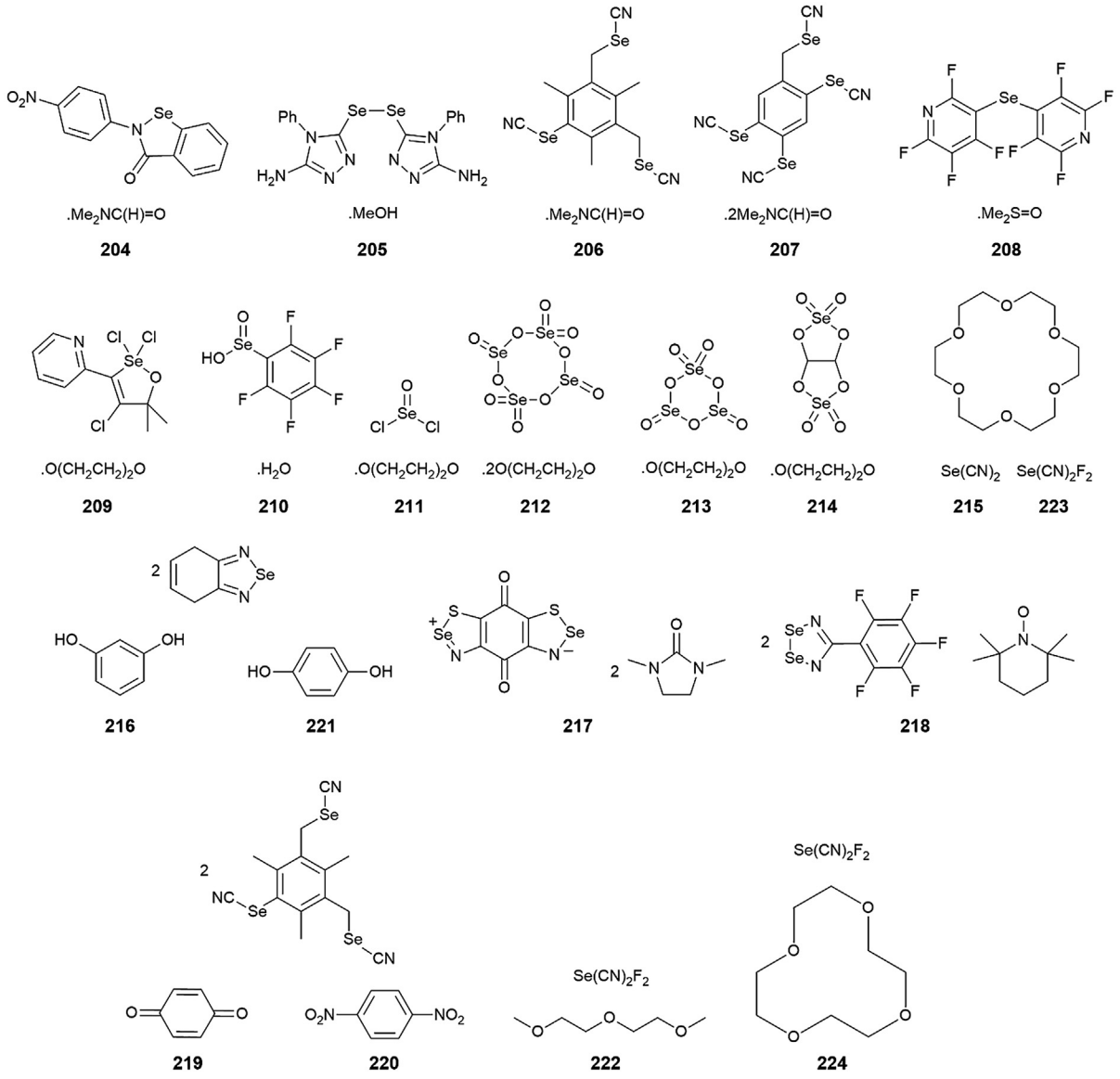

Fig. 25. Chemical diagrams for the interacting species, **204**–**224**, in selenium(II) and selenium(IV) crystals featuring Se···O contacts leading to supramolecular, two-dimensional arrays.

nitrogen-oxo-containing molecule; both species are radicals. The oxo atoms atom accepts four Se···O(oxo) interactions, one each from each of the selenium atoms of the two co-formers, Fig. 28d. The tri-nuclear molecules in each of **219** and **220** [244] featured earlier in **206**, i.e. forming a two-molecule aggregate with a solvent molecule, Fig. 26c. In **219** and **220**, Fig. 28e, this molecule is also a co-former in 2:1 co-crystals with potentially bridging molecules, at least via Se···O interactions; the organic co-former is disposed about a centre of inversion in both co-crystals. Indeed, one selenium(II) atom in each molecule is connected by Se···O(carbonyl) and Se···O(nitro) interactions in **219** and **220**, respectively, to form a three-molecule aggregate in each case.

The only one-dimensional chain in this section is formed in the 2:1 co-crystal **221** [241]; the selenium(II) molecule also formed a solvate via a Se···O(hydroxyl) interaction in **216** [241], Fig. 28b. In **221**, the benzene-1,4-diol molecule is situated about a centre of inversion and the association between molecules is also through Se···O(hydroxyl) interactions. Centrosymmetric {···Se–O}$_2$ synthons are formed in the crystal leading to a linear, supramolecular chain, Fig. 28f.

7.3. Supramolecular assemblies in selenium(IV) co-crystals

There are three selenium(IV) molecules forming co-crystals based on Se···O chalcogen bonding, i.e. **222**, **223** and **224** [240]. In **222**, Fig. 28g, the selenium(IV) atom forms three Se···O(ether) contacts to form a zero-dimensional adduct. Similar, two molecule aggregates are formed in **223** and **224** where each selenium atom forms four Se···O(ether) contacts, resembling the situation illustrated for **215** [240] in Fig. 28a.

8. Overview

Allowing for multiple molecules in the asymmetric unit and the occurrence of several polymorphs, 224 distinct supramolecular aggregation patterns based on Se···O chalcogen bonding interaction are noted in the crystals of nearly 220 selenium compounds. The overwhelming majority of the compounds were homogeneous but examples of solvates and co-crystals are evident. By far the most predominant oxidation state is + II, with 163 examples (72%), followed by + IV (51) with a small number of compounds

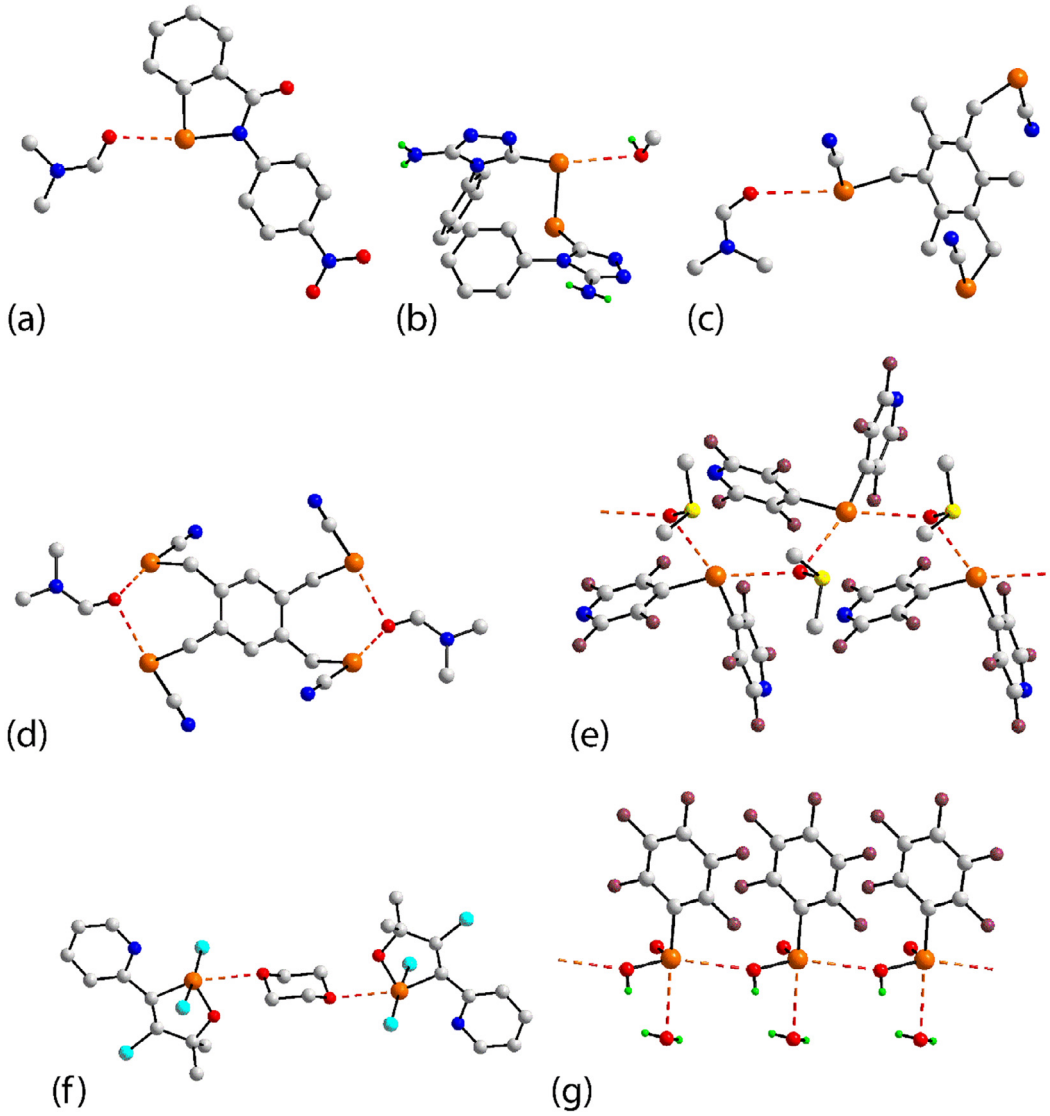

Fig. 26. Supramolecular association in selenium(II) and selenium(IV) crystals leading to zero- and one-dimensional assemblies based on Se···O chalcogen bonding interactions: (a) **204** [233; Se···O = 2.64 Å], (b) **205** [234; 3.06 Å], (c) **206** [235; 3.28 Å], (d) **207** [235; 2.94 & 2.95 Å], (e) **208** [236; 2.89 & 2.90 Å], (f) **209** [237; 2.83 Å] and (g) **210** [238; 2.92 & 3.03 Å].

with selenium in the + VI (8) oxidation state; two mixed valent selenium(IV)/(VI) compounds are also included in the survey. Over two-thirds of molecules are mono-nuclear (161), with decreasing numbers of bi-, tri- and tetra-molecules, i.e. 43, 11 and nine, respectively. A full range of zero-, one-, two- and three-dimensional patterns are noted with the majority, i.e. over 55% (128 examples), being one-dimensional with the next most significant being, zero-dimensional, with 69 examples. There are 22 examples of molecules assembled into two-dimensional arrays and five forming three-dimensional architectures. The average number of Se···O interactions per participating species varies from 0.5, i.e. for zero-dimensional aggregates sustained by a single interaction to four in several architectures. Of the nearly 300 different Se···O contacts in the supramolecular aggregates described herein, over three-quarters (78%) involve a single Se···O interaction and 18% involve two Se···O interactions. There are six examples each of molecules where the selenium forms three or four contacts, always in higher-dimensional aggregates. Of the zero-dimensional aggregates, the majority comprise two like-molecules sustained by one (9) or two (41) Se···O interactions but, examples of four- and six-molecule aggregates are also observed. A variety of topologies are noted among the 125 zero-dimensional chains, including linear (38), zig-zag (52), helical (30) and twisted (5).

The large range of supramolecular aggregation patterns is complimented by the diversity in the oxygen donors participating in Se···O interactions. When aggregates featuring one type of Se···O interaction only, 41% involve carbonyl donors. The next most prevalent are ether (including methoxy) and Se=O donors, each at 12%, followed by nitro-, sulphoxide- and hydroxyl-donors at 9, 8 and 6%, respectively.

Attention is now directed on the propensity of molecules to form Se···O chalcogen bonding in their crystals. Herein, 224 examples of aggregates sustained by Se···O chalcogen bonding interactions were identified. Put into perspective, after a search of the CSD [65] following the protocols outlined in section 2, there are 1722 "hits" for crystals containing both selenium and oxygen. This implies the percentage adoption of Se···O chalcogen bonding approximates 13% of all possible structures where these interactions can occur. This percentage is an underestimate as in the present survey as

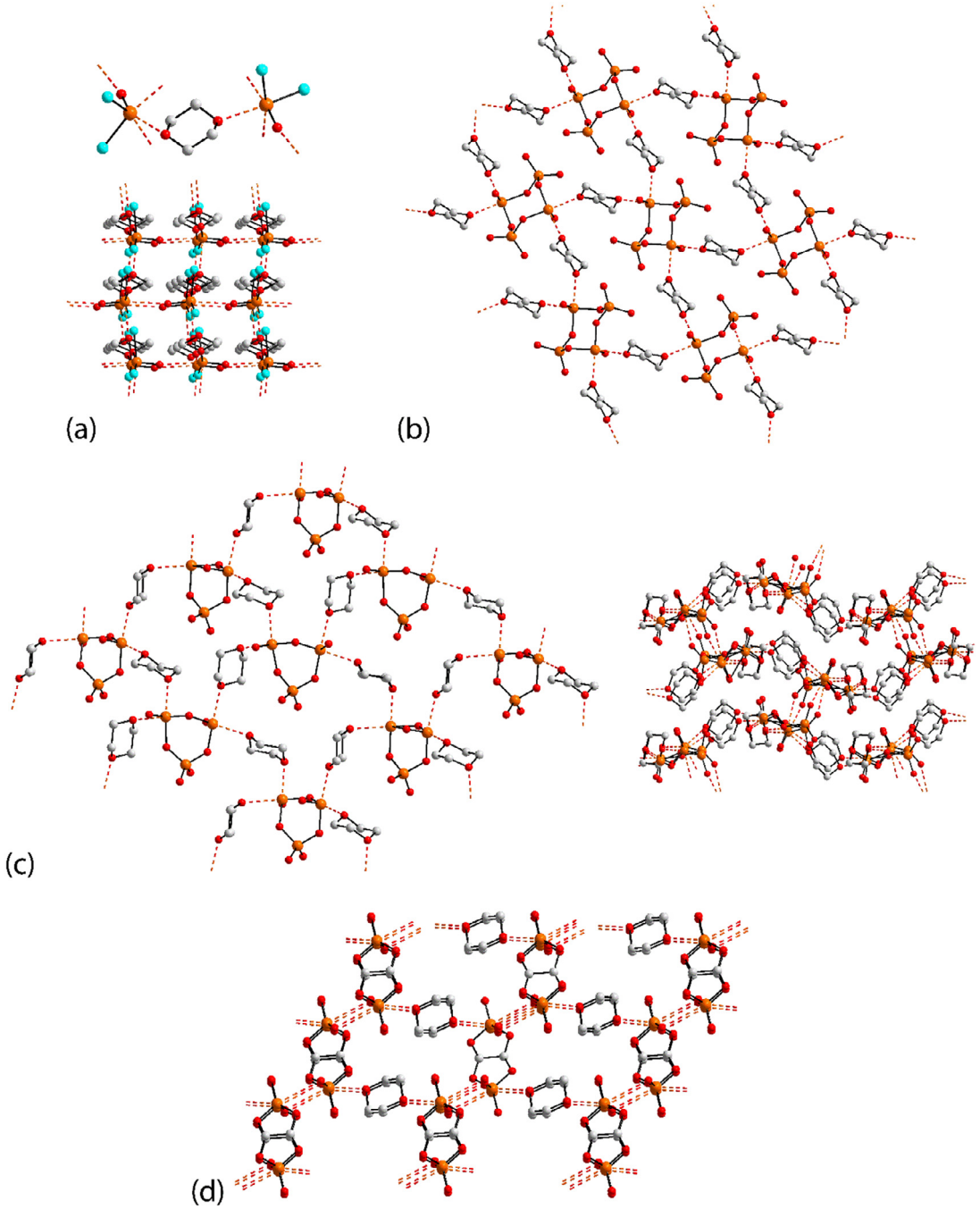

Fig. 27. Supramolecular association in selenium(IV), mixed selenium(IV)/(VI) and selenium(VI) crystals leading to two- and three-dimensional assemblies based on Se···O chalcogen bonding interactions: (a) **211** [239; Se···O = 2.61, 2.72 & 2.90 Å], (b) **212** [118; 2.40 & 2.44 Å], (c) **213** [118; Se···O(ether) 2.44–2.62 Å and Se···O(oxide) 2.82 & 3.07 Å] and (d) **214** [118; 2.83 & 3.13 Å].

crystals where Se···O interactions were acting in concert with other identifiable intermolecular forces, the notable example being hydrogen bonding, were omitted. This percentage compares favourably to the 6% of selenium(lone-pair)···π(arene) interactions in crystals where these interactions can potentially form [248,249]. Over and above different chemical composition, as alluded to above, secondary bonding interactions, including chalcogen bonding interactions, are notoriously subject to steric effects in that these interactions are mitigated when bulky metal-bound and/or ligand-bound substituents are present [54,56–63]. To probe further the likely adoption of Se···O interactions in crystals, the likelihood of specific classes of compounds to form Se···O chalcogen bonds was ascertained.

As noted above, Se···O(carbonyl) interactions featured in 41% of the crystals in the present survey. Hence, the CSD was searched for "selenium" and "carbonyl-oxygen" using the established protocols. This indicated that almost 50% of all crystals having these two components actually formed Se···O(carbonyl) interactions. An analogous search for residues containing Se=O, often observed in the selenium(IV) compounds included herein, was conducted. This analysis indicated a smaller percentage adoption of about 25%. Throughout this survey, the 5-selanylidene-1H-pyrrol-2-one core,

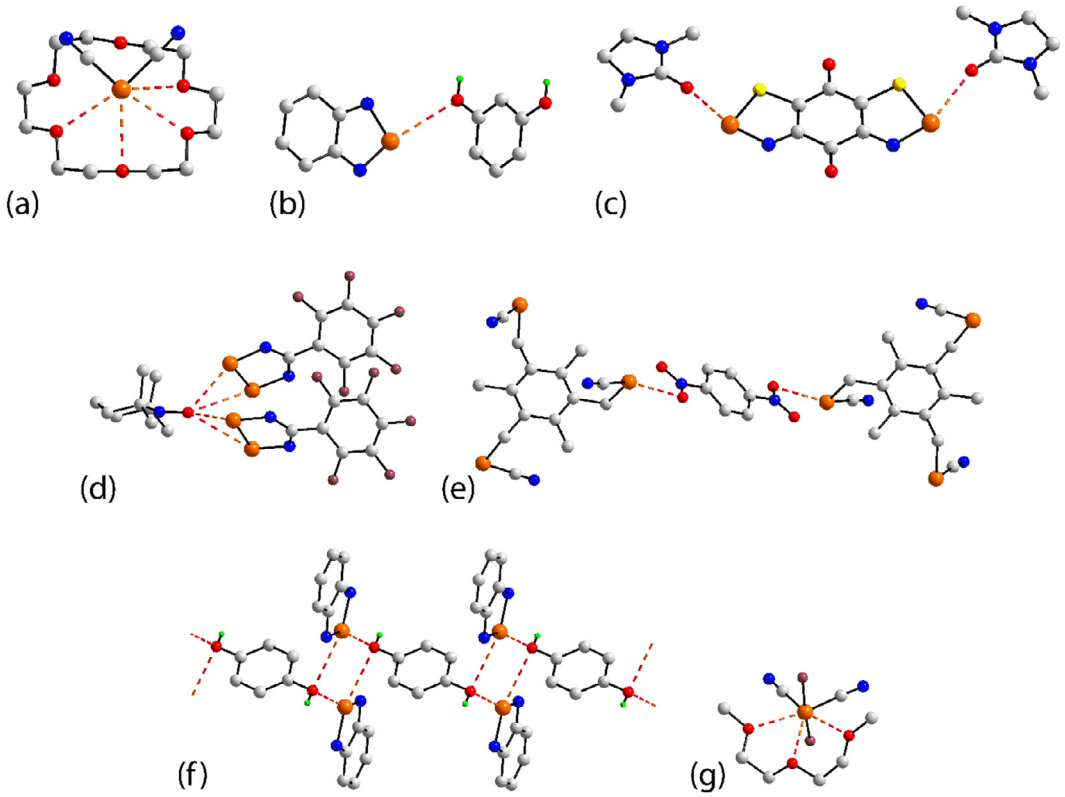

Fig. 28. Supramolecular association in selenium(II) and selenium(IV) co-crystals leading to zero- and one-dimensional assemblies based on Se···O chalcogen bonding interactions: (a) **215** [240; Se···O = 2.87–3.40 Å], (b) **216** [241; 3.18 Å], (c) **217** [242; 2.83 Å], (d) **218** [243; 2.90–3.35 Å], (e) **220** [244; 3.23 Å], (f) **221** [241; 3.14 & 3.28 Å] and (g) **222** [240; 2.66–2.85 Å].

as found in Ebselen™, has been mentioned a good number of times. This core has a three-bond separation between the selenium and carbonyl-oxygen atoms, and with these acceptor and donor atoms largely constrained to a fixed disposition owing to their relationship through the five-membered ring. A search of the CSD revealed this core features in 52 crystals. With Se···O(carbonyl) interactions forming in 25 examples, the percentage adoption is over 48%. Interestingly, five others of these structures formed Se···O interactions in their crystals but, with selenide- (1), nitro- (1) and hydroxyl-oxygen (3) donors. With this relatively high adoption rate, the propensity of selenium molecules with selenium incorporated within a five-membered ring comprising four unspecified atoms and unspecified bonds between them was then evaluated. The CSD has about 945 "hits" for this fragment and with 102 examples having unassisted Se···O chalcogen bonding interactions, the percentage adoption is at least 10%, indicating this fragment alone does not promote Se···O interactions.

Consideration is now directed towards the geometric parameters characterising the observed Se···O secondary bonding interactions. The Se···O separations span a wide range, i.e. from a short 2.40 Å, indicative of some covalent character, right out to the van der Waals limit of 3.42 Å; the average distance of a Se···O interaction computes to 3.11 Å and the median value is 3.17 Å. It is noted that while many of the shorter interactions were in the dioxane adducts, such as **212** which exhibited the short contact cited above, short contacts were often noted in one-dimensional chains involving molecules incorporating the 5-selanylidene-1H-pyrrol-2-one core, e.g. the next shortest separation of 2.41 Å is observed in **118**. However, these are only generalisations, with each class of molecule, respectively, also having longer contacts, e.g. 3.35 Å in **8** and 3.38 Å in **23**. This observation is entirely consistent with the well-known axiom in supramolecular chemistry that geometric correlations of weak intermolecular interactions are not generally possible unless the molecules/interactions are very closely related/isostructural [245–247]. In the present case, the lack of systematic trends is not surprising considering the different chemical composition of the interacting species, different oxidation states and geometries, and range of oxygen donors engaged in the Se···O interactions.

Up to this point, no specific mention of the angles associated with the supramolecular Se···O interactions has been made; key angles subtended at oxygen donor atoms and selenium acceptor atoms are collated in Appendix A. Just as distance correlations are not reliable for intermolecular interactions [245–247], correlations involving angles are also problematic, as commented upon recently for secondary bonding interactions formed between selenium and the heavier main group elements [250]. This is because, as for distances, angles are going to be moderated by the chemical/electronic environment of the participating atoms. Based on the assumption that for the specified Se···O contacts, the oxygen atom is the Lewis base, providing the charge to the σ-hole located on the selenium atom of the Lewis acid, there are several variables impacting upon the magnitude of the Se···O interaction and the angles subtended at the interacting oxygen atom. In the case of the oxygen donor, these factors include but, are not limited to the steric and electronic profiles of the residues bound to oxygen, the hybridisation of the oxygen atom and, when the interacting oxygen atom is part of a nitro group, for example, the partial charge on the oxygen atom. For the selenium acceptor, again the steric and electronic profiles of bound atoms/groups come into play, as does the ligand donor set about the selenium atom along with the oxidation state of the selenium atom which, in turn, impacts on the number of sterically active lone-pairs of electrons about the selenium atom and therefore, stereochemistry.

These points are highlighted in the following observations on the sub-set of structures where the donor oxygen and acceptor selenium atoms participate in one contact only. Considering the angles subtended at the oxygen donors first, in the surveyed structures featuring a single contact between the participating atoms, the minimum angle of 82.4° (the Se···O separation is 3.38 Å) was found in **105** where the donor atom is a carbonyl-O to a selenium(II) centre, and the maximum angle of 160.2° (Se···O = 2.83 Å) is seen in **217** where a carbonyl-O atom is the donor and the acceptor is a selenium(II) atom flanked by nitrogen and sulphur atoms within a five-membered ring. The large range observed overall is also reflected in more specific contacts, for example S–O···Se contacts with a range of over 70°, i.e. from 87.7° in **2** to 159.7° in **78** with a spread of values within this range for the 10 structures having the oxygen and selenium atoms forming a single contact only. The above notwithstanding, the following represents an analysis of specific types of Se···O interactions.

For the sp^3-hybridised hydroxyl-O atom, there are 11 examples and the range of values is somewhat reduced compared to the general survey, i.e. 94.1° in **13** to 126.2° in **15** if an outlier, i.e. **3** (144.7°), is ignored. While, to a first approximation, these values are in the generally expected range for a sp^3-hybridised-O(lone-pair)···σ-hole(Se) interaction, the influence of hydrogen bonding interactions, for example, might also be expected to cause distortions, as in outlier **3**. Conversely, if selenium-bound lone-pair of electrons is anticipated in a position diagonally opposite to a covalent bond involving selenium and carbon (or nitrogen or phosphorus), a close to linear angle at selenium would be anticipated. In the present series of structures involving hydroxyl-donors, these angles range from 148.6° for C–Se···O in **15**, where the selenium (II) atom is part of five-membered ring to 175.0° for N–Se···O in **118**, where the selenium(II) atoms is flanked by carbon and nitrogen donors within a five-membered ring.

A number of structures are constructed about a $\{\cdots Se{=}O\}_2$ core and these present a robust set of Se=O···Se and A–Se···O angles, where A = C, N or S. Only two examples of selenium(II) feature this core, i.e. **25** and **26**, each resulting in a zero-dimensional aggregation, with pairs of Se=O···Se and A–Se···O angles of 108.3 and 156.5°, and 111.2 and 156.1°, respectively. For the 15 selenium (IV) species, the Se=O···Se angles range from 88.0°, for **43**, to 121.4° for **44**. In fact, these are outliers (see below) with the remaining angles lying between 93.2°, for **37**, to 108.4° for **42**. In terms of A–Se···O angles, these are consistently wider than for the selenium(II) species, lying between 163.6°, for **37** (A = C), to 177.5° for **39** (A = O). The two exceptional selenium(II) structures in this regard are **42**, with C–Se···O = 144.9°, and **44** with C–Se···O = 138.9°. These, along with **43** mentioned above, feature concatenated, strained rings which readily account for the observed deviations. For the five zero-dimensional selenium(VI) structures featuring a $\{\cdots Se{=}O\}_2$ core, the Se=O···Se angles range from 105.3°, for **55**, to 111.5° for **53**, and the A–Se···O angles range from 167.5°, for **55** (A = O), to 174.1°, for **51** (A = C). The $\{\cdots Se{=}O\}_2$ core also features in eight one-dimensional aggregation patterns and present narrow ranges for both Se=O···Se, i.e. 94.6° (**168**) to 108.6° (**165**), and A–Se···O angles, i.e. 156.2° (**165**, A = O) to 176.8° (**164**, A = C). Finally, taking the sub-set of 29 zero-dimensional selenium(II) examples where the selenium atom forms one Se···O interaction only, there are two exceptional structures where A–Se···O lies between 127 and 128°, i.e. **8** and **22**. Indeed, 21 examples have A–Se···O > 160°.

From the A–Se···O data included in Appendix A, it is a generalisation that the angle about the selenium atom, regardless of oxidation state, generally lies between 140 and 180°. This observation is consistent with expectation in terms of the σ-hole model to explain the nature of these interactions [45–47,251]. It might be concluded that while to a first approximation, there is a general understanding of the mode of bonding leading to Se···O and related secondary bonding interactions, further investigations, such high-level crystallographic, including charge density studies and analysis [11,252,253], along with reliable computational chemistry studies [254–256] are required in order to gain a more complete picture of Se···O interactions. Also of interest would be the determination, experimental and theoretical, of the energies of stabilisation provided by specific Se···O contacts. Thus far, these are comparatively rare, e.g. 10–40 kJ/mol for molecules based on the Ebselen™ (**89** & **90**) structure [11], i.e. as noted previously [54], an energy in the range observed for conventional hydrogen bonding interactions.

Finally, while the focus of the present review has been upon the identification of intermolecular Se···O interactions in crystals of molecular selenium compounds, the relevance of Se···O secondary bonding interactions in the biological context was alluded to in the Introduction. With the present covid-19 pandemic confronting the World, it is not surprising that Ebselen™ and analogues have already been evaluated as potential inhibitors of the active site of the main protease (M^{pro}) of the severe acute respiratory syndrome coronavirus 2 (SARS-CoV-2) [257] in a classic case of drug repurposing [258]. On-going crystallographic, spectroscopic, e.g. ^{77}Se NMR [259], and computational studies [260,261] should also be alert for the potential influence of Se···O interactions in providing stability to poses adopted by selenium compounds in relevant active sites of target macromolecules.

9. Conclusions

Chalcogen bonding of the type Se···O contribute to the stability of crystals where they can form and are shown to sustain a full range of supramolecular aggregates: any complete analysis of the molecular packing of relevant compounds should include an analysis of these and other secondary bonding interactions. In the same way, any evaluations of the biological mechanisms of action, catalytic processes, rationalisation of chemical reactivity, etc. should be on the alert to the possible role of Se···O secondary bonding. Most notably by the prevalence of linear A–Se···O angles, for A = C, N, S and Se, the concept of the σ-hole provides a key impetus for the rationalisation of these interactions for selenium(II)- and selenium(IV)-containing compounds in the above contexts. However, further studies are required, both experimental and computational, for a more complete understanding of the formation of Se···O interactions and the energies of their association.

Declaration of Competing Interest

The author declares that there are no known competing financial interests or personal relationships that could have appeared to influence the work reported in this paper.

Acknowledgements

The author gratefully acknowledges Sunway University Sdn Bhd (Grant no. STR-RCTR-RCCM-001-2019) for support of crystallographic studies.

Appendix A. Supplementary data

Supplementary data to this article (details of crystals featuring Se···O chalcogen bonding interactions: composition, diagram, distance and angle data, citation and commentary) can be found online at https://doi.org/10.1016/j.ccr.2020.213586.

References

[1] T.C. Stadtman, Ann. Rev. Biochem. 65 (1996) 83–100, https://doi.org/10.1146/annurev.bi.65.070196.000503.
[2] V.N. Gladyshev, D.L. Hatfield, J. Biomed. Sci. 6 (1999) 151–160, https://doi.org/10.1159/000025383.
[3] , Eur. J. Biochem. 264 (1999) 607–609.
[4] J. Nordberg, E.S.J. Arnér, Free Radic. Biol. Med. 31 (2001) 1287–1312, https://doi.org/10.1016/S0891-5849(01)00724-9.
[5] A.C. Bianco, D. Salvatore, B. Gereben, M.J. Berry, P.R. Larsen, Endocr. Rev. 23 (2002) 38–89, https://doi.org/10.1210/edrv.23.1.0455.
[6] M. Allingstrup, A. Afshari, Cochrane Database Syst. Rev. (2015) CD003703; doi: 10.1002/14651858.CD003703.pub3
[7] E.R.T. Tiekink, Dalton Trans. 41 (2012) 6390–6395, https://doi.org/10.1039/c2dt12225a.
[8] H.-L. Seng, E.R.T. Tiekink, Appl. Organomet. Chem. 26 (2012) 655–662, https://doi.org/10.1002/aoc.2928.
[9] N.V. Barbosa, C.W. Nogueira, P.A. Nogara, A.F. de Bem, M. Aschner, J.B.T. Rocha, Metallomics 9 (2017) 1703–1734, https://doi.org/10.1039/c7mt00083a.
[10] Z. Chen, H. Lai, L. Hou, T. Chen, Chem. Commun. 56 (2020) 179–196, https://doi.org/10.1039/C9CC07683B.
[11] S.P. Thomas, K. Satheeshkumar, G. Mugesh, T.N. Guru Row, Chem. Eur. J. 21 (2015) 6793–6800, https://doi.org/10.1002/chem.201405998.
[12] H. Wang, J. Liu, W. Wang, Phys. Chem. Chem. Phys. 20 (2018) 5227–5234, https://doi.org/10.1039/c7cp08215k.
[13] W. Wang, B. Ji, Y. Zhang, J. Phys. Chem. A 113 (2009) 8132–8135, https://doi.org/10.1021/jp904128b.
[14] C.B. Aakeröy, D.L. Bryce, G.R. Desiraju, A. Frontera, A.C. Legon, F. Nicotra, K. Rissanen, S. Scheiner, G. Terraneo, P. Metrangolo, G. Resnati, Pure Appl. Chem. 91 (2019) 1889–1892, https://doi.org/10.1515/pac-2018-0713.
[15] R.M. Minyaev, V.I. Minkin, Can. J. Chem. 76 (1998) 776–778, https://doi.org/10.1139/v98-080.
[16] R.J. Fick, G.M. Kroner, B. Nepal, R. Magnani, S. Horowitz, R.L. Houtz, S. Scheiner, R.C. Trievel, A.C.S. Chem, Biol. 11 (2016) 748–754, https://doi.org/10.1021/acschembio.5b00852.
[17] S. Mondal, G. Mugesh, Chem. Eur. J. 25 (2019) 1773–1780, https://doi.org/10.1002/chem.201805112.
[18] S.P. Thomas, V. Kumar, K. Alhameedi, T.N.G. Guru Row, Chem. Eur. J. 25 (2019) 3591–3597, https://doi.org/10.1002/chem.201805131.
[19] N. Biot, D. Bonifazi, Coord. Chem. Rev. 413 (2020) 213243, https://doi.org/10.1016/j.ccr.2020.213243.
[20] S. Scheiner, M. Michalczyk, W. Zierkiewicz, Coord. Chem. Rev. 405 (2020) 213136, https://doi.org/10.1016/j.ccr.2019.213136.
[21] M.S. Taylor, Coord. Chem. Rev. 413 (2020) 213270, https://doi.org/10.1016/j.ccr.2020.213270.
[22] E. Navarro-García, B. Galmés, M.D. Velasco, A. Frontera, A. Caballero, Chem. Eur. J. 26 (2020) 4706–4713, https://doi.org/10.1002/chem.201905786.
[23] P. Wonner, T. Steinke, L. Vogel, S.M. Huber, Chem. Eur. J. 26 (2020) 1258–1262, https://doi.org/10.1002/chem.201905057.
[24] C.M. Young, A. Elmi, D.J. Pascoe, R.K. Morris, C. McLaughlin, A.M. Woods, A.B. Frost, A. de la Houpliere, K.B. Ling, T.K. Smith, A.M.Z. Slawin, P.H. Willoughby, S.L. Cockroft, A.D. Smith, Angew. Chem. Int. Ed. 59 (2020) 3705–3710, https://doi.org/10.1002/anie.201914421.
[25] K.T. Mahmudov, M.N. Kopylovich, M.F.C. Guedes da Silva, A.J.L. Pombeiro, Dalton Trans. 46 (2017) 10121–10138, https://doi.org/10.1039/c7dt01685a.
[26] M. Fourmigué, A. Dhaka, Coord. Chem. Rev. 403 (2020) 213084, https://doi.org/10.1016/j.ccr.2019.213084.
[27] S. Scheiner, Int. J. Quantum Chem. 113 (2013) 1609–1620, https://doi.org/10.1002/qua.24357.
[28] R. Gleiter, G. Haberhauer, D.B. Werz, Chem. Rev. 118 (2018) 2010–2041, https://doi.org/10.1021/acs.chemrev.7b00449.
[29] L. Vogel, P. Wonner, S.M. Huber, Angew. Chem. Int. Ed. 58 (2019) 1880–1891, https://doi.org/10.1002/anie.201809432.
[30] P. Scilabra, G. Terraneo, G. Resnati, Acc. Chem. Res. 52 (2019) 1313–1324, https://doi.org/10.1021/acs.accounts.9b00037.
[31] A.C. Legon, Phys. Chem. Chem. Phys. 19 (2017) 14884–14896, https://doi.org/10.1039/c7cp02518a.
[32] M. Juanes, R.T. Saragi, W. Caminati, A. Lesarri, Chem. Eur. J. 25 (2019) 11402–11411, https://doi.org/10.1002/chem.201901113.
[33] V. Kumar, Y. Xu, C. Leroy, D.L. Bryce, Phys. Chem. Chem. Phys. 22 (2020) 3817–3824, https://doi.org/10.1039/C9CP06267J.
[34] H.A. Bent, Chem. Rev. 68 (1968) 587–648, https://doi.org/10.1021/cr60255a003.
[35] O. Hassel, Science 170 (1970) 497–502, https://doi.org/10.1126/science.170.3957.497.
[36] N.W. Alcock, Adv. Inorg. Chem. Radiochem. 15 (1972) 1–58, https://doi.org/10.1016/S0065-2792(08)60016-3.
[37] N.W. Alcock, Bonding and Structure: Structural Principles in Inorganic and Organic Chemistry, Ellis Horwood, New York, 1990.
[38] P. Pyykkö, Chem. Rev. 97 (1997) 597–636, https://doi.org/10.1021/cr940396v.
[39] I. Haiduc, Coord. Chem. Rev. 158 (1997) 325–358, https://doi.org/10.1016/S0010-8545(97)90063-1.
[40] , Encyclopaedia of Supramolecular Chemistry vol. 2 (2004) 1215–1224.
[41] N.W. Alcock, R. Countryman, Acta Crystallogr., Section A 13 (1975) S62.
[42] N.W. Alcock, R.M. Countryman, J. Chem. Soc., Dalton Trans. (1977) 217–219, https://doi.org/10.1039/DT9770000217.
[43] J. Starbuck, N.C. Norman, A.G. Orpen, New. J. Chem. 23 (1999) 969–972, https://doi.org/10.1039/A906352H.
[44] G. Cavallo, P. Metrangolo, R. Milani, T. Pilati, A. Priimagi, G. Resnati, G. Terraneo, Chem. Rev. 116 (2016) 2478–2601, https://doi.org/10.1021/acs.chemrev.5b00484.
[45] J.S. Murray, P. Lane, T. Clark, P. Politzer, J. Mol. Model. 13 (2007) 1033–1038, https://doi.org/10.1007/s00894-007-0225-4.
[46] P. Politzer, J.S. Murray, Crystals 7 (2017) 212, https://doi.org/10.3390/cryst7070212.
[47] M.H. Kolář, P. Hobza, Chem. Rev. 116 (2016) 5155–5187, https://doi.org/10.1021/acs.chemrev.5b00560.
[48] D.J. Pascoe, K.B. Ling, S.L. Cockroft, J. Am. Chem. Soc. 139 (2017) 15160–15167, https://doi.org/10.1021/jacs.7b08511.
[49] S. Scheiner, J. Phys. Chem. A 121 (2017) 5561–5568, https://doi.org/10.1021/acs.jpca.7b05300.
[50] W. Dong, Q. Li, S. Scheiner, Molecules 23 (2018) 1681, https://doi.org/10.3390/molecules23071681.
[51] J.D. Velásquez, G. Mahmoudi, E. Zangrando, A.V. Gurbanov, F.I. Zubkov, Y. Zorlu, A. Masoudias, J. Echeverría, CrystEngComm 21 (2019) 6018–6025, https://doi.org/10.1039/C9CE00959K.
[52] J.S. Murray, P. Politzer, Crystals 10 (2020) 76, https://doi.org/10.3390/cryst10020076.
[53] B. Galmés, A. Juan-Bals, A. Frontera, G. Resnati, Chem. Eur. J. 26 (2020) 4599–4606, https://doi.org/10.1002/chem.201905498.
[54] E.R.T. Tiekink, Coord. Chem. Rev. 345 (2017) 219–228, https://doi.org/10.1016/j.ccr.2017.01.009.
[55] D.P. Malenov, G.V. Janjiae, V.B. Medakoviae, M.B. Hall, S.D. Zarić, Coord. Chem. Rev. 345 (2017) 318–341, https://doi.org/10.1016/j.ccr.2016.12.020.
[56] E.R.T. Tiekink, CrystEngComm 5 (2003) 101–113, https://doi.org/10.1039/B301318A.
[57] M.A. Buntine, F.J. Kosovel, E.R.T. Tiekink, CrystEngComm 5 (2003) 331–336, https://doi.org/10.1039/B308922C.
[58] Y. Liu, E.R.T. Tiekink, CrystEngComm 7 (2005) 20–27, https://doi.org/10.1039/B416493H.
[59] E.R.T. Tiekink, CrystEngComm 8 (2006) 104–118, https://doi.org/10.1039/B517339F.
[60] C.S. Lai, E.R.T. Tiekink, Z. Kristallogr, Cryst. Mater. 222 (2007) 532–538, https://doi.org/10.1524/zkri.2007.222.10.532.
[61] E.R.T. Tiekink, Appl. Organomet. Chem. 22 (2008) 533–550, https://doi.org/10.1002/aoc.1441.
[62] E.R.T. Tiekink, J. Zukerman-Schpector, Coord. Chem. Rev. 254 (2010) 46–76, https://doi.org/10.1016/j.ccr.2009.09.007.
[63] E.R.T. Tiekink, Crystals 8 (2018) 292, https://doi.org/10.3390/cryst8070292.
[64] S.M. Lee, P.J. Heard, E.R.T. Tiekink, Coord. Chem. Rev. 375 (2018) 410–423, https://doi.org/10.1016/j.ccr.2018.03.001.
[65] R. Taylor, P.A. Wood, Chem. Rev. 119 (2019) 9427–9477, https://doi.org/10.1021/acs.chemrev.9b00155.
[66] I.J. Bruno, J.C. Cole, P.R. Edgington, M. Kessler, C.F. Macrae, P. McCabe, J. Pearson, R. Taylor, Acta Crystallogr., Sect. B: Struct. Sci., Cryst. Eng. Mater. 58 (2002) 389–397, https://doi.org/10.1107/S0108768102003324.
[67] A. Spek, A. Crystallogr, E. Sect, Cryst. Commun. 76 (2020) 1–11, https://doi.org/10.1107/S2056989019016244.
[68] C.F. Macrae, I. Sovago, S.J. Cottrell, P.T.A. Galek, P. McCabe, E. Pidcock, M.I. Platings, G.P. Shields, J.S. Stevens, M. Towler, P.A. Wood, J. Appl. Crystallogr. 53 (2020) 226–235, https://doi.org/10.1107/S1600576719014092.
[69] K. Brandenburg, DIAMOND. Visual Crystal Structure Information System, version 3.1, Crystal Impact, Bonn, Germany, 2006.
[70] F. Wang, P.L. Polavarapu, J. Drabowicz, P. Kiełbasinski, M.J. Potrzebowski, M. Mikołajczyk, M.W. Wieczorek, W.W. Majzner, I. Łażewska, J. Phys. Chem. A 108 (2004) 2072–2079, https://doi.org/10.1021/jp031270h.
[71] P.P. Phadnis, A. Kunwar, M. Kumar, R. Mishra, A. Wadawale, K.I. Priyadarsini, V.K. Jain, J. Organomet. Chem. 852 (2017) 1–7, https://doi.org/10.1016/j.jorganchem.2017.09.029.
[72] S. Goswami, A. Hazra, R. Chakrabarty, H.-K. Fun, Org. Lett. 11 (2009) 4350–4353, https://doi.org/10.1021/ol901737s.
[73] M. Ruamps, N. Lugan, V. Cesar, Eur. J. Inorg. Chem. (2017) 4167–4173, https://doi.org/10.1002/ejic.201700883.
[74] E. Block, E.V. Dikarev, R.S. Glass, J. Jin, B. Li, X. Li, S.-Z. Zhang, J. Am. Chem. Soc. 128 (2006) 14949–14961, https://doi.org/10.1021/ja065037j.
[75] J.Y. See, H. Yang, Y. Zhao, M.W. Wong, Z. Ke, Y.-Y. Yeung, ACS Catalysis 8 (2018) 850–858, https://doi.org/10.1021/acscatal.7b03510.
[76] G. Hua, J. Du, A.M.Z. Slawin, J.D. Woollins, J. Org. Chem. 79 (2014) 3876–3886, https://doi.org/10.1021/jo500316v.
[77] A.M. Toma, A. Nicoară, A. Silvestru, T. Rüffer, H. Lang, M. Mehring, J. Organomet. Chem. 810 (2016) 33–39, https://doi.org/10.1016/j.jorganchem.2016.03.002.
[78] C. Allen, J.C.A. Boeyens, A.G. Briggs, L. Denner, A.J. Markwell, D.H. Reid, B.G. Rose, J. Chem. Soc. Chem. Comm. (1987) 967–968, https://doi.org/10.1039/C39870000967.
[79] M. Iyoda, R. Watanabe, Y. Miyake, Chem. Lett. 33 (2004) 570–571, https://doi.org/10.1246/cl.2004.570.

[80] P. Bhattacharyya, A.M.Z. Slawin, J.D. Woollins, Chem. Eur. J. 8 (2002) 2705–2711, https://doi.org/10.1002/1521-3765(20020617)8:12<2705::AID-CHEM2705>3.0.CO;2-2.
[81] G. Karabanovich, J. Roh, Z. Padělková, K. Vávrová Novák, Z.A. Hrabálek, Tetrahedron 69 (2013) 8798–8808, https://doi.org/10.1016/j.tet.2013.07.103.
[82] B.M. Laloo, H. Mecadon, Md.R. Rohman, I. Kharbangar, I. Kharkongor, M. Rajbangshi, R. Nongkhlaw, B. Myrboh, J. Org. Chem. 77 (2012) 707–712, https://doi.org/10.1021/jo201985n.
[83] C. Gicquel-Mayer, G. Perez, P. Lerouge, C. Paulmier, Acta Crystallogr., Sect. C: Cryst. Struct. Commun. 43 (1987) 284–287, https://doi.org/10.1107/S0108270187096112.
[84] V. Kubát, M. Babiak, Z. Trávníček, J. Novosad, Polyhedron 124 (2017) 62–67, https://doi.org/10.1016/j.poly.2016.12.034.
[85] P. Arsenyan, E. Paegle, S. Belyakov, Chem. Heterocycl. Compd. 49 (2013) 791–796, https://doi.org/10.1007/s10593-013-1310-5.
[86] P. Arsenyan, E. Vasiljeva, S. Belyakov, Chem. Heterocycl. Compd. 47 (2011) 237–241, https://doi.org/10.1007/s10593-011-0746-8.
[87] K.M. Aumann, P.J. Scammells, J.M. White, C.H. Schiesser, Org. Biomol. Chem. 5 (2007) 1276–1281, https://doi.org/10.1039/b700812k.
[88] X. Chen, K.-H. Baek, Y. Kim, S.-J. Kim, I. Shin, J. Yoon, Tetrahedron 66 (2010) 4016–4021, https://doi.org/10.1016/j.tet.2010.04.042.
[89] K. Matoba, T. Yamazaki, Chem. Pharm. Bull. 35 (1987) 4967–4971, https://doi.org/10.1248/cpb.35.4967.
[90] J. Zhou, J.-M. Huang, Y. Tang, R.-Y. Chen, Chin. J. Struct. Chem. 18 (1999) 103–106.
[91] K. Satheeshkumar, G. Mugesh, Chem. Eur. J. 17 (2011) 4849–4857, https://doi.org/10.1002/chem.201003417.
[92] K. Shimada, A. Moro-oka, A. Maruyama, H. Fujisawa, T. Saito, R. Kawamura, H. Kogawa, M. Sakuraba, Y. Takata, S. Aoyagi, Y. Takikawa, C. Kabuto, Bull. Chem. Soc. Jpn. 80 (2007) 567–577, https://doi.org/10.1246/bcsj.80.567.
[93] V.P. Singh, H.B. Singh, R.J. Butcher, Chem. Commun. 47 (2011) 7221–7223, https://doi.org/10.1039/c1cc12152a.
[94] L. Dupont, M. Messali, L. Christiaens, Acta Crystallogr., Sect. E: Struct. Rep. Online 59 (2003) o547–o549, https://doi.org/10.1107/S1600536803006433.
[95] V.P. Singh, H.B. Singh, R.J. Butcher, Chem. Asian J. 6 (2011) 1431–1442, https://doi.org/10.1002/asia.201000858.
[96] F.-Y. Meng, Y.-A. Chen, C.-L. Chen, P.-T. Chou, ChemPhotoChem 2 (2018) 475–480, https://doi.org/10.1002/cptc.201800066.
[97] V. Kumar, Y. Xu, D.L. Bryce, Chem. Eur. J. 26 (2020) 3275–3286, https://doi.org/10.1002/chem.201904795.
[98] G.M. Arvanitis, M.E. Berardini, D. Allardice, P.E. Dumas, J. Chem. Cryst. 24 (1994) 421–423, https://doi.org/10.1007/BF01666088.
[99] A.S. Hodage, P.P. Phadnis, A. Wadawale, K.I. Priyadarsini, V.K. Jain, Phosphorus, Sulfur, Silicon, Relat. Elem. 189 (2014) 700–710, https://doi.org/10.1080/10426507.2013.844144.
[100] K.P. Bhabak, G. Mugesh, Chem. Asian J. 4 (2009) 974–983, https://doi.org/10.1002/asia.200800483.
[101] P. Arsenyan, E. Paegle, S. Belyakov, I. Shestakova, E. Jaschenko, I. Domracheva, J. Popelis, Eur. J. Med. Chem. 46 (2011) 3434–3443, https://doi.org/10.1016/j.ejmech.2011.05.008.
[102] S. Braverman, M. Cherkinsky, Y. Kalendar, R. Jana, M. Sprecher, I. Goldberg, Synthesis 46 (2014) 119–125, https://doi.org/10.1055/s-0033-1338555.
[103] Y. Kim, T. Jun, S.V. Mulay, S.T. Manjare, J. Kwak, Y. Lee, D.G. Churchill, Dalton Trans. 46 (2017) 4111–4117, https://doi.org/10.1039/C7DT00555E.
[104] S. Hayashi, H. Wada, T. Ueno, W. Nakanishi, J. Org. Chem. 71 (2006) 5574–5585, https://doi.org/10.1021/jo060527f.
[105] S.-C. Yu, H. Kuhn, C.-G. Daniliuc, I. Ivanov, P.G. Jones, W.-W. du Mont, Org. Biomol. Chem. 8 (2010) 828–834, https://doi.org/10.1039/b918778b.
[106] T.M. Klapötke, B. Krumm, M. Scherr, Z. Anorg, Allg. Chem. 636 (2010) 1955–1961.
[107] T. Annaka, N. Nakata, A. Ishii, New J. Chem. 43 (2019) 11643–11652, https://doi.org/10.1039/C9NJ02813G.
[108] T. Kawashima, F. Ohno, R. Okazaki, J. Am. Chem. Soc. 115 (1993) 10434–10435.
[109] T. Kataoka, S. Watanabe, K. Yamamoto, M. Yoshimatsu, G. Tanabe, O. Muraoka, J. Org. Chem. 63 (1998) 6382–6386, https://doi.org/10.1021/jo980999x.
[110] E.C. Llaguno, I.C. Paul, J. Chem. Soc., Perkin Trans. 2 (1972) 2001–2006; doi: 10.1039/p29720002001
[111] R. Betz, M. Pfister, M.M. Reichvilser, P. Klüfers, Z. Anorg, Allg. Chem. 634 (2008) 1393–1396, https://doi.org/10.1002/zaac.200800097.
[112] T. Maaninen, T. Chivers, R. Laitinen, G. Schatte, M. Nissinen, Inorg. Chem. 39 (2000) 5341–5347, https://doi.org/10.1021/ic000598b.
[113] P. Klüfers, M.M. Reichvilser, Eur. J. Inorg. Chem. (2008) 384–396, https://doi.org/10.1002/ejic.200700837.
[114] T.M. Klapötke, B. Krumm, P. Mayer, H. Piotrowski, O.P. Ruscitti, Z. Naturforsch B, Chem. Sci. 57 (2002) 145–150.
[115] A.G. Makarov, A.Yu. Makarov, I.Yu. Bagryanskaya, M.M. Shakirov, A.V. Zibarev, J. Fluorine Chem. 144 (2012) 118–123, https://doi.org/10.1016/j.jfluchem.2012.08.002.
[116] M. Budesinsky, V. Vanek, M. Dracinsky, R. Pohl, L. Postova-Slavetinska, V. Sychrovsky, I. Cisarova Picha, Tetrahedron 70 (2014) 3871–3886, https://doi.org/10.1016/j.tet.2014.04.047.
[117] Z. Žák, J. Marek, L. Keznikl, Z. Anorg, Allg. Chem. 622 (1996) 1101–1105, https://doi.org/10.1002/zaac.19966220628.
[118] L. Richtera, V. Jancik, D. Martínez-Otero, A. Pokluda, Z. Zak, J. Taraba, J. Touzin, Inorg. Chem. 53 (2014) 6569–6577, https://doi.org/10.1021/ic500137z.
[119] L. Richtera, J. Taraba, J. Toužín, Z. Anorg, Allg. Chem. 629 (2003) 716–721, https://doi.org/10.1002/zaac.200390121.
[120] C. Ghiazza, L. Khrouz, C. Monnereau, T. Billard, A. Tlili, Chem. Commun. 54 (2018) 9909–9912, https://doi.org/10.1039/C8CC05256E.
[121] P.G. Jones, A. Chrapkowski, Private Communication to the Cambridge Structural Database (2004) Refcode YADVOP.
[122] H.-Q. Wu, S.-H. Luo, L. Cao, H.-N. Shi, B.-W. Wang, Z. Wang, Private Communication to the Cambridge Structural Database (2019) Refcode VIWNAT.
[123] H.J. Traesel, P.R. Olivato, J. Valenca, D.N.S. Rodrigues, J. Zukerman-Schpector, M.D. Colle, J. Mol. Struct. 1157 (2018) 29–39, https://doi.org/10.1016/j.molstruc.2017.12.040.
[124] S. Kumar, N. Sharma, I.K. Maurya, A. Verma, S. Kumar, K.K. Bhasin, R.K. Sharma, New J. Chem. 41 (2017) 2919–2926, https://doi.org/10.1039/C7NJ00338B.
[125] P.S. Engl, R. Senn, E. Otth, A. Togni, Organometallics 34 (2015) 1384–1395, https://doi.org/10.1021/acs.organomet.5b00137.
[126] D. Das, G. Roy, G. Mugesh, J. Med. Chem. 58 (2008) 7313–7317, https://doi.org/10.1021/jm800894m.
[127] W.-J. Chang, C.-M. Sun, Private Communication to the Cambridge Structural Database (2012) Refcode GOHPEA.
[128] M.S. Afzal, J.-P. Pitteloud, D. Buccella, Chem. Commun. 50 (2014) 11358–11361, https://doi.org/10.1039/C4CC04460F.
[129] G.A. Brown, K.M. Anderson, M. Murray, T. Gallagher, N.J. Hales, Tetrahedron 56 (2000) 5579–5586, https://doi.org/10.1016/S0040-4020(00)00408-7.
[130] G. Hua, J. Du, A.M.Z. Slawin, J.D. Woollins, Synlett 25 (2014) 2189–2195, https://doi.org/10.1055/s-0034-1378525.
[131] T. Laitalainen, T. Simonen, R. Kivekas, M. Klinga, J. Chem. Soc., Perkin Trans. 1 (1983) 333–340, https://doi.org/10.1039/p19830000333.
[132] K. Okuma, Y. Mori, T. Shigetomi, M. Tabuchi, K. Shioji, Y. Yokomori, Tetrahedron Lett. 48 (2007) 8311–8313, https://doi.org/10.1016/j.tetlet.2007.09.120.
[133] S.J. Balkrishna, A.S. Hodage, S. Kumar, P. Panini, S. Kumar, RSC Adv. 4 (2015) 11535–11538, https://doi.org/10.1039/C4RA00381K.
[134] M. Iwasaki, N. Miki, Y. Tsuchiya, K. Nakajima, Y. Nishihara, Org. Lett. 19 (2017) 1092–1095, https://doi.org/10.1021/acs.orglett.7b00116.
[135] Y.S. Peng, H.S. Xu, P. Naumov, S.S.S. Raj, H.-K. Fun, I.A. Razak, S.W. Ng, Acta Crystallogr., Sect. C: Cryst. Struct. Commun. 56 (2000) 1386–1388, https://doi.org/10.1107/S0108270100011276.
[136] S. Sankari, P. Sugumar, P. Manisankar, S. Muthusubramanian, M.N. Ponnuswamy, Acta Crystallogr., Sect. E: Struct. Rep. Online 68 (2012) o871, https://doi.org/10.1107/S1600536812007027.
[137] K. Doudin, K.W. Tornrös, J. Mol. Struct. 1134 (2017) 611–616, https://doi.org/10.1016/j.molstruc.2016.12.067.
[138] C.J. Narangoda, T.R. Lex, M.A. Moore, C.D. McMillen, A. Kitaygorodskiy, J.E. Jackson, D.C. Whitehead, Org. Lett. 20 (2018) 8009–8013, https://doi.org/10.1021/acs.orglett.8b03590.
[139] S.S. Zade, S. Panda, H.B. Singh, R.B. Sunoj, R.J. Butcher, J. Org. Chem. 70 (2005) 3693–3704, https://doi.org/10.1021/jo0478656.
[140] U. Flörke; Private Communication to the Cambridge Structural Database (2019) Refcode KIXTUJ
[141] A. Blaschette, M. Naveke, P.G. Jones, Chem. Zeit. 114 (1990) 384–386.
[142] Q. Glenadel, C. Ghiazza, A. Tlili, T. Billard, Adv. Synth. Catal. 359 (2017) 3414–3420, https://doi.org/10.1002/adsc.201700904.
[143] G.M. Li, R.A. Zingaro, M. Segi, J.H. Reibenspies, T. Nakajima, Organometallics 16 (1997) 756–762, https://doi.org/10.1021/om960883w.
[144] M. Yamamura, T. Nabeshima, Bull. Chem. Soc. Jpn. 89 (2016) 42–49, https://doi.org/10.1246/bcsj.20150288.
[145] G. Hua, J. Du, A.M.Z. Slawin, J.D. Woollins, Chem. Sel. 1 (2016) 6810–6817, https://doi.org/10.1002/slct.201601577.
[146] G. Hua, J. Du, A.M.Z. Slawin, J.D. Woollins, Molecules 22 (2017) 46, https://doi.org/10.3390/molecules22010046.
[147] J.-B. Shen, X. Lv, J.-F. Chen, Y.-F. Zhou, G.-L. Zhao, Acta Crystallogr., Sect. E: Struct. Rep. Online 67 (2011) o803, https://doi.org/10.1107/S1600536811007185.
[148] G.L. Sommen, A. Linden, H. Heimgartner, Tetrahedron 62 (2006) 3344–3354, https://doi.org/10.1016/j.tet.2006.01.077.
[149] T. Fellowes, J.M. White, CrystEngComm 21 (2019) 1539–1542, https://doi.org/10.1039/C8CE01853G.
[150] L. Dupont, O. Dideberg, P. Jacquemin, Acta Crystallogr., Sect. C: Cryst. Struct. Commun. 46 (1990) 484–486, https://doi.org/10.1107/S0108270189007894.
[151] S.-X. Feng, C.-M. Yang, J.-L. Wang, J.-Y. Ma, Chem. Res. Appln. 30 (2018) 840–845, https://doi.org/10.3969/j.issn.1004-1656.2018.05.030.
[152] K.P. Bhabak, G. Mugesh, Chem. Eur. J. 13 (2007) 4594–4601, https://doi.org/10.1002/chem.200601584.
[153] M. Piatek, B. Oleksyn, J. Sliwinski, Acta Crystallogr., Sect. C: Cryst. Struct. Commun. 51 (1995) 298–301, https://doi.org/10.1107/S0108270193012983.
[154] R. Shukla, N. Claiser, M. Souhassou, C. Lecomte, S.J. Balkrishna, S. Kumar, D. Chopra, IUCrJ 5 (2018) 647–653, https://doi.org/10.1107/S2052252518011041.
[155] L. Wang, Y. Xu, Z. Guo, X. Wei, IUCrData 2 (2017) x170532, https://doi.org/10.1107/S2414314617005326.
[156] X. Zhu, Y. Xu, H. Han, Z. Guo, X. Wei, Acta Crystallogr., Sect. E: Struct. Rep. Online 69 (2013) o1538, https://doi.org/10.1107/S1600536813024744.

[157] H. Ungati, V. Govindaraj, M. Narayanan, G. Mugesh, Angew. Chem., Int. Ed. 58 (2019) 8156–8160, https://doi.org/10.1002/anie.201903958.
[158] S.J. Balkrishna, B.S. Bhakuni, D. Chopra, S. Kumar, Org. Lett. 12 (2010) 5394–5397, https://doi.org/10.1021/ol102027j.
[159] M.J. Laws, C.H. Schiesser, J.M. White, S.-L. Zheng, Aust. J. Chem. 53 (2000) 277–283, https://doi.org/10.1071/CH99127.
[160] S.J. Balkrishna, B.S. Bhakuni, S. Kumar, Tetrahedron 67 (2011) 9565–9575, https://doi.org/10.1016/j.tet.2011.09.141.
[161] L. Dupont, P. Jacquemin, Acta Crystallogr Sect. C: Cryst. Struct. Commun. 50 (1994) 1801–1802, https://doi.org/10.1107/S0108270194001691.
[162] V.A. Potapov, E.O. Kurkutov, M.V. Musalov, S.V. Amosova, Tetrahedron Lett. 51 (2010) 5258–5261, https://doi.org/10.1016/j.tetlet.2010.07.133.
[163] R.A. Bragg, J. Clayden, M. Bladon, O. Ichihara, Tetrahedron Lett. 42 (2001) 3411–3414, https://doi.org/10.1016/S0040-4039(01)00502-0.
[164] S.E. Brantley, B. Gerlach, M.M. Olmstead, K.M. Smith, Tetrahedron Lett. 38 (1997) 937–940, https://doi.org/10.1016/S0040-4039(97)00002-6.
[165] I.V. Svistunova, G.O. Tretyakova, K.A. Gayvoronskaya, Phosphorus, Sulfur, Silicon, Relat. Elem. 192 (2017) 1177–1187, https://doi.org/10.1080/10426507.2017.1354210.
[166] M.B. Hursthouse, D.S. Hughes, A.L. Redfern, D.W. Knight, Private Communication to the Cambridge Structural Database (2013) Refcode TELLIH.
[167] G. Roy, P.N. Jayaram, G. Mugesh, Chem. Asian J. 8 (2013) 1910–1921, https://doi.org/10.1002/asia.201300274.
[168] O.R. Shangpliang, B. Kshiar, K. Wanniang, I.D. Marpna, T.M. Lipon, B.M. Laloo, B. Myrboh, J. Org. Chem. 83 (2018) 5829–5835, https://doi.org/10.1021/acs.joc.8b00558.
[169] J. Yu, J.-H. Kim, H.W. Lee, V. Alexander, H.-C. Ahn, W.J. Choi, J. Choi, L.S. Jeong, Chem. Eur. J. 19 (2013) 5528–5532, https://doi.org/10.1002/chem.201300741.
[170] G. Adiwidjaja, O. Schulze, J. Voss, J. Wirsching, Carbohydr. Res. 325 (2000) 107–119, https://doi.org/10.1016/S0008-6215(99)00321-3.
[171] Z. Majeed, W.R. McWhinnie, K. Paxton, T.A. Hamor, J. Organomet. Chem. 577 (1999) 15–18, https://doi.org/10.1016/S0022-328X(98)01019-5.
[172] Y.A. Getmanenko, T.G. Allen, H. Kim, J.M. Hales, B. Sandhu, M.S. Fonari, K.Yu. Suponitsky, Y. Zhang, V.N. Khrustalev, J.D. Matichaz, T.V. Timofeeva, S. Barlow, S.-H. Chi, J.W. Perry, S.R. Marder, Adv. Funct. Mater. 28 (2018) 1804073, https://doi.org/10.1002/adfm.201804073.
[173] P.C. Ho, J. Rafique, J. Lee, L.M. Lee, H.A. Jenkins, J.F. Britten, A.L. Braga, I. Vargas-Baca, Dalton Trans. 46 (2017) 6570–6579, https://doi.org/10.1039/C7DT00612H.
[174] Y.-X. Xiao, X.-F. Liu, H.-S. Xu, J. Zhu Jun, Y.-Q. Huang, S.-Z. Hu, Chin. J. Struct. Chem. 16 (1997) 42–47.
[175] S.J. Balkrishna, S. Kumar, G.K. Azad, B.S. Bhakuni, P. Panini, N. Ahalawat, R.S. Tomar, M.R. Detty, S. Kumar, Org. Biomol. Chem. 12 (2014) 1215–1219, https://doi.org/10.1039/C4OB00027G.
[176] A. Gieren, V. Lamm, Acta Crystallogr. Sect. B: Struct. Crystallogr. Cryst. Chem. 38 (1982) 2605–2611, https://doi.org/10.1107/S0567740882009443.
[177] M. Sbit, L. Dupont, O. Dideberg, C. Lambert, Acta Crystallogr., Sect. C: Cryst. Struct. Commun. 44 (1988) 340–342, https://doi.org/10.1107/S0108270187010837.
[178] S.J. Balkrishna, Ch.D. Prasad, P. Panini, M.R. Detty, D. Chopra, S. Kumar, J. Org. Chem. 77 (2012) 9541–9552, https://doi.org/10.1021/jo301486c.
[179] Z.-L. Zuo, Acta Crystallogr Sect. E: Struct. Rep. Online 69 (2013) o636, https://doi.org/10.1107/S1600536813007526.
[180] I. Trentin, C. Schindler, C. Schulzke, Acta Crystallogr., Sect. E: Cryst. Commun. 74 (2018) 840–845, https://doi.org/10.1107/S2056989018007454.
[181] K. Sivapriya, P. Suguna, S. Shubashree, P.R. Sridhar, S. Chandrasekaran, Carbohydr. Res. 342 (2007) 1151–1158, https://doi.org/10.1016/j.carres.2007.02.035.
[182] D. Sureshkumar, S. Koutha, S. Chandrasekaran, Eur. J. Org. Chem. (2007) 4543–4551, https://doi.org/10.1002/ejoc.200700357.
[183] P. Kuronen, T. Laitalainen, O. Orama, J. Heterocycl. Chem. 30 (1993) 961–965, https://doi.org/10.1002/jhet.5570300420.
[184] J.T. Lowe, A. Chandrasekaran, R.O. Day, W. Rosen, Chem. Commun. (2001) 1390–1391, https://doi.org/10.1039/b103499p.
[185] R.J. Adrien, R.W. Gable, B.F. Hoskins, D. Dakternieks, J. Organomet. Chem. 359 (1989) 33–39, https://doi.org/10.1016/0022-328X(89)85248-9.
[186] O. Foss, F. Kvammen, K. Marøy, J. Chem. Soc., Dalton Trans. (1985) 231–237, https://doi.org/10.1039/dt9850000231.
[187] E.A. Meyers, R.A. Zingaro, N.L.M. Dereu, Z. Kristallogr, Cryst. Mater. 210 (1995) 305, https://doi.org/10.1524/zkri.1995.210.4.305.
[188] S. Kumar, S. Panda, H.B. Singh, G. Wolmershäuser, R.J. Butcher, Struct. Chem. 18 (2007) 127–132, https://doi.org/10.1007/s11224-006-9082-5.
[189] A.S. Hodage, P.P. Phadnis, A. Wadawale, K.I. Priyadarsini, V.K. Jain, Anal. Sci.: X-Ray Struct. Anal. Online 25 (2009) 101–102, https://doi.org/10.2116/xraystruct.25.101.
[190] D. Sureshkumar, V. Ganesh, S. Chandrasekaran, J. Org. Chem. 72 (2007) 5313–5319, https://doi.org/10.1021/jo070705k.
[191] D.R. Garud, M. Koketsu, M. Ebihara, H. Ishihara, Acta Crystallogr., Sect. E: Struct. Rep. Online 62 (2006) o2133–o2134, https://doi.org/10.1107/S1600536806015212.
[192] A. Chesney, M.R. Bryce, M.A. Chalton, A.S. Batsanov, J.A.K. Howard, J.-M. Fabre, L. Binet, S. Chakroune, J. Org. Chem. 61 (1996) 2877–2881, https://doi.org/10.1021/jo951979n.
[193] D.M. Freudendahl, M. Iwaoka, T. Wirth, Eur. J. Org. Chem. (2010) 3934–3944, https://doi.org/10.1002/ejoc.201000514.
[194] M.J. Potrzebowski, M. Michalska, J. Blaszczyk, M.W. Wieczorek, W. Ciesielski, S. Kazmierski, J. Pluskowski, J. Org. Chem. 60 (1995) 3139–3148, https://doi.org/10.1021/jo00115a033.
[195] J. Hildebrandt, T. Niksch, R. Trautwein, N. Häfner, H. Görls, M.-C. Barth, M. Dürst, I.B. Runnebaum, W. Weigand, Phosphorus, Sulfur, Silicon, Relat. Elem. 192 (2017) 182–186, https://doi.org/10.1080/10426507.2016.1250760.
[196] A. Linden, Y. Zhou, H. Heimgartner, Acta Crystallogr Sect. C: Cryst, Struct. Chem. 70 (2014) 482–487, https://doi.org/10.1107/S2053229614008237.
[197] M.W. Carland, C.H. Schiesser, J.M. White, Aust. J. Chem. 57 (2004) 97–100, https://doi.org/10.1071/CH03210.
[198] C.P. Prabhu, P.P. Phadnis, A.P. Wadawale, K.I. Priyadarsini, V.K. Jain, J. Organomet. Chem. 713 (2012) 42–50, https://doi.org/10.1016/j.jorganchem.2012.04.014.
[199] G.D. Morris, F.W.B. Einstein, Acta Crystallogr Sect. C: Cryst. Struct. Commun. 42 (1986) 1433–1435, https://doi.org/10.1107/S0108270186092004.
[200] P. Maity, D. Kundu, R. Roy, B.C. Ranu, Org. Lett. 16 (2014) 4122–4125, https://doi.org/10.1021/ol501820e.
[201] G. Cooke, M.R. Bryce, M.C. Petty, D.J. Ando, M.B. Hursthouse, Synthesis (1993) 465–467, https://doi.org/10.1055/s-1993-25881.
[202] P. Kumar, V.S. Kashid, J.T. Mague, M.S. Balakrishna, Tetrahedron Lett. 55 (2014) 5232–5235, https://doi.org/10.1016/j.tetlet.2014.08.005.
[203] T. Shirahata, M. Kibune, H. Yoshino, T. Imakubo, Chem. Eur. J. 13 (2007) 7619–7630, https://doi.org/10.1002/chem.200700314.
[204] T. Imakubo, T. Shirahata, M. Kibune, Chem. Commun. (2004) 1590–1591, https://doi.org/10.1039/b403559c.
[205] K. Sivapriya, P. Suguna, S. Chandrasekaran, Tetrahedron Lett. 48 (2007) 2091–2095, https://doi.org/10.1016/j.tetlet.2007.01.128.
[206] J. Beckmann, A. Duthie, Z. Anorg. Allg. Chem. 631 (2005) 1849–1855, https://doi.org/10.1002/zaac.200500167.
[207] A.S. Filatov, E. Block, M.A. Petrukhina, Acta Crystallogr., Sect. C: Cryst. Struct. Commun. 61 (2005) o596–o598, https://doi.org/10.1107/S0108270105027587.
[208] V.P. Singh, J.-F. Poon, R.J. Butcher, L. Engman, Chem. Eur. J. 20 (2014) 12563–12571, https://doi.org/10.1002/chem.201403229.
[209] H. Ge, Q. Shen, Org. Chem. Front. 6 (2019) 2205–2209, https://doi.org/10.1039/C8QO01249K.
[210] D. Dakternieks, R.W. Gable, B.F. Hoskins, Acta Crystallogr., Sect. C: Cryst. Struct. Commun. 45 (1989) 206–208, https://doi.org/10.1107/S0108270188011126.
[211] J. Toužín, K. Neplechová, Z. Žák, M. Černík, Collect. Czech. Chem. Commun. 67 (2002) 577–586, https://doi.org/10.1135/cccc20020577.
[212] B. Dahlén, Acta Crystallogr Sect. B: Struct. Crystallogr. Cryst. Chem. 30 (1974) 647–651, https://doi.org/10.1107/S0567740874003463.
[213] P.R. Prasad, H.B. Singh, R.J. Butcher, Molecules 20 (2015) 12670–12685, https://doi.org/10.3390/molecules200712670.
[214] N. Kamigata, Y. Nakamura, K. Kikuchi, I. Ikemoto, T. Shimizu, H. Matsuyama, J. Chem. Soc., Perkin Trans. 1 (1992) 1721–1728, https://doi.org/10.1039/p19920001721.
[215] T. Takahashi, N. Nakao, T. Koizumi, Tetrahedron: Asymm. 8 (1997) 3293–3308, https://doi.org/10.1016/S0957-4166(97)00423-0.
[216] Y. Nakahima, T. Shimizu, K. Hirabayashi, N. Kamigata, M. Yasui, M. Nakazato, F. Iwasaki, Tetrahedron Lett. 45 (2004) 2301–2303, https://doi.org/10.1016/j.tetlet.2004.01.107.
[217] D.S. Lamani, D. Bhowmick, G. Mugesh, Org. Biomol. Chem. 10 (2012) 7933–7943, https://doi.org/10.1039/c2ob26156a.
[218] K. Maartmann-Moe, K.A. Sanderud, J. Songstad, Acta Chem. Scand. 38 (1984) 187–200, https://doi.org/10.3891/acta.chem.scand.38a-0187.
[219] M.R. Detty, H.R. Luss, Organometallics 11 (1992) 2157–2162, https://doi.org/10.1021/om00042a032.
[220] T.G. Back, B.P. Dyck, S. Nan, M. Parvez, Acta Crystallogr., Sect. C: Cryst. Struct. Commun. 54 (1998) 425–427, https://doi.org/10.1107/S0108270197015916.
[221] X. Yan, R. Long, F. Luo, L. Yang, X. Zhou, Tetrahedron Lett. 58 (2017) 54–58, https://doi.org/10.1016/j.tetlet.2016.11.098.
[222] D.B. Werz, R. Gleiter, F. Rominger, Eur. J. Org. Chem. (2003) 151–154; doi: https://doi.org/10.1002/1099-0690(200301)2003:1<151::AID-EJOC151>3.0.CO;2-7
[223] R. Kivekas, T. Laitalainen, T. Simonen, Acta Chem. Scand. 40 (1986) 98–100, https://doi.org/10.3891/acta.chem.scand.40b-0098.
[224] L. Boudiba, L. Ouahab, A. Gouasmia, Tetrahedron Lett. 47 (2006) 3123–3125, https://doi.org/10.1016/j.tetlet.2006.02.145.
[225] C. Schindler, C. Schulzke, Inorg. Chem. Commun. 77 (2017) 80–82, https://doi.org/10.1016/j.inoche.2017.02.005.
[226] G. Hua, A.L. Fuller, A.M.Z. Slawin, J.D. Woollins, Eur. J. Org. Chem. (2010) 2607–2615, https://doi.org/10.1002/ejoc.201000075.
[227] R. Kapoor, P. Wadhawan, P. Kapooor, J.F. Sawyer, Can. J. Chem. 66 (1988) 2367–2374, https://doi.org/10.1139/v88-374.
[228] S.K. Tripathi, U. Patel, D. Roy, R.B. Sunoj, H.B. Singh, G. Wolmershäuser, R.J. Butcher, J. Org. Chem. 70 (2005) 9237–9247, https://doi.org/10.1021/jo051309+.
[229] S. Claeson, V. Langer, S. Allenmark, Chirality 12 (2000) 71–75, https://doi.org/10.1002/(SICI)1520-636X(2000)12:2<71::AID-CHIR3>3.0.CO;2-S.
[230] B. Dahlen, B. Lindgren, Acta Chem. Scand. 33 (1979) 403–405, https://doi.org/10.3891/acta.chem.scand.33a-0403.

[231] T. Maaninen, R. Laitinen, T. Chivers, Chem. Commun. (2002) 1812–1813, https://doi.org/10.1039/b205011k.
[232] J. Beck, P. Krieger-Beck, K. Kelm, Z. Naturforsch B, Chem. Sci. 61 (2006) 123–132.
[233] H.-Y. Li, H.-F. Han, W.-J. Li, X.-H. Wei, Chin. J. Struct. Chem. 31 (2012) 910–914.
[234] G.L. Sommen, A. Linden, H. Heimgartner, Helv. Chim. Acta 90 (2007) 641–651, https://doi.org/10.1002/hlca.200790067.
[235] O. Jeannin, H.-T. Huynh, A.M.S. Riel, M. Fourmigué, New J. Chem. 42 (2018) 10502–10509, https://doi.org/10.1039/C8NJ00554K.
[236] S. Aboulkacem, D. Naumann, W. Tyrra, I. Pantenburg, Organometallics 31 (2012) 1559–1565, https://doi.org/10.1021/om201195j.
[237] P. Arsenyan, J. Vasiljeva, S. Belyakov, E. Liepinsh, M. Petrova, Eur. J. Org. Chem. (2015) 5842–5855, https://doi.org/10.1002/ejoc.201500582.
[238] T.M. Klapötke, B. Krumm, K. Polborn, Eur. J. Inorg. Chem. (1999) 1359–1366, https://doi.org/10.1002/(SICI)1099-0682(199908)1999:8<1359::AID-EJIC1359>3.3.CO;2-3.
[239] N.W. Alcock, J.F. Sawyer, Dalton Trans. (1980) 115–120, https://doi.org/10.1039/dt9800000115.
[240] S. Fritz, C. Ehm, D. Lentz, Inorg. Chem. 54 (2015) 5220–5231, https://doi.org/10.1021/acs.inorgchem.5b00107.
[241] K. Eichstaedt, A. Wasilewska, B. Wicher, M. Gdaniec, T. Polonski, Cryst. Growth Des. 16 (2016) 1282–1293, https://doi.org/10.1021/acs.cgd.5b01356.
[242] K. Lekin, A.A. Leitch, A. Assoud, W. Yong, J. Desmarais, J.S. Tse, S. Desgreniers, R.A. Secco, R.T. Oakley, Inorg. Chem. 57 (2018) 4757–4770, https://doi.org/10.1021/acs.inorgchem.8b00485.
[243] M.A. Nascimento, E. Heyer, J.J. Clarke, H.J. Cowley, A. Alberola, N. Stephaniuk, J.M. Rawson, Angew. Chem., Int. Ed. 58 (2018) 1371–1375, https://doi.org/10.1002/anie.201812132.
[244] A.M.S. Riel, O. Jeannin, O.B. Berryman, M. Fourmigué, Acta Crystallogr., Sect. B: Struct. Sci., Cryst. Eng. Mat. 75 (2019) 34–38, https://doi.org/10.1107/S2052520618017778.
[245] J.D. Dunitz, R. Taylor, Chem. Eur. J. 3 (1997) 89–98, https://doi.org/10.1002/chem.19970030115.
[246] E.R.T. Tiekink, J. Zukerman-Schpector, CrystEngComm 11 (2009) 2701–2711, https://doi.org/10.1039/B910209D.
[247] I. Caracelli, I. Haiduc, J. Zukerman-Schpector, E.R.T. Tiekink, Coord. Chem. Rev. 257 (2013) 2863–2879, https://doi.org/10.1016/j.ccr.2013.05.022.
[248] I. Caracelli, J. Zukerman-Schpector, E.R.T. Tiekink, Coord. Chem. Rev. 256 (2012) 412–438, https://doi.org/10.1016/j.ccr.2011.10.021.
[249] I.S. Đorđević, M. Popadić, M. Sarvan, M. Petković-Benazzouz, G.V. Janjić, Acta Crystallogr B. Sect Struct. Sci., Cryst. Eng. Mater. 76 (2020) 122–136, https://doi.org/10.1107/S2052520619016287.
[250] E.R.T. Tiekink, Crystals 10 (2020) article no. 503; doi: https://doi.org/10.3390/cryst10060503
[251] T. Clark, M. Hennemann, J.S. Murray, P. Politzer, J. Mol. Model. 13 (2007) 291–296, https://doi.org/10.1007/s00894-006-0130-2.
[252] M.E. Brezgunova, J. Lieffrig, E. Aubert, S. Dahaoui, P. Fertey, S. Lebègue, J.G. Ángyán, M. Fourmigué, E. Espinosa, Cryst. Growth Des. 13 (2013) 3283–3289, https://doi.org/10.1021/cg400683u.
[253] K. Alhameedi, A. Karton, D. Jayatilaka, S.P. Thomas, IUCrJ 5 (2018) 635–646, https://doi.org/10.1107/S2052252518010758.
[254] X. Guo, X. An, Q. Li, J. Phys. Chem. A 119 (2015) 3518–3527, https://doi.org/10.1021/acs.jpca.5b00783.
[255] P. Politzer, J.S. Murray, T. Clark, G. Resnati, Phys. Chem. Chem. Phys. 19 (2017) 32166–32178, https://doi.org/10.1039/C7CP06793C.
[256] R. Wysokiński, M. Michalczyk, W. Zierkiewicz, S. Scheiner, Phys. Chem. Chem. Phys. 21 (2019) 10336–10346, https://doi.org/10.1039/C9CP01759C.
[257] Z. Jin, X. Du, Y. Xu, Y. Deng, M. Liu, Y. Zhao, B. Zhang, X. Li, L. Zhang, C. Peng, Y. Duan, J. Yu, L. Wang, K. Yang, F. Liu, R. Jiang, X. Yang, T. You, X. Liu, X. Yang, F. Bai, H. Liu, X. Liu, L.W. Guddat, W. Xu, G. Xiao, C. Qin, Z. Shi, H. Jiang, Z. Rao, H. Yang, Nature 582 (2020) 289–293, https://doi.org/10.1038/s41586-020-2223-y.
[258] H. Sies, M.J. Parnham, Free Radic. Biol. Med. 156 (2020) 107–112, https://doi.org/10.1016/j.freeradbiomed.2020.06.032.
[259] J. Struppe, Y. Zhang, S. Rozovsky, J. Phys. Chemistry B 119 (2015) 3643–3650, https://doi.org/10.1021/jp510857s.
[260] C.A. Bayse, S. Antony, Main Group Met. Chem. 6 (2007) 185–200, https://doi.org/10.1080/10241220801994700.
[261] R. Kheirabadi, M. Izadyar, J. Phys. Chem. A 120 (2016) 10108–10115, https://doi.org/10.1021/acs.jpca.6b11437.